

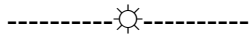
The function of the $\beta 6$ /Pre7 propeptide for 20S proteasome biogenesis in baker's yeast

Von der Fakultät Geo-und Biowissenschaften der Universität Stuttgart
zur Erlangung der Würde eines
Doktors der Naturwissenschaften (Dr. rer. nat.)
genehmigte Abhandlung

Vorgelegt von
Saravanakumar Iyappan
aus India

Vorsitzender des Prüfungsausschusses: **Prof. Dr. Holger Jeske**
Hauptberichter: **PD Dr. Wolfgang Heinemeyer**
Mitberichter: **Prof. Dr. Dieter H. Wolf**
Tag der mündlichen Prüfung: **14.12.2004**

Institut für Biochemie
der Universität Stuttgart
2004



	Abbreviations	7
	Zusammenfassung	9
	Summary	13
1	Introduction	
1.1	Cellular Proteolysis.	16
1.2	The Ubiquitin-Proteasome System	
1.2.1	A retrospective on the proteasome.	16
1.2.2	The ubiquitin-conjugating system.	17
1.2.3	The proteasome and its regulatory complexes.	20
1.3	The 20S core particle	
1.3.1	Subunit comparison of 20S proteasome.	20
1.3.2	Subunit arrangement in 20S proteasome.	21
1.3.3	Structural details of the yeast 20S proteasome.	22
1.3.4	Active site formation and catalytic mechanism.	24
1.4	The assembly of 20S proteasomes	
1.4.1	Preteasome assembly intermediates.	25
1.4.2	Accessory proteins in proteasome biogenesis.	28
1.4.3	Propeptides and their requirements in the proteasome assembly.	28
2	Scope of this work	32
3	Materials and methods	
3.1	Materials	
3.1.1	Media for yeast cultures.	35
3.1.2	Media for <i>Escherichia coli</i> cultures.	35
3.1.3	Chemicals and their Suppliers.	35

3.1.4	Antibodies used in this study.	37
3.1.5	Instruments used in this study.	38
3.1.6	Yeast Strains.	39
3.1.7	Bacterial Strains.	42
3.1.8	Oligonucleotides.	43
3.1.9	Plasmid vectors.	46
3.1.10	Plasmid constructs	47
3.2	Methods	
3.2.1	Molecular biological methods	
3.2.1.1	Plasmid construction.	51
3.2.1.2	Site-directed mutagenesis by recombinant PCR.	51
3.2.1.3	Site-directed mutagenesis by “Quick-Change” mutagenesis.	51
3.2.1.4	Construct maps.	52
3.2.1.5	Yeast colony PCR.	54
3.2.2	Yeast techniques	
3.2.2.1	Strain construction.	54
3.2.2.2	Generation of <i>ump1Δ::HIS3</i> strains and verification by Southern blot analysis.	54
3.2.3	Biochemical methods	
3.2.3.1	Protein sample preparation and quantification.	55
3.2.3.2	Gel electrophoresis and immuno-blotting of proteins.	55
3.2.3.3	Stripping and re-probing of membranes.	55
3.2.3.4	Antibody production against the Pre7 subunit and immuno-affinity purification of the anti Pre7 polyclonal antibody	
3.2.3.4.1	Antibody production and analysis.	56
3.2.3.4.2	Antigen column preparation.	56
3.2.3.4.3	Antibody purification.	57

3.2.3.5	Fractionation of whole-cell extracts by gel-filtration.	57
3.2.3.6	Pulse-chase analysis and immuno-precipitation analysis.	58
3.2.3.7	Non-denaturing PAGE and an in-gel protease assay.	58
3.2.3.8	Non-denaturing PAGE and immuno-blotting analysis.	59
3.2.3.9	Assays for proteolytic activities with fluorogenic peptide substrates.	59
3.2.3.10	Induction of Ump1 protein expression and immunoblot analysis.	60
3.2.3.11	Fusion protein expression in <i>E. coli</i>	60
3.2.3.12	Binding of proteasome complexes to immobilized GST-Ump1.	61
3.2.3.13	<i>In vitro</i> transcription/translation and interaction assay.	61

4 Results

4.1 Genetic analysis of the requirements of proteasomal β -subunit propeptides

4.1.1	The β 6/Pre7 propeptide is essential for yeast cell viability, in contrast to the propeptides of other inactive β -type proteasome subunits.	63
4.1.2	The propeptide remnant in the Pre7 subunit is necessary for proteasome function.	65
4.1.3	Deletion of Ump1 suppresses lethality caused by the Pre7 propeptide deletion.	68
4.1.4	The Pre7 propeptide does not function as separate component.	71
4.1.5	The <i>pre1-1</i> mutation does not suppress the Pre7 truncation phenotype.	72
4.1.6	Genetic evidence for Ump1 independent propeptide functions in proteasome assembly intermediates.	75

4.2 Biochemical analysis of proteasome biogenesis

4.2.1	The Ump1 protein interacts with proteasome assembly intermediates.	77
4.2.2	The Ump1 protein interacts with proteasomal β -type subunits <i>in vitro</i>	79
4.2.3	Epitope tagging of the Pre7 subunit causes impaired cell growth.	80
4.2.4	Polyclonal antibody production against the Pre7 subunit.	81
4.2.5	Precursor subunits accumulate in Pre7 truncation mutants.	82

4.2.6	Pre7 mutant strains are impaired in the proteasome assembly.	83
4.2.7	The Pre7 mutant strains show reduced proteasomal activity.	88
4.2.8	Proteasome maturation is diminished in mutant Pre7 strains.	90
4.2.9	Visualization of proteasome assembly intermediates accumulating in Pre7 mutant strains.	92
4.2.10	The effect of Ump1 induction in Pre7 truncation mutants.	94
4.3	Structure-based mutation analysis of the β6/Pre7 subunit	
4.3.1	The Pre7 propeptide remnant adheres to the Pre7 surface via a hydrophobic pocket.	104
4.3.2	Conserved amino acids in the Pre7 subunit are essential for proteasome biogenesis.	105
5	Discussion	
5.1	The role of propeptides in proteasome biogenesis.	109
5.2	Additional requirements for proteasome assembly.	112
5.3	Defects in proteasome function up-regulate the precursor expression.	114
5.4	Complete maturation of 20S proteasomes requires the function of propeptides and accurate particle assembly.	115
5.5	Proteasome assembly occurs via half-proteasome.	118
5.6	Induction of Ump1 in Pre7 truncation mutants causes defects in the proteasome assembly process.	119
5.7	Genetic dissection of structural requirements in Pre7 for proper Ump1 function.	120
6	A model of the yeast 20S proteasome biogenesis.	123
7	References.	127
	Acknowledgments.	139
	Curriculum vitae.	140
	Declaration.	141

Abbreviations

Amp	ampicillin
ATP	adenosine triphosphate
~	approximately
bp	base pairs
BSA	bovine serum albumin
X-Gal	5-bromo-4-chloro-3-indoxyl- β -D-galactosid
CEN	centromeric
Δ	deletion
DTT	dithiotreitol
$^{\circ}$ C	degree celsius
DMF	dimethylformamid
DMSO	dimethylsulfoxid
<i>E. coli</i>	<i>Escherichia coli</i>
Et-OH	ethanol
EDTA	ethylenediamine-tetraacetic acid
EGTA	ethylene glycol-bis-[β -aminoethyl ether]-N,N,N',N'-tetraacetic acid
5-FOA	5-Fluoroorotic acid
G418	geneticin disulfate
Gal	galactose
Glu	glucose
GST	glutathione S-transferase
H	helix
HIS	histidine
hrs	hours
HCl	hydrochloric acid
HEPES	N-[2-Hydroxyethyl] piperazine-N'-[2-ethanesulfonic acid]
HRPO	peroxidase conjugate
IPTG	isopropyl- β -D-thiogalactosid
Kan	kanamycin
KDa	kilodalton
(μ ,m) l	(micro, milli) liter
(m, μ ,p) g	(milli, micro, pico) gram
LEU	leucin
L	loop
LB	luria broth
β -ME	2-mercapto ethanol
MgCl ₂	magnesium chloride
min	minutes
mA	milli ampere
MW	molecular weight
MCS	multi cloning site
nm	nanometer
Native-PAGE	native polyacrylamide gel electrophoresis
OD	optical density
ORF	open reading frame
%	percentage

PGPH	peptidylglutamyl peptide hydrolyzing
PMSF	phenylmethylsulfonyl fluoride
PAGE	polyacrylamide gel electrophoresis
PCR	polymerase chain reaction
PBS	phosphate buffered saline
KH_2PO_4	potassium phosphate monobasic
KOAc	potassium acetate
rpm	rotations per minute
RT	room temperature
RNAse	ribonuclease
<i>S. cerevisiae</i>	<i>Saccharomyces cerevisiae</i>
S	sedimentation
NaCl	sodium chloride
SDS	sodium dodecyl sulfate
NaOH	sodium hydroxide
Na_2HPO_4	sodium phosphate dibasic
NaN_3	sodium azide
SC	synthetic complete (minimal growth medium)
SR	synthetic complete (minimal growth medium with raffinose)
TCA	trichloro acetic acid
TEMED	N,N,N',N'-tetramethylethylenediamin
Tris	tris [hydroxymethyl] aminomethane (Trizma ® base)
TBS	tris buffer saline
T-X100	Triton X 100
T-20	Tween 20
UBI	ubiquitin
U	units
URA	uracil
WT	wild type
YPD	yeast-peptone-dextrose (rich growth medium)

Zusammenfassung

Regulierte Proteolyse von intrazellulären Proteinen findet in Eukaryonten über eine spezialisierte enzymatische Maschinerie statt, das Ubiquitin-Proteasomen-System. Dabei werden Proteine spezifisch erkannt und für ihren Abbau durch Anknüpfen von Poly-Ubiquitinketten markiert, bevor sie durch das 26S Proteasom zerlegt werden. Das 20S Proteasom ist die katalytische Kerneinheit des 26S Proteasoms und setzt sich aus zwei Sätzen von jeweils 7 verschiedenen α - und β -Typ Untereinheiten zusammen, die einen fassförmigen Komplex aufbauen. Der Zusammenbau und die Reifung des eukaryontischen 20S Proteasoms ist ein mehrstufiger Prozess, bei dem sich zunächst freie α - und β -Typ Untereinheiten zu dem vollständigen, aber noch inaktiven Komplex zusammenschlagern. Die Aktivierung geschieht abschließend mit der Überführung von drei der β -Typ Untereinheiten in ihre reife Form durch die autokatalytische Entfernung von N-terminalen Propeptiden, was zur Freilegung von katalytischen Threoninen an deren N-Termini führt. Der Beitrag der Propeptide dieser aktiven β -Typ Untereinheiten zur Assemblierung der Partikel reicht in der Bäckerhefe von absoluter Notwendigkeit bis zur Entbehrlichkeit. Weiterhin werden drei der vier nicht aktiven β -Typ Untereinheiten ebenfalls mit Propeptid synthetisiert, welches entweder unprozessiert bleibt ($\beta 3$ /Pup3) oder nur partiell entfernt wird ($\beta 7$ /pre4 und $\beta 6$ /Pre7), wofür aktivierte benachbarte β -Typ Untereinheiten verantwortlich sind. Die resultierenden kurzen N-terminalen Verlängerungen von 8-9 Resten befinden sich in der Kristallstruktur der 20S Proteasoms von Hefe in einer gestreckten Konformation und reichen jeweils bis zu den Verengungen, welche die zentrale proteolytische Kammer von den Vorkammern abgrenzen.

In dieser Arbeit werden mehrere Fragestellungen angegangen hinsichtlich der Funktion der während der Proteasomenevolution erhalten gebliebenen Propeptide von inaktiven Untereinheiten. Die Arbeit konzentriert sich besonders auf die Struktur und Funktion des $\beta 6$ /Pre7 Propeptids und dessen Beitrag zur Proteasomenbiogenese, da es essentiell für die Lebensfähigkeit von Hefe ist, im Gegensatz zu dem $\beta 3$ /Pup3 Propeptid, welches für die Proteasomenfunktion entbehrlich ist, wie auch bereits für das $\beta 7$ /Pre4 Propeptid beschrieben. Der Teil des $\beta 6$ /Pre7 Propeptids, der durch die benachbarte aktive

β -Typ Untereinheit $\beta 2$ /Pup1 abgeschnitten wird, ist nicht essentiell, doch die 9 Reste, die im reifen Proteasom zu finden sind, sind unentbehrlich für dessen Funktion. Die Analyse von schrittweisen Verkürzungen des Propeptid-Überbleibels ergab, dass die 6 am meisten C-terminal gelegenen Aminosäuren ausreichend fürs Überleben der Zelle sind, jedoch ist das Zellwachstum beträchtlich verlangsamt, wenn dieses Stück von 9 auf 6 Reste verkürzt wird.

Überraschenderweise ist die Notwendigkeit dieses Propeptid-Überbleibels nur in Anwesenheit des Proteasomenassemblierungsfaktors Ump1 gegeben. Von Ump1 war bekannt, dass es die Dimerisierung von zwei Halbproteasomen-Vorläufern erleichtert und außerdem die Proteasomenreifung unterstützt. Die Fraktionierung von Vorläufer- und reifen Proteasomenformen durch Gel-Filtration sowie "pulse-chase"-Analysen deckten auf, dass im *UMP1* Wildtyp-Stammhintergrund die Pre7-Mutante mit einem Propeptid-Überbleibsel von 6 Resten starke Defekte bei der Partikelassemblierung und dessen Reifung aufweist. Im Gegensatz dazu lassen sich in *ump1* Δ Zellen solche Störungen des Zusammenbaus und der Reifung bereits in Gegenwart von Wildtyp-Pre7 feststellen, und diese Defekte werden durch Verkürzungen der Pre7 Propeptid-Restregion nicht weiter verstärkt. In ähnlicher Weise reduzieren sich die proteasomalen Peptidase-Aktivitäten bei Anwesenheit von Ump1 schrittweise mit zunehmender Verkürzung des Pre7 Propeptid-Rests, wogegen sich die Aktivitätsprofile im *ump1* Δ Stammhintergrund nicht verändern.

Durch nicht-denaturierende Gel-Elektrophorese wurde ersichtlich, dass Verkürzungen des Pre7 Propeptid-Überbleibels von bis zu 3 Resten mit der Dimerisierung von zwei Halb-Proteasomen zu Pre-Holoproteasomen interferieren und somit zur Anhäufung dieser Assemblierungsprodukte führen, jedoch wiederum nur in Anwesenheit von Ump1. Das Abbruchstadium in der Proteasomenassemblierung in solchen Stämmen, die nur in der Abwesenheit von Ump1 lebensfähig sind, wurde durch Expression von Ump1 von einem induzierbaren Promoter analysiert. Wie erwartet, inhibiert das Erscheinen von Ump1 die Zellvermehrung nach wenigen Teilungen vollständig in Zellen, die Pre7 Propeptid-Reste mit weniger als 6 Resten enthielten. Die Analyse dieser Zellen zeigte, dass der Prozess der Proteasomenassemblierung auf der Stufe von Ump1 enthaltenden Halb-Proteasomen-Assemblierungsintermediaten blockiert ist. Des weiteren war die Interaktion von Ump1 auf Halb-Proteasomen beschränkt, während in Stämmen mit

Wildtyp-Pre7 Ump1 in einem wahrscheinlich früheren Assemblierungsintermediat zu finden war. Somit könnte die Bindung von Ump1 an frühe Assemblierungsstadien den Dimerisierungsprozess effizienter vorantreiben als seine Interaktion mit den vollständig assemblierten Halb-Proteasomen. Die Analyse von in-vitro Interaktionen und GST-„pull-down“-Experimente deuteten darüber hinaus an, dass die Bildung von Halb-Proteasomen mit dem Einbau von Ump1 einhergeht und dass dessen Assoziierung von den spät eingeführten Untereinheiten Pre2, Pre4 und Pre7 abhängig ist, sehr wahrscheinlich vermittelt durch deren Propeptide.

Versuche zur Austauschbarkeit der Pre7 Propeptid-Restregion zeigten, dass deren Funktion spezifisch von seiner Aminosäuresequenz abhängt. Ein Sequenzvergleich der Primärstrukturen von $\beta 6$ Orthologen aus verschiedenen Arten erhellte, dass ein Prolin an Position -6 und ein Tyrosin an Position -5 in der Evolution streng konserviert wurden. Zusätzlich dazu ließ sich in allen bekannten $\beta 6$ -Untereinheiten eine konservierte Abfolge von hydrophoben Aminosäuren feststellen, die eine hydrophobe Tasche ausbilden und das Propeptid im gereiften Proteasom binden. Das Tyrosin an Position -5 stellte sich als bedeutsam für die Funktion des Pre7 Propetid-Überbleibels heraus, denn sein Austausch durch Alanin war in *UMPI* Wildtyp-Zellen letal. Die aromatische Seitenkette dieses Tyrosins wird benötigt, um den Propeptid-Rest durch Interaktionen mit der hydrophoben Tasche an der Oberfläche der Pre7-Untereinheit zu fixieren, während die Hydroxylgruppe entbehrlich ist. Zwei Phenylalanin-Reste in der hydrophoben Tasche wurde ebenso als essentiell identifiziert, was impliziert, dass diese Reste entweder wichtig sind, das Propetid in bestimmten Stadien des Assemblierungsprozesses zu fixieren oder für die strukturelle Integrität der Pre7-Untereinheit benötigt werden. Bemerkenswerterweise war die durch Mutationen in der hydrophoben Tasche verursachte Letalität wiederum an die Anwesenheit von Ump1 gekoppelt. Vielleicht führt die Exponierung der hydrophoben Oberfläche, bedingt durch das Fehlen des Pre7 Propeptids oder durch Verlust von dessen Bindefähigkeit, zu unzulässigen Interaktionen des Ump1 Proteins mit dieser Region, was weitere Assemblierungs- und Reifungsschritte ausschließen könnte. Obwohl das Propeptid der Pre7-Untereinheit kritisch dafür zu sein scheint, solche unerwünschten Interaktionen von Ump1 mit der hydrophoben Oberfläche zu verhindern, scheint eine primäre Rolle darin zu bestehen, die strukturelle Integrität zu bewahren, welche eine

Voraussetzung für das Fortschreiten des Assemblierungs- und Reifungsprozesses ist. Dies wird durch die Tatsache impliziert, dass der Austausch des Tyrosins in der Propeptid-Region in Kombination mit Austauschungen irgendeiner der hydrophoben Aminosäuren in der hydrophoben Tasche gravierende Wachstumsdefekte sogar in *ump1Δ*-Zellen verursacht und dass das Ersetzen aller konservierten Reste der Tasche durch Alanine letal ist.

Zusammengefasst belegt diese Arbeit eine kritische Rolle des Pre7 Propeptids in der Assemblierung und der Reifung des 20S Proteasoms in Hefe. Die konservierten Reste im Propeptid und in der hydrophoben Tasche der Pre7-Untereinheit sind gemeinsam notwendig für eine korrekte Faltung zu einer Tertiärstruktur, die einen effizienten Einbau der Untereinheit ins Proteasom gestattet. Darüber hinaus wird das Propeptid von Pre7 spezifisch für das Funktionieren des Proteasomenassemblierungs- und Reifungsfaktors Ump1 während der Proteasomenbiogenese benötigt. Weiterhin könnte es an Interaktionen mit anderen proteasomalen Proteinen oder an der Übertragung struktureller Veränderungen in proteasomalen Assemblierungsintermediaten beteiligt sein.

Summary

In eukaryotes, the regulated proteolysis of intracellular proteins occurs through a specialized enzymatic machinery, the ubiquitin-proteasome system. Here proteins are specifically recognized and marked for degradation by addition of poly-ubiquitin chains before being degraded by the 26S proteasome. The 20S proteasome is the catalytic core of the 26S proteasome, composed of two copies of each 7 different α - and β -type subunits forming a barrel-shaped complex. Assembly and maturation of the eukaryotic 20S proteasome is a multi-step process, in which the free α - and β -type subunits are first assembled into the complete but still inactive complex. Final activation occurs after conversion of three of the β -type subunits into their mature form by autocatalytic removal of N-terminal propeptides leading to the exposure of catalytic threonines at their N-termini. The contribution of the propeptides of these active β -type subunits to particle assembly in baker's yeast ranges from absolute necessity to dispensability. In addition, of the four inactive β -type subunits three are also synthesized with a propeptide which stays either unprocessed (β 3/Pup3) or is only partially removed (β 7/Pre4 and β 6/Pre7) by the action of the activated neighbour β -type subunits. The resulting short N-terminal extensions of 8-9 residues are found in the crystal structure of the yeast 20S proteasome in an extended conformation each reaching the restrictions separating the central proteolytic chamber from the antechambers.

In this work multiple questions are addressed regarding the function of propeptides of the inactive subunits that have been preserved during proteasome evolution. The work focusses especially on the structure and function of the β 6/Pre7 propeptide and its contribution to proteasome biogenesis, because it is essential for yeast cell viability in contrast to the β 3/Pup3 propeptide that is dispensable for proteasome function, like already reported for the β 7/Pre4 propeptide. The region in the β 6/Pre7 propeptide that is cleaved off by the neighboring active β -type subunit β 2/Pup1 is not essential, but the remaining 9 residues found in the mature proteasome are indispensable for its function. Stepwise truncation analysis in the Pre7 propeptide remnant region revealed that the six most C-terminal amino acids are sufficient for cell survival, but cell growth is considerably retarded if this piece is shortened from 9 to 6 residues. Surprisingly, the

need for this propeptide remnant is restricted to the presence of the proteasome assembly factor Ump1. Ump1 was shown to enhance the dimerization of two half-proteasome precursor complexes and in addition to promote proteasome maturation. Fractionation of precursor and mature proteasome species by gel-filtration analysis as well as pulse-chase analysis elucidated that in a *UMPI* wild-type strain background the Pre7 mutant bearing a propeptide remnant with 6 residues has severe defects in particle assembly and maturation. In contrast to this, in *ump1Δ* cells such perturbation in assembly and maturation was found even in the presence of wild-type Pre7 and these defects were not enhanced by the truncations in the Pre7 propeptide region. Similarly, the proteasomal peptidase activities were reduced gradually along with stepwise truncations in the Pre7 propeptide region in the presence of Ump1, but the activity profiles were not altered in the *ump1Δ* strain background.

As seen in non-denaturing gel electrophoresis, truncations in the Pre7 propeptide remnant region by up to 3 residues interfered with the dimerization of two half-proteasomes to the pre-holoproteasome and thus led to accumulation of these assembly products, but again only in the presence of Ump1. The obstruction stage in the proteasome assembly in those strains that are viable only in the absence of Ump1 was analysed by expressing the Ump1 protein from an inducible promoter. As expected, in cells carrying a Pre7 propeptide remnant shorter than 6 residues, the appearance of Ump1 completely inhibited their proliferation after few cell divisions. Analysis of these cells revealed that the proteasome assembly process is blocked at the state of half-proteasome assembly intermediates containing Ump1. Furthermore, interaction of Ump1 was restricted to the half-proteasome, whereas in strains carrying wild-type Pre7 Ump1 was found in a putative earlier assembly intermediate. Thus, the binding of Ump1 to early assembly stages might trigger the dimerization process more efficiently than its interaction with completely assembled half-proteasomes. *In vitro* interaction and GST-pull down analysis additionally indicated that formation of half-proteasomes is coupled with incorporation of Ump1 and that its association depends on the late incorporating subunits Pre2, Pre4 and Pre7, most likely mediated by their propeptides.

Replacement analysis of the Pre7 propeptide remnant region showed that its function specifically depends on its amino acid sequence. Sequence comparison of the primary structure of $\beta 6$ orthologues from different species enlightened that a proline at

position -6 and a tyrosine at -5 have been absolutely conserved during evolution. In addition to this, a stretch of hydrophobic amino acids that forms a hydrophobic pocket and binds the propeptide in the mature proteasome was also found to be conserved in all known $\beta 6$ subunits. The tyrosine at position -5 turned out to be crucial for the function of the Pre7 propeptide remnant, since its exchange with alanine was lethal in *UMP1* wild-type cells. The aromatic side chain of this tyrosine is required to fix the propeptide remnant on the Pre7 subunit surface by interacting with the hydrophobic pocket, whereas the hydroxyl group is dispensable. Two phenylalanines in the hydrophobic pocket were also found to be essential, suggesting that these residues are either crucial to fix the propeptide at any stage of the assembly process or required for the structural integrity of the Pre7 subunit. Remarkably, the lethality caused by the mutations in the hydrophobic pocket was again coupled to the presence of the Ump1 protein. Probably, the exposure of this hydrophobic surface due to the absence of the Pre7 propeptide or due to loss of its ability to bind it might lead to unfavorable interactions of the Ump1 protein with this area and so might preclude further assembly and maturation steps. Although the propeptide of the Pre7 subunit seems to be crucial to avoid such unfavorable interactions of Ump1 with the hydrophobic surface, a primary role might lie in maintaining a structural integrity, which is a prerequisite for the proceeding of the assembly and maturation process. This is implicated by the fact that replacing the tyrosine in the propeptide region in combination with replacements of any of the hydrophobic amino acids in the hydrophobic pocket causes severe growth defects even in *ump1 Δ* cells and that exchanging all conserved residues in the pocket by alanines is lethal.

Taken together this work establishes a critical role of Pre7 propeptide in the yeast 20S proteasome assembly and in its maturation. The conserved residues found in the propeptide and in the hydrophobic pocket of the Pre7 subunit are concertedly necessary for proper folding into a tertiary structure that allows efficient incorporation of the subunit into the proteasome. Moreover, the propeptide of Pre7 is specifically required for the function of the proteasome assembly and maturation factor Ump1 during proteasome biogenesis. In addition, it might be involved in interactions with other proteasomal proteins or in the transmission of structural alterations in the proteasomal assembly intermediates.

1 Introduction

1.1 Cellular Proteolysis

Life from molecule to species manifests pursuing aspects: creation, maintenance, and destruction or re-utilization. As cellular structures are continually rebuilt, the homeostatic levels must be maintained by a delicate balance between anabolic and catabolic pathways, which is important for cell survival. Misfolded and malfunctioning proteins, prone to aggregation, must be scavenged and degraded. In addition to such “house-keeping” functions, protein degradation has a key regulatory role in many cellular pathways and must therefore be subject to spatial and temporal control.

Studies in cellular biochemistry during the past several decades have provided a refined understanding of the nature of protein synthesis, its constituents, enzymatic reactions and regulatory mechanisms. Little more than a decade ago, the lysosomes, with their substantial complement of broad-specificity proteases, were considered the locus of cellular protein degradation by relatively non-selective bulk processes (Bohley and Seglen, 1992; Harris, 1968; Knop et al., 1993).

Since lysosomal degradation of intracellular proteins occurs mostly under stress conditions such as starvation, for researchers it was hard to imagine how such highly unspecific terminal scavenger process could be responsible for selective protein degradation, when they came to know that the proteolysis of cellular proteins is highly complex and tightly regulated during cell life and death. In contrast to the lysosome the “nonlysosomal system” is responsible for the remarkably selective turnover of intracellular proteins that occurs under basal metabolic and in stress conditions (Larsen, 2002). The most important nonlysosomal proteolytic system is the ubiquitin-mediated proteolytic system, in which soluble nuclear and cytoplasmic proteins are specifically recognized and finally removed by the proteasome.

1.2 The Ubiquitin-Proteasome System

1.2.1 A retrospective on the proteasome

The first description of a “cylinder-shaped” complex dates back to the late sixties. Since its first sighting in erythrocytes (Harris, 1968) and other cells (Kleinschmidt et al.,

1983; Narayan and Rounds, 1973; Shelton et al., 1970; Smulson, 1974), it has accumulated a variety of names such as *cylindrin* (Harris, 1988), *prosome* (Schmid et al., 1984), *multicatalytic protease complex* (Orlowski and Wilk, 1988), *alkaline protease* (Hase et al., 1980), *ingensin* (Ishiura and Sugita, 1986), *low-molecular weight protein* (Monaco and McDevitt, 1984) and *macropain* (McGuire and DeMartino, 1986) and almost as many functions were proposed.

In recognition of its only established function, the “multicatalytic protease complex” was named “proteasome”, a designation that prevailed from the late eighties on (Arrigo et al., 1988). Two forms were distinguished by their sedimentation constant as 26S proteasome and 20S proteasome (Driscoll and Goldberg, 1990; Hough et al., 1987). The 20S proteinase was found to be a component of the ATP-dependent 26S proteinase (Eytan et al., 1989)

Identification of 20S proteasomes in the archaeobacterium *Thermoplasma acidophilum* (Dahlmann et al., 1989) and electron microscopic studies (Grziwa et al., 1991; Puhler et al., 1992) paved the way to elucidate the structural details of the 20S particle (Zwickl et al., 1992). The crystal structure of the *Thermoplasma* 20S proteasome provided detailed insights into the architecture and catalytic mechanism of the particle (Löwe et al., 1995). This barrel-shaped complex is constructed by 14 copies of two different subunits, namely alpha and beta, in the two outer and the two inner rings, respectively (Löwe et al., 1995). The catalytic center in the β -subunits was identified by co-crystallization of a tripeptide aldehyde inhibitor and site-directed mutagenic studies (Seemüller et al., 1995a). A major insight concerning the function of this enzyme complex came from genetic and biochemical studies in yeast (Heinemeyer et al., 1991). The following X-ray structure analysis of the more complex yeast and bovine 20S proteasome certainly represents the largest breakthrough towards understanding structure-function relationships of the eukaryotic core particle (Groll et al., 1997; Heinemeyer et al., 1997; Unno et al., 2002b; Voges et al., 1999).

1.2.2 The ubiquitin-conjugating system

The ubiquitin-mediated proteolytic system is the major mechanism for regulated degradation of intracellular proteins in eukaryotes. Short-lived proteins such as cell cycle and growth regulators, components of signal transduction pathways, enzymes of house

keeping and cell specific metabolic pathways, immune and inflammatory regulators, mutated and denatured or misfolded proteins from the cytosol, nucleus and endoplasmic reticulum, are specifically recognized and removed efficiently (Etlinger, 1977; Ciechanover et al., 2000; Ciechanover, 2003; Glickman, 2002; Hilt and Wolf, 2004). The system is also involved in generation of peptides destined for presentation by class I molecules of the major histocompatibility complex (Rock et al., 1994). In this capacity, the system is involved in the regulation of many basic cellular processes besides playing a key role in cellular quality control and defense mechanisms.

The ubiquitin-conjugation system is a specialized recognition apparatus that operates functionally and possibly spatially detached from the ubiquitin-conjugate-specific protease, the proteasome (Jentsch and Schlenker, 1995; Glickman, 2004). This system has been well characterized in the recent decade (Ciechanover, 1998a). It consists of several essentially required components. One of these has been identified as ubiquitin, an abundant, 76-residue polypeptide that is found in all eukaryotic cells. The C-terminal glycine of ubiquitin is activated by the ubiquitin activating enzyme E1 in an ATP-requiring reaction to generate a high-energy thiol ester intermediate (E1-S~ubiquitin). This activated ubiquitin is then transferred to ubiquitin-conjugating enzymes E2 or ubiquitin-carrier proteins, again yielding a high-energy thiol ester intermediate (E2-S~ubiquitin), and finally to the substrate that is specifically bound to an ubiquitin protein ligase E3 (see Fig 1). Alternatively, ubiquitin is transferred from the E2 enzyme to the active site Cys residue on another type of E3 enzyme to generate a third high-energy thiol ester intermediate (E3-S~ubiquitin) before its transfer to the ligase-bound substrate. Covalent attachment of ubiquitin to the ϵ -amino group of Lys residues in the substrate via an isopeptide bond is thus directly catalyzed or mediated by E3 enzymes (Glickman, 2002; Hershko, 1998). Subsequent addition of activated ubiquitin moieties to internal Lys residues in the previously conjugated ubiquitin molecule leads to synthesis of a poly-ubiquitin chain on the substrate. Ubiquitin chains of four or more ubiquitin molecules linked through lysine 48 (K48) serve as a proteasome targeting signal. The poly-ubiquitinated substrate protein is then recognized and degraded by the 26S proteasome complex, whereby free and re-utilizable ubiquitin is released (Ciechanover, 1998b).

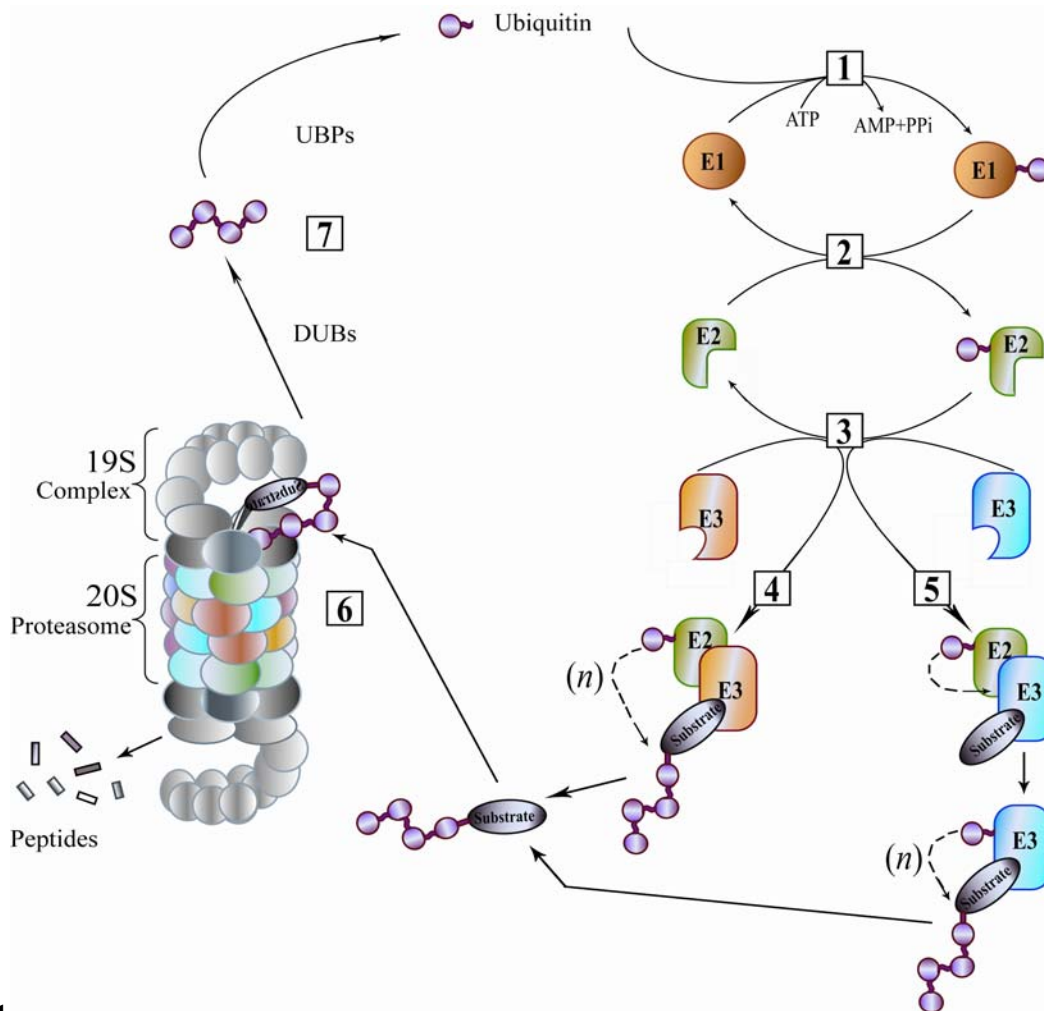


Fig1
The Ubiquitin-proteasome proteolytic pathway

The reactions of the pathway are represented in seven steps. 1) Activation of ubiquitin by an ubiquitin-activating enzyme (E1) and ATP. 2) Transfer of activated ubiquitin from E1 to a member of the ubiquitin-carrier or conjugating enzymes (E2). 3) Formation of a E2-E3 complex by binding of E2 either to a RING Finger¹ E3 (shown in yellow) or a HECT domain² type E3 (shown in blue), which might not or might have substrate already bound via a defined recognition motif. 4) Direct transfer of activated ubiquitin from E2 to a lysine of the E3-bound substrate via an isopeptide bond occurs in substrates targeted by RING finger E3s. Multiple (n) cycles of ubiquitin conjugation to previously bound ubiquitin moieties on the target substrate leads to synthesis of a poly-ubiquitin chain. 5) As in step 4, but the activated ubiquitin moiety is first transferred from the E2 to the E3, yielding a high-energy thiol ester intermediate, before its conjugation to the E3-bound substrate or to the previously conjugated ubiquitin moiety of the substrate. 6) Binding of the poly-ubiquitinated substrate to the ubiquitin receptor subunit in the 19S complex of the 26S proteasome and degradation of the substrate to short peptides by the 20S complex with release of short peptides. 7) Recycling of ubiquitin via the activity of the deubiquitinating enzymes (DUBs) or ubiquitin hydrolases and ubiquitin-specific processing proteases (UBPs).

1. RING finger

Defined structurally by two interleaved metal-coordinating sites. The consensus sequence for the RING finger is: CX2CX(9-39)CX(1-3)HX(2-3)C/HX2CX(4-48)CX2C. The cysteines and histidines represent metal-binding sites with the first, second, fifth and sixth of these binding one zinc ion and the third, fourth seventh and eighth binding the second.

2. HECT domain

Stands for homologous to E6-AP carboxyl terminus. The HECT domain is a ~ 350 - amino acid domain, highly conserved among a family of E3 enzymes.

1.2.3 The proteasome and its regulatory complexes

Initially energy dependent 26S proteasomes were found by electron micrographic studies as an elongated structure (~ 45 nm long) consisting of a central 20S complex capped at either one or both ends by 19S complexes facing in opposite directions (see Fig1) (Peters et al., 1993; Yoshimura et al., 1993). The 19S complex or regulatory particle is also referred to as PA700 in mammals, and as μ particle in *Drosophila melanogaster*. Each 19S complex contains at least seventeen different subunits and is assembled from two main subcomplexes, a base that contains six ATPases plus two non-ATPase subunits and abuts on the 20S proteasome, and a lid subcomplex that sits on the top of the base (Glickman et al., 1998a; Glickman et al., 1998b). An 11S activator complex also called PA26 or PA28 can alternatively bind to the 20S core. It is found in species ranging from *Trypanosoma* to mammals and is implicated in antigen processing. Another activator complex named PA200 exists in mammals and has been implicated in DNA excision repair (Ustrell et al., 2002). The related Blm3 protein complex in yeast may regulate proteasome maturation. The presence of Blm3 seems to protect nascent 20S proteasomes from premature assembly with regulatory 19S particles (Fehlker et al., 2003).

The proteolytically active sites of the proteasome are found in the core 20S particle (see Fig 2), where they are sequestered within the lumen of this cylindrical complex (Groll et al., 1997; Löwe et al., 1995). Proteins apparently enter the lumen of the core particle through channels located at each end of the cylinder. The binding of the regulatory particle to the outer port of the core particle implies that the 19S particle initiates recognition, unfolding, de-ubiquitylation and translocation of the substrate into the lumen of the core particle, where the substrate chains are degraded into oligopeptides (Baumeister et al., 1998; Larsen, 1997).

1.3 The 20S core particle

1.3.1 Subunit comparison of 20S proteasome

Proteasomes are found in all three domains of life: archaea, bacteria, and eukarya. This bears testimony to an old evolutionary principle. All subunits have a comparable tertiary fold. Sequence identities among subunits within a species are usually ~ 20-50 %, but orthologous subunits from different species often have identities in the 55-95 % range.

Although the molecular architecture of proteasomes isolated from all types of species is strikingly similar, their subunit complexity is different (Baumeister et al., 1998).

Proteasomes are ubiquitously present in archaeons, and are composed of only two types of subunits, α and β (Löwe et al., 1995). In eubacteria, the occurrence of proteasomes is possibly restricted to actinomycetales. Here, the biochemical and structural studies on the proteasome from *Rhodococcus* confirmed the existence of two different α - and two different β -type subunits (Tamura et al., 1995). In some bacteria, the chambered proteases HslV and ClpP are composed of two rings built from one type of subunit with $\sim 20\%$ sequence similarity to the proteasomal β -type subunits (Missiakas et al., 1996; Rohrwild et al., 1996; Wang and Flanagan, 1997).

The eukaryotic proteasomes in comparison to those in prokaryotes are characterized by an increased subunit complexity, in which each ring is composed of seven distinct α -type and seven distinct β -type subunits (Arendt and Hochstrasser, 1997; Enenkel et al., 1994; Heinemeyer et al., 1993; Heinemeyer et al., 1994). Of the β -type subunits, only three have active sites (Arendt and Hochstrasser, 1997; Heinemeyer et al., 1997; Seemüller et al., 1996). In mammals three additional γ -interferon inducible genes encode variants of the three active site subunits, called $\beta 1i/LMP2$, $\beta 2i/MECL-1$ and $\beta 5i/LMP7$. Incorporation of these subunits results in the formation of a proteasome subtype termed the immunoproteasome. In *Drosophila melanogaster*, of the 14 subunits of the proteasome, six testis-specific isoforms have been found (Ma et al., 2002). In the plant *Arabidopsis thaliana* 23 genes encode proteasomal subunits. These can be assigned to the established 14 subfamilies of α - and β -subunits by sequence comparison (Fu et al., 1998).

1.3.2 Subunit arrangement in 20S proteasome

The 20S proteasomes of prokaryotes and eukaryotes both contain 28 subunits but differ in complexity, as described above. The prokaryotic proteasomes consist of 14 copies each of 2 distant but related polypeptides, α and β , eukaryotic proteasomes are built of 2 copies of each of 7 distinct α - and β -type subunits. Electron microscopic studies (Grziwa et al., 1991; Puhler et al., 1992) showed that the *Thermoplasma* 20S proteasome forms a cylinder of four ring structures, whereby the two outer rings are composed of seven α -subunits each, and the two inner rings of seven β -subunits each ($\alpha 7\beta 7\beta 7\alpha 7$). The 20S

proteasome architecture of the model eukaryote baker's yeast (Groll et al., 1997) is similar to that of the archaebacterial proteasome, though each subunit occupies a unique location (α 1-7, β 1-7, β 1-7, α 1-7) (see Fig 2). In mammals the additional three γ -interferon inducible β -subunits (β 1i, β 2i and β 5i) can replace the constitutive active subunits (β 1, β 2 and β 5) in their location.

With respect to symmetry, the prokaryotic and eukaryotic enzymes differ considerably in their quaternary structure. The symmetry in the eukaryotic proteasome is reduced due to its increased subunit complexity. In place of the seven-fold symmetry in the *Thermoplasma* proteasome (Löwe et al., 1995), the eukaryotic proteasome has two-fold symmetry (Kopp et al., 1995; Schauer et al., 1993). The available crystal structures of the yeast 20S proteasome (Groll et al., 1997) and more recently of the bovine 20S proteasome (Unno et al., 2002a; Unno et al., 2002b) clarified that the fixed arrangement and topology of the subunits in the complex is conserved from yeast to mammals.

1.3.3 Structural details of the yeast 20S proteasome

20S proteasomes are defined by a characteristic architecture, a barrel-shaped complex, 15 nm in length and 11 nm in diameter, which is traversed from one end to the other by a channel that widens into three internal cavities separated by narrow constrictions (Baumeister et al., 1988; Hegerl et al., 1991). The central cavity, which harbours the active sites, is formed by two face to face-oriented β -rings and is separated by approximately 3 nm wide β -annuli from two antechambers formed by the other side of the β -ring and a α -ring (see Fig 2). The constrictions in the α -subunit rings that give access to the antechambers are narrow (1.3 nm) and are lined with loops of the α -subunits with a highly conserved RPXG motif.

The seminal ascertainment of the molecular structure of the yeast 20S core by X-ray crystallography (Groll et al., 1997) showed that all α - and β -subunits have a common fold characterized by a central five-stranded β -sheet sandwich (S1 through S10), flanked by two helices H1 and H2 on one side and by three helices H3, H4 and H5 on the other side. The helices H1 and H2 mediate the association of α - and β -subunit rings by intercalating in a wedge-like fashion between two subunits of the facing ring; H3 and H4 which are located on the opposite side provide contacts between the β -subunit rings. Differences between the subunits appear in turns, which vary in length by one or two

residues, in long insertions connecting secondary structural elements, and in the N-terminal and especially the C-terminal regions. A unique element in the α -subunit is the H0 helix (residues 20-30) at the highly conserved N-terminal extensions. Access to the antechambers is possible only after reorganization of the N-terminal H0 helices of the α -type subunits. In the so-called latent state of the core particle these N-terminal tails of its α -subunits block substrate access to the lumen. Deletion of this stretch yields crystal structures with an open channel, where all the α -subunit N-termini point upward and surround a pore wide enough to let a peptide chain or even a loop of an extended polypeptide pass through (Groll et al., 2000). Within the α -rings, intimate α -*cis* contacts are made by the intertwined N-terminal segments of subunits α 1/C7, α 2/Y7, α 3/Y13 and α 7/C1 in the centre of the heptameric rings. Thus, the principal rate-limiting step in the hydrolysis of even small peptides by the free core particle is their entry into the lumen. The channel opening is mediated by the ATPases in the regulatory particle when it binds to the core particle to form the 26S proteasome holoenzyme (Kohler et al., 2001).

Instead of this N-terminal H0 helix, most of the β -subunits have prosequences of varying lengths, which are removed in active subunits by autolysis during proteasome maturation, thus rendering the cleft between the central β -sandwich freely accessible from the central cavity. The prosequences of the inactive subunits β 7/Pre4 and β 6/Pre7 is cleaved at position -8 and -9, respectively by the next neighbour active center (Heinemyer et al., 1997). In contrast, β 4/Pre1 and β 3/Pup3 are not processed from their primary translation products.

Additional contacts between subunits are characteristic for yeast and eukaryotic 20S proteasomes in general. Within β -rings, a very specific contact exists between β 2/Pup1 and β 3/Pup3, mediated by the long C-terminal arm of β 2/Pup1, which embraces β 3/Pup3, touching the next-nearest neighbour β 4/Pre1. These unique structural elements are important features that determine the specific subunit interactions within the α - or β -rings and between the rings (α -trans- β and β -trans- β). These interactions target each of the 14 subunits to unique locations within the structure of the proteasome (Groll et al., 1997; Unno et al., 2002b). Differences between the yeast and bovine 20S particle concern especially these extensions and seem to be related to the ability of the mammalian particle to accommodate either the constitutive or the inducible subunit type in a given location.

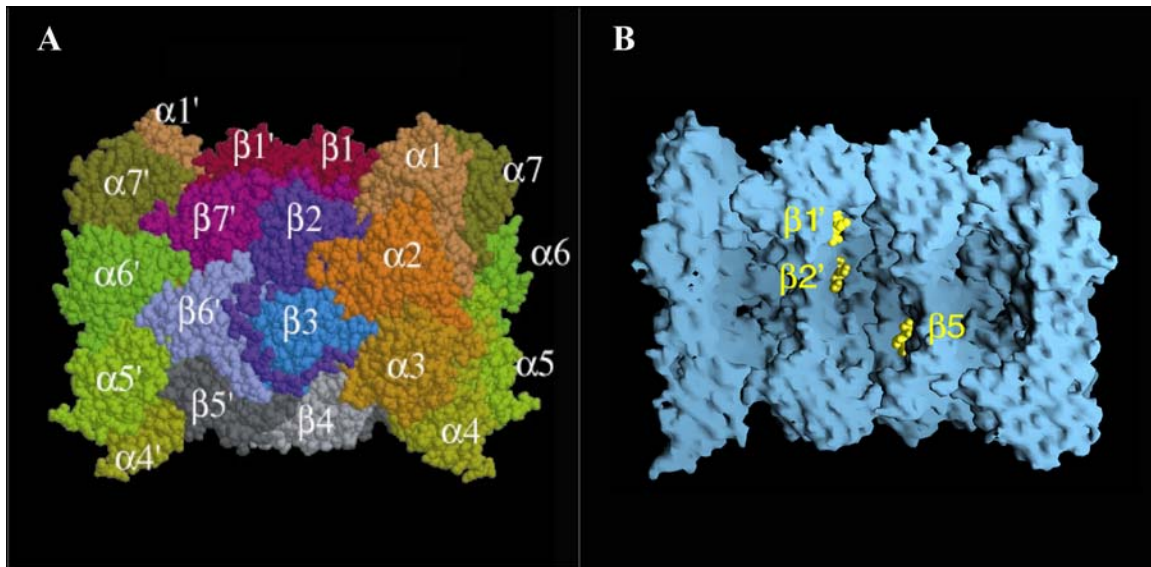


Fig2
Structure of the *Saccharomyces cerevisiae* 20S proteasome

A. Slightly tilt side view in space-filling mode showing the overall subunit arrangement, which results in a C2 symmetry of the particle. All seven α - and β -type subunits are marked and shown in different colors. B. Surface view of the proteasome molecule clipped along the cylinder axis shows the central active chamber (formed by two face to face-oriented β -rings) which is separated from two antechambers (formed by the β - and α -ring) by narrow constrictions. The catalytic Thr1 residues of active subunits in the central active chamber have calpain inhibitor molecules bound (shown as space-filling models in yellow).

1.3.4 Active site formation and catalytic mechanism

The β -type subunits in which the proteolytic activities reside are members of the N-terminal nucleophile (Ntn) hydrolase protein family (Brannigan et al., 1995). Common to this family is the ability to hydrolyze amide bonds, but only proteasomal β -subunits cleave peptide bonds. The precursors of the proteasomal β -subunits are synthesized as proproteins and become active by autolytic processing between Gly-1 and Thr1 in a process that requires the presence of Thr1, Gly-1 and Lys33 (Chen and Hochstrasser, 1996; Schmidtke et al., 1996). This *intra*-subunit autolysis is mediated by Thr1-O γ acting as the nucleophile for the catalytic attack of the carbonyl atom of Gly-1 (Schmidtke et al., 1996). In this autolysis reaction, no N-terminal amino group is available as proton acceptor; a water molecule is predicted to mediate the nucleophile addition of the Thr1-O γ to the carbonyl atom of Gly-1 in the preceding peptide bond (Ditzel et al., 1998b; Groll et al., 1997; Seemüller et al., 1995a). In the mature particle

the N-terminal Thr1 amino acid residue acts as ‘single residue active site’ with its hydroxyl side chain providing the nucleophile and the free amino group acting as the general base for the hydrolysis reaction. This Thr1 is surrounded by the highly conserved residues Asp17 (Glu17 in the *Thermoplasma* β -subunit), Lys33, Ser129, Asp166 and Ser169. These amino acids constitute a charge relay system, which is required to polarize atoms in the participating substrate as well as in the enzyme itself, for instance delocalizing the proton from the Thr1 hydroxyl group to enhance its nucleophilic character.

Only three of the seven distinct eukaryotic β -type subunits (β 1, β 2 and β 5) in a given 20S particle appear to have all the necessary residues required for peptide bond hydrolysis besides an N-terminal propeptide in the precursor that is missing in the matured purified protein (Seemüller et al., 1995b). In contrast the unprocessed or intermediately processed subunits β 3/Pup3 (C10), β 4/Pre1 (C11) and β 6/Pre7 (C5) lack Thr1, and in β 7/Pre4(N3) Lys33 is replaced by Arg.

The eukaryotic β -type subunits provide the active-site nucleophiles for the three distinct catalytic activities of the eukaryotic 20S proteasome conferring “chymotrypsin-like” (cleavage after hydrophobic residues) activity to Pre2/ β 5, “trypsin-like” (cleavage after basic residues) activity to Pup1/ β 2 and the “peptidylglutamyl peptide hydrolyzing (PGPH)” activity to Pre3/ β 1 to the enzyme complex (Bochtler et al., 1997; Chen and Hochstrasser, 1996; Heinemeyer et al., 1997). The cleavage specificities of the enzyme are determined by the sizes and charge distributions of the three different S1 peptide binding pockets, where the substrate is bound and cut at its C-terminal side. In the base of the β 1/Pre3 pocket, Arg45 can balance the charge of acidic P1 residues, favoring the PGPH activity of β 1. The presence of Glu53 at the bottom of its S1 pocket and an acidic side wall contributed by the β 3/Pup3 neighbor subunit favors the trypsin-like activity of β 2/Pup1 and an apolar character in the pocket of β 5/Pre2 explains its chymotrypsin-like peptidase activity.

1.4 The assembly of 20S proteasomes

1.4.1 Preteasome assembly intermediates

In *Thermoplasma acidophilum* formation of seven-membered α -rings is the first step in the proteasome assembly and subsequently, these α -rings function as docking platform for the β -subunit precursors (Baumeister et al., 1998). Possibly, conformational changes

in the β -subunits, induced upon binding to the α -ring, are the prerequisite for the dimerization of the two half-proteasome precursors, which again is needed to trigger processing of the β -subunits (see Fig3) (Seemüller et al., 1996; Zwickl et al., 1994). In contrast, four different subunits ($\alpha 1$, $\alpha 2$, $\beta 1$, and $\beta 2$) of *Rhodococcus* proteasomes assemble into α/β precursor heterodimers that quickly are converted into half-proteasomes (Fig 3) (Zühl et al., 1997a). Upon dimerization of half-proteasomes processing of the β -type precursors occurs, concomitantly yielding fully assembled proteolytically active particles both *in vivo* and *in vitro* (Zühl et al., 1997b).

Up to now, the complex eukaryotic proteasome assembly is not well understood. It requires a highly orchestrated process to ensure proper positioning of each of the 14 different subunits in the particle (Schmidt and Kloetzel, 1997). The assembly properties of recombinant human α -subunits were studied *in vitro*, indicating that at least not all α -subunits contain the information for their correct positioning within a ring of subunits, which argues against a model of a pre-assembled α -ring as an early intermediate. This probably means that α -subunits require additional guidance through their interaction with β -subunits for correct positioning in the ring (Gerards et al., 1998; Gerards et al., 1997). It is interesting that, of the 14 20S proteasome subunits in the yeast *S. cerevisiae*, the only non-essential subunit is $\alpha 3$ /Pre9 (Emori et al., 1991). Surprisingly, this subunit is substituted by another neighboring α -subunit, $\alpha 4$ /Pre6 that takes the position normally occupied by $\alpha 3$ /Pre9, suggesting an advantage for Pre9 over Pre6 incorporation at the $\alpha 3$ position (Velichutina et al., 2004).

The analysis of the mammalian and yeast proteasome assembly gave an insight in the occurrence of distinct and more complex intermediates (Chen and Hochstrasser, 1996; Frentzel et al., 1994; Ramos et al., 1998; Yang et al., 1995). The first detected assembly intermediate or incomplete precursor complex contains all the α -type subunits and a subset of the β -type subunits ($\beta 2$ (Z), $\beta 3$ (C10) and $\beta 4$ (C7)) in a 13S complex (see Fig 3). Subsequent incorporation of the remaining β -type subunits ($\beta 1$ (δ), $\beta 5$ (MB1), $\beta 6$ (C5) and $\beta 7$ (N3)) complete the assembly of 15S half-proteasome precursor complexes which triggers fast dimerization into short-lived processing competent 16S pre-holoproteasomes (Nandi et al., 1997). Processing of $\beta 1/\delta$ or $\beta 1i$ /LMP2 appears in this complex (Schmidtke et al., 1997). The incorporation of the three immuno-subunits also occurs at the precursor level and is a cooperative event (Groettrup et al., 1997; Nandi et al., 1997).

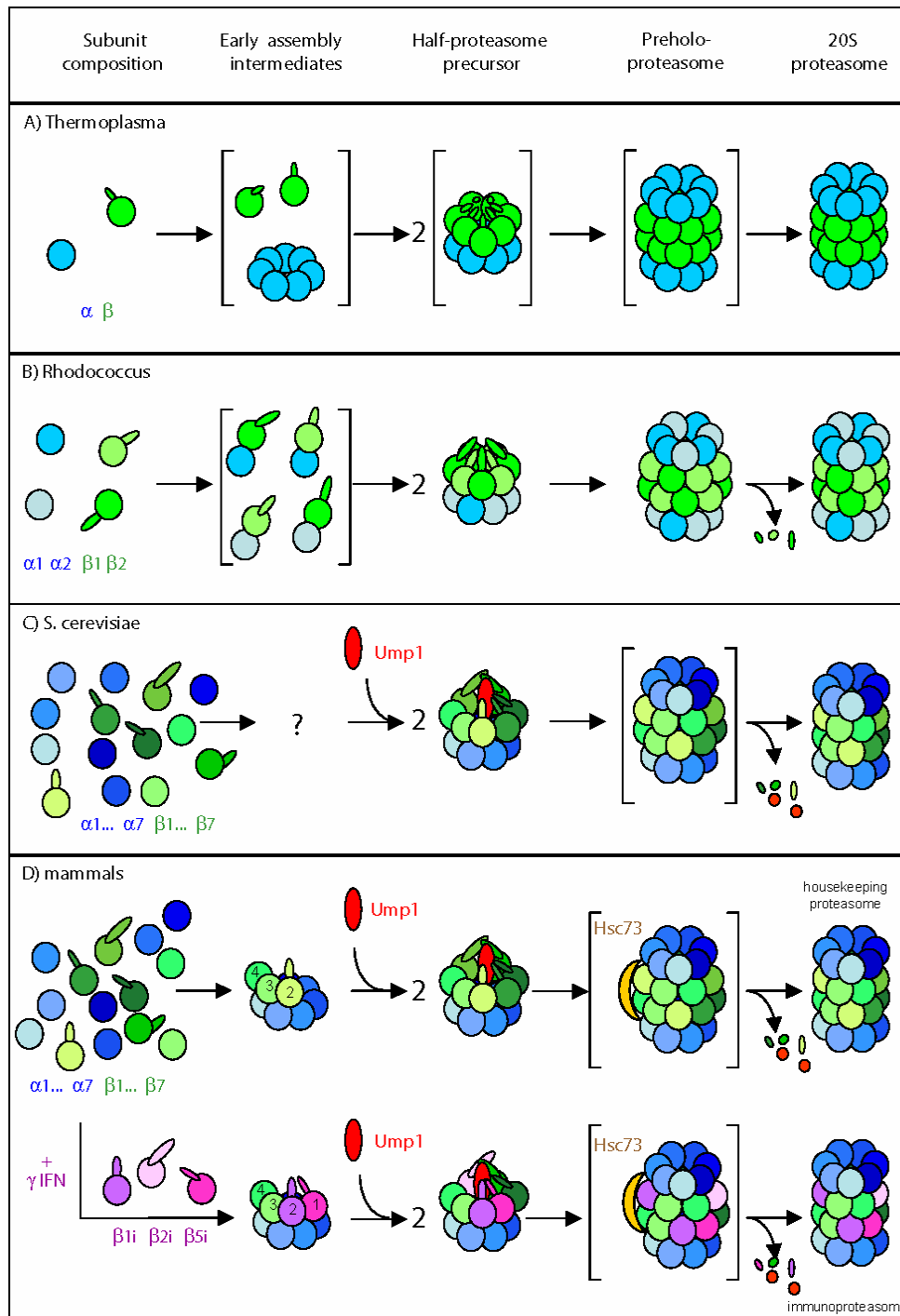


Fig3
Models of the 20S proteasome biogenesis in different organisms
(Picture taken from Heinemeyer et al., 2004)

The models are represented in five stages: free subunits, early assembly intermediates, half-proteasome precursors, pre-holoproteasome and the mature 20S proteasome (see text for details). The intermediates in brackets are too unstable to be detected *in vivo*. Colors: α -subunits, various shades of blue; β -subunits, shades of green; β -subunits induced by γ -interferon (γ -IFN), shades of purple; factor underpinning maturation of the proteasome, Ump1, red; heat shock protein Hsc73; yellow. Respective propeptides are represented as extensions on β -subunits. The assembly pathways of 20S proteasomes from *Thermoplasma*, *Rhodococcus*, *S. cerevisiae* and mammals are represented in column A, B, C and D, respectively (see text for details).

Dimerization of half-proteasome precursor complexes is mediated by multiple interactions between the two β -rings. A long C-terminal extension (37 residues) of β 2/Pup1, wrapping around β 3/Pup3 within the same ring contacts β 6/Pre7 of the opposite ring and thus may contribute to the stability of the assembly intermediate. The most prominent connection between the two β -rings is mediated by the subunit β 7/Pre4. Its C-terminal extension intercalates between the β 1/Pre3 and β 2/Pup1 subunits in the opposite ring and facilitates the formation of 20S particles from two half-proteasome precursor complexes and/or stabilizes mature 20S proteasomes (Ramos et al., 2004).

1.4.2 Accessory proteins in proteasome biogenesis

Proteasome assembly depends on additional factors that probably act as chaperons. They are only transiently associated with the nascent complex and assist the final maturation steps. The chaperone hsc73 is associated with 16S proteasome precursor complexes and may keep assembly intermediates in a partially unfolded state to allow subunit processing, correct folding and incorporation of proteasome subunits (Schmidtke et al., 1997).

Another novel factor that plays a crucial role in proteasome maturation is the dedicated short-lived chaperone termed Ump1 that underpins the maturation of the proteasome in yeast (Ramos et al., 1998). Ump1 is part of the 15S half-proteasome precursor complexes and becomes degraded upon final proteasome maturation. In the absence of Ump1, the formation of 20S structures from two half-proteasome precursors appears to be less efficient and maturation of the precursors of the three active subunits is drastically reduced. During the assembly process, Ump1 was shown to be transiently buried inside the nascent proteasome to coordinate the processing of the β -type subunits (Ramos et al., 1998). Ump1 homologues in mammals were identified and referred to as POMP (proteasome maturation protein) (Witt et al., 2000), protoassemblin (Griffin et al., 2000) or h/mUMP (human / mouse UMP) (Burri et al., 2000).

1.4.3 Propeptides and their requirements in the proteasome assembly

In general, posttranslational removal of a propeptide is a common mechanism for controlling the activity of proteolytic enzymes (Baker et al., 1988). In such a way proteasomal propeptides may exert an inhibitory function by preventing gain of premature proteolytic

activity and a chaperoning function by assisting the correct incorporation-competent folding of the subunit.

Thermoplasma β -subunits are synthesized as a precursor with an N-terminal propeptide of eight amino acid residues, which are autocatalytically cleaved off during proteasome assembly (Zwickl et al., 1992). The minor importance of the short 8 residue β -subunit propeptide was apparent upon its genetic deletion which only slightly reduced the assembly rate and did not affect gain of full activity (Zwickl et al., 1994). In addition, the ability to reconstitute the *Thermoplasma* proteasome after complete dissociation and unfolding of its monomers corroborated the dispensability of the propeptide in subunit folding as well as in the assembly of the particle (Grziwa et al., 1994). In contrast to the *Thermoplasma* proteasome, the long 65 and 58 residue β -subunit propeptides in the *Rhodococcus* proteasome were found to promote both initial folding of the precursor proteins to allow their incorporation into and subsequent dimerization of half-proteasomes. Interestingly this propeptide was found to function *in trans* during the assembly processes (Zühl et al., 1997a).

In eukaryotic proteasomes the N-terminal propeptides of precursors of active site subunits have both common and distinct functions in proteasome biogenesis. Considering the degree of inter-species primary sequence conservation among the propeptides of individual β -subunit subfamily members, a minor role of the short β 1 propeptides, probably restricted to inhibit subunit inactivation (see below), is consistent with the lowest sequence conservation. In contrast, the β 2 prosegments of intermediate length show considerably lesser diversification, including high conservation between the mammalian β 2i and β 2 propeptide sequences, which supports a central, evolutionary conserved role of the β 2 prosequence in promoting 20S proteasome maturation. The long β 5 propeptides are quite uniform in length, but the primary sequence diversification is considerably high, especially between the mammalian β 5 and β 5i propeptides. This might reflect a co-evolution of the prosequence in the eukaryotic β 5 and β 5i branches with different assembly factors.

The short propeptide of the β 1/Pre3 propeptide is dispensable for cell viability, because deletion of this prosequence did not affect the yeast cell growth. However, strains expressing the Pre3 subunit without covalently bound propeptide lost the activity of Pre3. This effect is due to modification of the Thr1 amino group by N- α -acetylation

(Arendt and Hochstrasser, 1999). Thus, propeptide of Pre3 functions as a protector from irreversible modification of the catalytic Thr1 amino group rather than as a temporary inhibitor that prevents premature activity of the subunit before its enclosure in the sealed particle (Jäger et al., 1999).

The β 2/Pup1 propeptide is required for normal viability of yeast cells, since removal of this propeptide retards the proteasome assembly and lowers the trypsin-like peptidase activity (Jäger et al., 1999). Supply of this propeptide *in trans* partially restores growth and the rate of proteasome assembly, but not the peptidase activity, suggesting that one distinct function of the propeptide is exerted only *in cis* apart from other functions *in trans* (Jäger et al., 1999). The nature of the assembly-promoting function of the Pup1 propeptide is not clear. It might involve interactions with assembly factors or with integral proteasome components during the assembly processes.

The propeptide of β 5/Pre2 is essential for proteasome assembly, since its deletion was found to be lethal in yeast cells (Chen and Hochstrasser, 1996). However, this propeptide can function *in trans* like a chaperone in proteasome biosynthesis (Chen and Hochstrasser, 1996; Jäger et al., 1999). Interestingly, the β 5/Pre2 propeptide became dispensable when the proteasome assembly factor Ump1 was missing in the yeast cells (Ramos et al., 1998). This propeptide is required during the assembly process of the 20S particle, where it might function to induce an alteration of conformation or position of Ump1 in the complex (Ramos et al., 1998). In contrast to yeast, the presence of the β 5 propeptide is not essential for incorporation of β 5i/LMP7 into the proteasome complex in human cells suggesting that the β 5i propeptide is dispensable for the association of POMP with proteasome precursors (Burri et al., 2000; Ramos et al., 1998; Witt et al., 2000). Thus, prosequences of other β -subunits may serve as well as binding sites of POMP in the precursor complex.

Therefore, a critical and common function of the propeptides in precursors of active subunits is to protect the N-terminal catalytic threonine residue against N- α -acetylation until the catalytic chamber has been sealed off by formation of the 20S proteasome from two half-complexes. In addition to this, propeptides exert additional functions in the proteasome assembly (Arendt and Hochstrasser, 1999; Jäger et al., 1999). One might also anticipate a targeting function of the propeptide to ensure the correct localization of the given subunit in the complex, and finally, interactions of propeptides

with other subunits or components aiding the eukaryotic core particle assembly might promote certain transformations at the maturation stages, which are still obscure.

In contrast to the active subunits, three of the four inactive subunits ($\beta 6$ /Pre7, $\beta 7$ /Pre4 and $\beta 3$ /Pup3) are also synthesized with prosegments of variable lengths and of low sequence conservation among species. These N-terminal propeptides that in case of $\beta 6$ and $\beta 7$ are partially processed by a neighboring active site after proteasome maturation are not functionally characterized (Groll et al., 1997; Heinemeyer et al., 1997). Their functions and requirement in the 20S proteasome biogenesis will be discussed in this work.

2 Scope of this work

The 20S proteasome is a complex multi-subunit enzyme. In eukaryotes most of the proteasomal β -type subunits are synthesized with N-terminal propeptide regions that are cleaved off by *inter* or *intra*-molecular processing during particle maturation (Fig 4) (Heinemeyer et al., 1997; Seemüller et al., 1996). The contribution of propeptides of active β -type subunits to the assembly of the eukaryotic 20S core particle ranges from absolute necessity to dispensability (Arendt and Hochstrasser, 1999; Chen and Hochstrasser, 1996; Jäger et al., 1999).

		Ta-beta		*	*	mammalian																																		
			mnqtleTg	TTTVGITLKDAVIMATERVTMENFIMHKN	GKLF...	homologues																																		
			-8	1	33																																			
active	$\beta 5$	Sc-Pre2	63aa..rnpdckikiahg	TTTLA	FRFQGGII	VAVDSRATAGN	WVASQTVK	KVI...	X/ ϵ ; LMP7																															
	$\beta 1$	Sc-Pre3	7aa..inrlkkgvslg	TSIMAV	TFKDG	VILGADSR	TTTGAYIANR	VTDKLT...	Y/ δ ; LMP2																															
	$\beta 2$	Sc-Pup1	17aa..nshtqpkatstg	TTIVG	VKFNN	GVVIAADR	TRSTQGP	IVADKNCA	KLH...	Z/ α ; MECL1																														
inactive	$\beta 7$	Sc-Pre4	29aa..pmvn	TQQPI	VTGTS	SVISMKYD	NGVIIAAD	NLGSYG	SLLRFNG	VERLI...	N3																													
	$\beta 6$	Sc-Pre7	16aa..ieh	QFN	PYGD	NGTIL	GIAGED	FAVLAG	DTRNIT	DYSINS	RYEP	KYF...	C5																											
	$\beta 3$	Sc-Pup3		M	S	P	S	I	N	G	V	S	N	K	F	E	K	I	F	...	C10																			
	$\beta 4$	Sc-Pre1		M	D	I	I	L	G	I	R	V	Q	D	S	V	I	L	A	S	S	K	A	V	T	R	G	I	S	V	L	K	D	S	D	D	K	T	R	...
				S1		S2		L		S3																														

Fig 4

Sequence alignment of the N-terminal regions of the *T. acidophilum* proteasome β -subunit (Ta-beta) and the seven *S. cerevisiae* (Sc) proteasomal β -type subunits

The N-terminal sequences of the Ta-beta precursor and corresponding fragments of the yeast proteasome β -type subunit precursors are aligned. The propeptides (green lower case letters) and the N-terminal mature parts (upper case letters) are numbered below the Ta-beta sequence with the N-terminus of active subunits defining position 1. Omitted propeptide residues (numbers to the left of the yeast sequences) and the position of the catalytically important residues (*symbol and red letters) are indicated. In yeast (Sc) the propeptide remnants of inactive β -subunits that stay in the mature proteasome are indicated in uppercase letters with light green. Active and inactive β -subunits are indicated at the left side of yeast proteins. In the right column, mammalian homologues of the yeast β -subunits are shown. The β -strands (S1, S2 and S3) and a loop region (L) in the mature subunits are marked.

In this work, the contribution of inactive β -type subunit propeptides to and their requirement for proteasome biogenesis are explored in detail. In addition, the function of propeptide remnants that stay in the mature particle is analysed. Interestingly, these

propeptide remnants consisting of 8 to 9 residues are directed towards the restrictions separating the central proteolytic chamber from the antechambers in the yeast 20S proteasome crystal structure (Fig 5). In addition, the residues Gln-9 and Thr-8 of Pre7 and Pre4, respectively, lie very close to each other at the sharp-edged inner annulus of the β -rings. Although in the crystal structure the propeptide remnants are bound tightly to the surface of the central chamber, they can move freely during particle assembly and thus movements of these propeptide remnants in the mature proteasome cannot be excluded. Based on this, the following questions can be investigated to understand the role of inactive β -type subunit propeptides, including their remnants, in particle assembly or maturation.

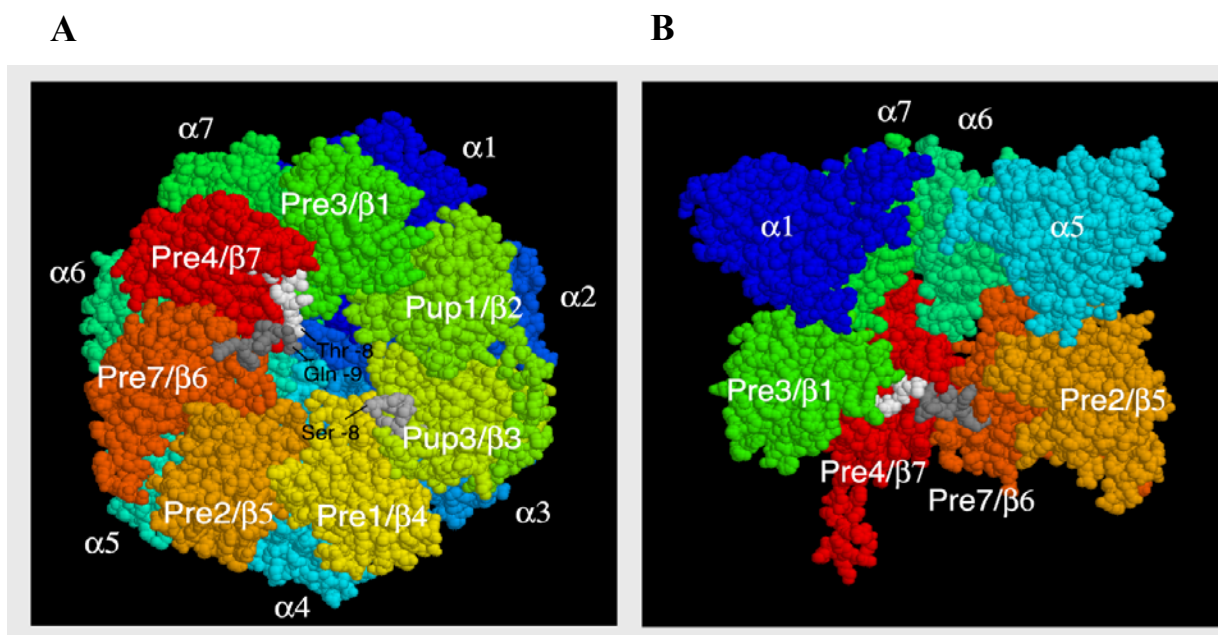


Fig 5

Structural views of half-proteasomes emphasizing the location of inactive subunit propeptide extensions in the mature particle

A. The 20S proteasome is cut along the central axis and the resulting half-proteasome is viewed from the interior (top view onto the β -ring) to show 9 residues of $\beta 6$ /Pre7 (grey), 8 residues of $\beta 7$ /Pre4 (white) and 8 residues of $\beta 3$ /Pup3 (light grey), defined as propeptide remnant region. The position of the N-terminal residues is labeled. B. The half-proteasome is clipped along the cylinder axis (side view into the interior) to indicate the location of the Pre7 (gray) and Pre4 (white) propeptide remnants at the subunit surface. All β -type and α -type subunits are marked.

An important question was why in the eukaryotic 20S proteasome four β -type subunits became inactive during evolution, but still some are synthesized with propeptides, that will be processed in the late assembly stage. Are these propeptides required to promote a specific step in the proteasome assembly process, and if so, do they function *in trans* and do they require specific interacting partners during this process? Next, do the propeptide remnants that are preserved in the mature proteasome contribute to this function, and if so, is the function of these propeptide residues sequence specific or does it only depend on its length? Finally, have these propeptide remnants acquired any novel function in the mature particle, for example by preventing deleterious interactions between protein substrates and the inner surface of the active chamber?

The results of this work will give insight into the crucial role of the β 6/Pre7 propeptide function and its requirements for proteasome biogenesis. In addition, these results will also help to understand the requirement of other inactive and active subunit propeptides in conjunction with the assembly factor Ump1 for efficient particle assembly and maturation. Ultimately, the results will be included in a detailed model for yeast 20S proteasome biogenesis.

3 Materials and methods

Methods specifically used or modified for this study are described in this section.

Appropriate references for all other standard methods applied for this work are cited.

3.1 Materials

3.1.1 Media for yeast cultures

Standard yeast rich (YPD) and minimal (SD) media were prepared as described (Ausubel et al., 1995; Rose et al., 1990) except for SG (synthetic minimal media with 2 % galactose) and SR medium (synthetic minimal media with 2 % raffinose). Geneticin (G418) resistant cells were grown on YPD plates containing 200 µg/ml of G418. Ura^r cells were selected on solid synthetic complete medium containing 5-FOA at 1 mg/ml.

3.1.2 Media for *Escherichia coli* cultures

Media were prepared as described (Sambrook et al., 1989). Ampicillin (stock solution of 50 mg/ml) was added to the medium to a final concentration of 50 µg/ml or 75 µg/ml according to the purpose.

3.1.3 Chemicals and their Suppliers

Suppliers	Chemicals
Amersham Biosciences, Buckinghamshire, UK	ECL Immunodetection kit Hypobond-N+ Nylon membrane for DNA blots Glutathione – Sepharose™ 4B CNBr-activated Sepharose 4B [³⁵ S]-methionine
Applied Biosystems, Norwalk, USA	X-Gal, IPTG
Bachem, Bubendorf, Switzerland	Peptide substrates Suc-Leu-Leu-Van-Tyr-AMC in (51) Cbz-Leu-Leu-Glu-4βNA (53) Cbz-Ala-Arg-Arg-4MβNA (54)

BioRad, München, DE	Prestained (Protein) Standard marker Immunoblot PVDF membrane
Merck, Darmstadt, DE	TEMED, APS, SDS and PMSF
MWG Biotech, Ebersberg or Metabion, Martinsried, DE	Oligonucleotides
New England Biolabs, UK	Restriction enzymes and DNA polymerases Calf intestinal alkaline phosphatase (CIP)
Perkin Elmer Inc, Boston, USA	Glusulase
Toronto Research chemicals, Northyork, Canada	5-FOA (5-fluoro-orotic acid)
Oncogene, San Diego, CA	Protein-G plus Protein-A agarose
Pall Gelman, Roßdorf, DE	Nitrocellulose
Promega, Madison, USA	TNT Coupled Reticulocyte Lysate System, Recombinant RNasein and Hering Sperm DNA
Quiagen, Hilden , DE	Plasmid prep, PCR clean and Gel extraction kit
Roth, Karlsruhe, DE	Solvents, Agarose
Roche Diagnostics, Mannheim, Germany	Nucleotides, Restriction enzymes, T4 DNA ligase, T4 DNA polymerase, Complete™ Inhibitor-Cocktail, RNaseA, DNA-ladder standards, Lumi-light Western blotting substrate, Lysozme, Ampicilin, Complete protease inhibitor and Taq DNA polymerase.
Seikagaku, Tokyo, Japan	Zymolyase 200T
Serva, Heidelberg, DE	Coomassie Brilliant Blue G250 and Bromophenol blue
Sigma, Deisenhofen, DE	All other chemicals if not otherwise indicated
Stratagene, Heidelberg, DE	PfuUltra™ High-fidelity DNA polymerase ExSite™ PCR-based site-directed mutagenesis kit Quikchange II XL site-directed mutagenesis kit Taqplus precision PCR system

3.1.4 Antibodies used in this study

Source/ Reference	Antibody	Dilutions	Buffer	Non-fat dry milk
Sigma, Deisenhofen, DE	anti-HA polyclonal antibody	1:5 000	T-TBS	-
	anti-Rabbit HRPO monoclonal antibody	1:5 000	T-TBS	0.5 %
	anti-FLAG polyclonal antibody	1:10 000	T-TBS	-
	anti-FLAG monoclonal antibody	1:20 000	T-PBS	3 %
Babco, Denver, PA, DE	Murine anti-HA 11 MMS-101p monoclonal antibody	1:10 000	T-PBS	-
Dianova, Hamburg, DE	AffiniPure Goat anti-Mouse IgG-HRPO monoclonal antibody	1:10 000	T-PBS	1 %
Affinity Research Products Ltd.,UK	anti-Rpt5 monoclonal antibody	1:20 000	T-TBS	1 %
Molecular probes Eugene, USA	anti-Pgk1 monoclonal antibody	1:10 000	T-PBS	-
This work	anti-Pre7 polyclonal antibody	1:500	T-TBS	-
Jäger et al., 2001	anti-Pre6 polyclonal antibody	1:5000	T-TBS	-
Hilt et al., 1994	anti-Pre4 polyclonal antibody	1:4000	T-TBS	-

T-TBS: Tris-buffered saline with 1 % or 0.5 % Tween20

T-PBS: Phosphate-buffered saline with 1 % Tween20

3.1.5 Instruments used in this study

Source	Instrument
Amersham Pharmacia Biotech AB, Uppsala, Sweden	FPLC and Superose-6 column
Bio Rad, München, DE	Gel electrophoresis (Poly acrylamid, Agarose) and Blotting apparatus
Midton Acrylics Ltd., Scotland, UK	Vacugene-vacuum blotting unit
Fröbel, Lindau, DE	Gel dryer, Semi-dry blotting system
Branson Sonic power, Danbury, USA	Sonifier
Beckman, California, USA	Optima™ TLX Ultra centrifuge
Sorvall products, Connecticut, USA	Sorvall RC5B plus centrifuge
Jasco, Gross Umstadt, DE	Photometer V530
Kontron, Neufarn, DE	Centrikon H-401 & T-124 and T-1065 rotors
Pharmacia, Freiburg, DE	Gelelectrophoresis camera
Stratagene, La Jolla, USA	Robocycler Gradient 40 PCR grade
Nikon, Tokyo, Japan	Micromanipulator
Shimadzu, Tokyo, Japan	RF-1502 Spectrofluorophotometer

3.1.6 Yeast Strains

Strain	Relevant genotype	Source
WCG4a	<i>MATa leu2-3,112 ura3 his3-11,15 Can^s GAL2</i>	Heinemeyer et al., 1993
WCG4 α	<i>MATa leu2-3,112 ura3 his3-11,15 Can^s GAL2</i>	Heinemeyer et al., 1993

All strains listed below are derivatives of either WCG4a or WCG4 α

Sky 144	<i>pup3Δ::HIS3 [pCEN-PUP3]</i>	Heinemeyer unpublished
Sky 145	<i>pup3Δ::HIS3 [pCEN-mmpup3]</i>	This study
Sky 110	<i>pre4Δ::HIS3 [pCEN-UBI/mmpre4]</i>	Jäger et al., 1999
Sky 106	<i>ump1Δ::HIS3</i>	As described in Ramos et al., 1998
Sky 138	<i>pre7Δ::KanMX4 [pCEN-PRE7]</i>	Heinemeyer unpublished
Sky 136	<i>pre7Δ::KanMX4 [pCEN-UBI/G+1pre7]</i>	Heinemeyer unpublished
Sky 139	<i>pre7Δ::KanMX4 [pCEN-UBI/Q-9pre7]</i>	Heinemeyer unpublished
Sky 140	<i>pre7Δ::KanMX4 [pCEN-UBI/N-7pre7]</i>	This study
Sky 201	<i>pre7Δ::KanMX4 [pCEN-UBI/P-6pre7]</i>	This study
Sky 141	<i>pre7Δ::KanMX4 [pCEN-Met Y-5pre7]</i>	This study
Sky 166	<i>pre7Δ::KanMX4 PRE2-HA::HIS3::URA3 [pCEN-PRE7]</i>	This study
Sky 168	<i>pre7Δ::KanMX4 PRE2-HA::HIS3::URA3 [pCEN-UBI/Q-9pre7]</i>	This study
Sky 171	<i>pre7Δ::KanMX4 PRE2-HA::HIS3::URA3 [pCEN-UBI/N-7pre7]</i>	This study
Sky 173	<i>pre7Δ::KanMX4 PRE2-HA::HIS3::URA3 [pCEN-Met Y-5pre7]</i>	This study
Sky 148	<i>pre7Δ::KanMX4 [pCEN-PRE7-3HA]</i>	This study
Sky 147	<i>pre7Δ::KanMX4 [pCEN-PRE7-(I-HA)]</i>	This study
Sky 175	<i>pre7Δ::KanMX4 [pCEN-PRE7-FLAG]</i>	This study
Sky 277	<i>pre7Δ::KanMX4 [pCEN-PRE7-(I-FLAG)]</i>	This study
Sky 278	<i>pre7Δ::KanMX4 [pCEN-UBI/Q-9pre7-FLAG]</i>	This study
Sky 279	<i>pre7Δ::KanMX4 [pCEN-UBI/Q-9pre7-(I-FLAG)]</i>	This study

Sky 120	<i>pre7Δ::KanMX4 ump1Δ::HIS3</i>	This study
Sky 121	<i>pre7Δ::KanMX4 ump1Δ::HIS3 [pCEN-UBI/Q-9pre7]</i>	This study
Sky 122	<i>pre7Δ::KanMX4 ump1Δ::HIS3 [pCEN-UBI/N-7pre7]</i>	This study
Sky 182	<i>pre7Δ::KanMX4 ump1Δ::HIS3 [pCEN-UBI/P-6pre7]</i>	This study
Sky 123	<i>pre7Δ::KanMX4 ump1Δ::HIS3 [pCEN-UBI/Y-5pre7]</i>	This study
Sky 124	<i>pre7Δ::KanMX4 ump1Δ::HIS3 [pCEN-UBI/D-3pre7]</i>	This study
Sky 125	<i>pre7Δ::KanMX4 ump1Δ::HIS3 [pCEN-UBI/G-1pre7]</i>	This study
Sky 126	<i>pre7Δ::KanMX4 ump1Δ::HIS3 [pCEN-Met Y-5pre7]</i>	This study
Sky 127	<i>pre7Δ::KanMX4 ump1Δ::HIS3 [pCEN-Met D-3pre7]</i>	This study
Sky 128	<i>pre7Δ::KanMX4 ump1Δ::HIS3 [pCEN-UBI/P3-8*pre7]</i>	This study
Sky 176	<i>pre7Δ::KanMX4 ump1Δ::HIS3 PRE2-HA::HIS3::URA3 [pCEN-PRE7]</i>	This study
Sky 177	<i>pre7Δ::KanMX4 ump1Δ::HIS3 PRE2-HA::HIS3::URA3 [pCEN-UBI/Q-9pre7]</i>	This study
Sky 179	<i>pre7Δ::KanMX4 ump1Δ::HIS3 PRE2-HA::HIS3::URA3 [pCEN-UBI/N-7pre7]</i>	This study
Sky 180	<i>pre7Δ::KanMX4 ump1Δ::HIS3 PRE2-HA::HIS3::URA3 [pCEN-Met Y-5pre7]</i>	This study
Sky 109	<i>pre2Δ::HIS3 [pCEN-PRE2]</i>	Heinemeyer et al., 1997
Sky 150	<i>pre1-1</i>	Heinemeyer et al., 1993
Sky 162	<i>pre1-1 pre7Δ::KanMX4 [pCEN-PRE7]</i>	This study
Sky 163	<i>pre1-1 pre7Δ::KanMX4 [pCEN-UBI/Q-9]</i>	This study
Sky 164	<i>pre1-1 pre7Δ::KanMX4 [pCEN-UBI/N-7]</i>	This study
Sky 153	<i>pre1-1 pre7Δ::KanMX4 ump1Δ::HIS3 [pCEN-PRE7]</i>	This study
Sky 154	<i>pre1-1 pre7Δ::KanMX4 ump1Δ::HIS3 [pCEN-UBI/Q-9pre7]</i>	This study
Sky 155	<i>pre1-1 pre7Δ::KanMX4 ump1Δ::HIS3 [pCEN-UBI/N-7pre7]</i>	This study
Sky 156	<i>pre1-1 pre7Δ::KanMX4 ump1Δ::HIS3 [pCEN-UBI/Y-5pre7]</i>	This study
Sky 157	<i>pre1-1 pre7Δ::KanMX4 ump1Δ::HIS3 [pCEN-UBI/D-3pre7]</i>	This study
Sky 158	<i>pre1-1 pre7Δ::KanMX4 ump1Δ::HIS3 [pCEN-UBI/G-1pre7]</i>	This study
Sky 159	<i>pre1-1 pre7Δ::KanMX4 ump1Δ::HIS3 [pCEN-Met Y-5pre7]</i>	This study
Sky 160	<i>pre1-1 pre7Δ::KanMX4 ump1Δ::HIS3 [pCEN-Met D-3pre7]</i>	This study
Sky 161	<i>pre1-1 pre7Δ::KanMX4 ump1Δ::HIS3 [pCEN-UBI/P3-8*pre7]</i>	This study

YWH 101	<i>UBI/mmPUP1</i>	Jäger et al., 1999
YWH 301	<i>UBI/mmPRE3</i>	Jäger et al., 1999
Sky 224	<i>UBI/mmPRE4</i>	This study
Sky 241	<i>ump1Δ::HIS3 UBI/mmPRE4</i>	This study
YHei 258	<i>ump1Δ::HIS3 UBI/mmPUP1</i>	This study
YHei 257	<i>ump1Δ::HIS3 UBI/mmPRE3</i>	This study
Sky 118	<i>ump1Δ::HIS3 pre2Δ::HIS3 [pCEN-UBI/mmPRE2]</i>	This study
Sky 260	<i>ump1Δ::HIS3 UBI/mmPRE2 pre7Δ::KanMX4 [pCEN-PRE7]</i>	This study
Sky 245	<i>ump1Δ::HIS3 pre7Δ::KanMX4 [pCEN-PRE7] [pGAL1::UMP1]</i>	This study
Sky 254	<i>ump1Δ::HIS3 pre7Δ::KanMX4 [pCEN-UBI/N-7pre7] [pGAL1::UMP1]</i>	This study
Sky 261	<i>ump1Δ::HIS3 pre7Δ::KanMX4 [pCEN-Met Y-5pre7] [pGAL1::UMP1]</i>	This study
Sky 264	<i>ump1Δ::HIS3 pre7Δ::KanMX4 [pCEN-UBI/Y-5pre7] [pGAL1::UMP1]</i>	This study
Sky 285	<i>ump1Δ::HIS3 pre7Δ::KanMX4 [pCEN-PRE7 GAL1::UMP1]</i>	This study
Sky 286	<i>ump1Δ::HIS3 pre7Δ::KanMX4 [pCEN-UBI/Q-9pre7 GAL1::UMP1]</i>	This study
Sky 287	<i>ump1Δ::HIS3 pre7Δ::KanMX4 [pCEN-UBI/N-7pre7 GAL1::UMP1]</i>	This study
Sky 288	<i>ump1Δ::HIS3 pre7Δ::KanMX4 [pCEN-UBI/P-6pre7 GAL1::UMP1]</i>	This study
Sky 289	<i>ump1Δ::HIS3 pre7Δ::KanMX4 [pCEN-Met Y-5pre7 GAL1::UMP1]</i>	This study
Sky 290	<i>ump1Δ::HIS3 pre7Δ::KanMX4 [pCEN-UBI/Y-5pre7 GAL1::UMP1]</i>	This study
Sky 291	<i>ump1Δ::HIS3 pre7Δ::KanMX4 [pCEN-Met D-3pre7 GAL1::UMP1]</i>	This study
Sky 293	<i>ump1Δ::HIS3 pre7Δ::KanMX4 [pCEN-UBI/D-3pre7 GAL1::UMP1]</i>	This study
Sky 304	<i>ump1Δ::HIS3 pre7Δ::KanMX4 PRE2-HA::HIS3::URA3 [pCEN-PRE7 GAL1::UMP1]</i>	This study
Sky 305	<i>ump1Δ::HIS3 pre7Δ::KanMX4 PRE2-HA::HIS3::URA3 [pCEN-UBI/Q-9pre7 GAL1::UMP1]</i>	This study
Sky 306	<i>ump1Δ::HIS3 pre7Δ::KanMX4 PRE2-HA::HIS3::URA3 [pCEN-UBI/N-7pre7 GAL1::UMP1]</i>	This study
Sky 307	<i>ump1Δ::HIS3 pre7Δ::KanMX4 PRE2-HA::HIS3::URA3 [pCEN-UBI/P-6pre7 GAL1::UMP1]</i>	This study
Sky 319	<i>ump1Δ::HIS3 pre7Δ::KanMX4 PRE2-HA::HIS3::URA3</i>	This study

	[pCEN-Met Y-5pre7 GAL1::UMP1]	
Sky 320	<i>ump1Δ::HIS3 pre7Δ::KanMX4 PRE2-HA::HIS3::URA3</i> [pCEN-UBI/Y-5pre7 GAL1::UMP1]	This study
Sky 321	<i>ump1Δ::HIS3 pre7Δ::KanMX4 PRE2-HA::HIS3::URA3</i> [pCEN-Met D-3pre7 GAL1::UMP1]	This study
Sky 322	<i>ump1Δ::HIS3 pre7Δ::KanMX4 PRE2-HA::HIS3::URA3</i> [pCEN-UBI/D-3pre7 GAL1::UMP1]	This study
Sky 181	<i>pre7Δ::KanMX4</i> [pCEN-UBI-Q-9pre7(P-6A)]	This study
Sky 222	<i>pre7Δ::KanMX4</i> [pCEN-UBI-Q-9pre7(P95A)]	This study
Sky 223	<i>pre7Δ::KanMX4</i> [pCEN-UBI-Q-9pre7(Y96A Y97A)]	This study
Sky 184	<i>pre7Δ::KanMX4 ump1Δ::HIS3</i> [pCEN-UBI/Q-9pre7(Y-5A)]	This study
Sky 183	<i>pre7Δ::KanMX4 ump1Δ::HIS3</i> [pCEN-UBI/Q-9pre7(P-6A)]	This study
Sky 185	<i>pre7Δ::KanMX4 ump1Δ::HIS3</i> [pCEN-UBI/Q-9pre7(P-6A Y-5A)]	This study
Sky 229	<i>pre7Δ::KanMX4 ump1Δ::HIS3</i> [pCEN-UBI/Q-9pre7(F93A F94A)]	This study
Sky 228	<i>pre7Δ::KanMX4 ump1Δ::HIS3</i> [pCEN-UBI/Q-9pre7(P95A)]	This study
Sky 230	<i>pre7Δ::KanMX4 ump1Δ::HIS3</i> [pCEN-UBI/Q-9pre7(Y96A Y97A)]	This study
Sky 323	<i>pre7Δ::KanMX4 ump1Δ::HIS3</i> [pCEN-UBI/Q-9pre7(Y-5A)(F93F94→AA)]	This study
Sky 324	<i>pre7Δ::KanMX4 ump1Δ::HIS3</i> [pCEN-UBI/Q-9pre7(Y-5A)(P95→A)]	This study
Sky 325	<i>pre7Δ::KanMX4 ump1Δ::HIS3</i> [pCEN-UBI/Q-9pre7(Y-5A)(Y96Y97→AA)]	This study

3.1.7 Bacterial Strains

Strain	Genotype	Source/Comments
DH5 α	F'(F'/endA1 hsdR17 (rK ⁻ mK ⁺) supE44 thi-1 recA-1 gyrA (Nal ^r)relA1 Δ (laZYA-argF) u169 (Δ 80lacZ Δ M15)	Hanahan
BL21	(DE3)F ⁻ <i>ompT</i> [<i>lon</i>] <i>hsdS_B</i> (r _B ⁻ m _B ⁻) with λ prophage DE3 q	Pharmacia
XL10-Gold	Tet ^R Δ (mcrA)183 Δ (mcrCB-hsdSMR-mrr)173 endA1 supE44 thi-1 recA1 gyrA96 relA1 lac The [F' proAB lacIq Z Δ M15 Tn10 (Tet ^R) Amy Cam ^R] ^{α}	Stratagene

-----Materials and methods

3.1.8 Oligonucleotides

Name	Sequence (purpose)
5/6Fprimer	GAAACAGCTATGACCATGAT (universal forward primer for MCS region of pCEN plasmid)
5/6Rprimer	GACGGCCAGTGAATTGTAAT (universal reverse primer for MCS region of pCEN plasmid)
UBI_+E3	ACTGACTTCGCCCTTTTTCAAACCACCTCTTAGCCTTAGCAC (for generation of UBI/E39 construct)
PRE2-5_618-634	GCGTTGGTTCAGGTCAA (for Pre2 subunit encoding region)
7_+5	TACGGTGATAATGGTGGTACAAT (for generation of UBI/Y-5 construct)
7_+7	AACCCTTACGGTGATAATGGTGGT (for generation of UBI/N-7 construct)
7_+6	CCTTACGGTGATAATGGTGGTAC (for generation of UBI/P-6 construct)
7_+6A	CCTTACGGTGATAATGGTGGTACA (for generation of UBI/P-6 construct)
7_E3	TTGAAAAAGGGCGAAGTCAGTTTAGGTGGTACAATCCTGGGCATTGC (for generation of UBI/E39 construct)
7_UBI-R	ACCACCTCTTAGCCTTAGCAC (for Ubiquitin encoding region)
UBI-F	ATGCAGATTTTCGTCAAGAC (for Ubiquitin encoding region)
NWPj_Pup3+1Fw	ATGGGTATCGTCGTTGCGATGAC (for generation of Met-mmPUP3 construct)
Pj_Pup3+1Fw	ATGGGTATCGTCGTAGCTATGAC (for generation of Met-mmPUP3 construct)
NWPj_Pup3+1Re	GTCATCGCAACGACGATACCCATTTTTTTTTTATGCTTTATTCAGTCTTC (for generation of Met-mmPUP3 construct)
Pj_Pup3+1Re	GTCATAGCTACGACGATACCCATTTTTTTTTTATGCTTTATTCAGTCTTC (for generation of Met-mmPUP3 construct)
Ura-del	GTATTGACGCTGGCGTACTGG (for Uracil encoding region)

PRE2-anti	CTTCCTTCATAATTCTATGGG (for Pre2 subunit terminator region)
F1	ATGTCGGCGAATGGATTGTC (for Pre7 encoding region)
7/+3	GATAATGGTGGTACAATCCTG (for generation of UBI/D-3 construct)
UBI-R-7/+3	CAGGATTGTACCACCATTATCACCACCTCTTAGCCTTAGCAC (for generation of UBI/D-3 construct)
7/+1	GGTGGTACAATCCTGGGCATT (for generation of UBI/G-1 construct)
UBI-R-7/+1	AATGCCCAGGATTGTACCACCACCACCTCTTAGCCTTAGCAC (for generation of UBI/G-1 construct)
Me7/+5	ATGTACGGTGATAATGGTGGTACA (for generation of Met Y-5 construct)
Me7/+5 R	ACCACCATTATCACCGTACATATTTGTTTAACTTTATAGTTCAA (for generation of Met Y-5 construct)
Me7/+3	ATGGATAATGGTGGTACAATCCTG (for generation of Met D-3 construct)
Me7/+3R	GATTGTACCACCATTATCCATATTTGTTTAACTTTATAGTTCAA (for generation of Met D-3 construct)
PUP3F/pre7	TCGGATCCAAGTTCTATTAACGGTGGTACAATCCTGGGCATTGCA (for generation of UBI/P3-8 construct)
PUP3R/pre7	GTTAATAGAACTTGGATCCGAACCACCTCTTAGCCTTAGCAC (for generation of UBI/P3-8 construct)
Loop/7F	TATGAGCCAGGTACAAACGGCGCCGCAAAGTCAAAAAGCCTTTGAAATAC (to introduce NotI site into Pre7 subunit loop region)
Loop/7R	GCGGCCGCCGTTTGTACCTGGCTCATATTG (to introduce NotI site into Pre7 subunit loop region)
UBI-R-7/+1	AATGCCCAGGATTGTACCACCACCACCTCTTAGCCTTAGCAC (for generation of UBI/G-1 construct)
E7ppNotI-FW	CAATCCTTACGGTGATAATGGCGGCCGCTAACTCGAGGGGAACACTACTC (to introduce NotI site into Pre7 propeptide region)
E7ppNotI-RE	GCGGCCGCCATTATCACCGTAAGGATTG (to introduce NotI site into Pre7 propeptide region)
E7 ORF	CAAAATATGGCCACTATTGCATC (for generation of T7-E7 construct)
E4 ORF	CCCACACGAATGAATCACG (for generation of T7-E4 construct)

E2 ORF	CAAACATGCAAGCTATTGCC (for generation of T7-E2 construct)
PRE7-A6FW	GCGTACGGTGATAATGGT (for generation of UBI/Q-9 [P6A] construct)
PRE7-A7FW	CCTGCAGGTTATAATGGT (for generation of UBI/Q-9 [Y5A] construct)
PRE7-AA6-7FW	GCTGCAGGTGATAATGGT (for generation of UBI/Q-9 [P6A, Y5A]construct)
UBI/E7-A6RE	CACCATTATCACC GTACGCATTGAATTGACCACCTCTTAGC (for generation of UBI/Q-9 [P6A] construct)
UBI/E7-A7RE	CACCATTATCACCTGCAGGATTGAATTGACCACCTCTTAGC (for generation of UBI/Q-9 [Y5A] construct)
UBI/E7-AA6-7RE	CACCATTATCACCTGCAGCATTGAATTGACCACCTCTTAGC (for generation of UBI/Q-9 [P6A, Y5A] construct)
E7ppNotI-FW	CAATCCTTACGGTGATAATGGCGGCCGCTAACTCGAGGGGAACACTACTC (to introduce NotI site into Pre7 propeptide region)
E7ppNotI-RE	GCGGCCGCCATTATCACCGTAAGGATTG (to introduce NotI site into Pre7 propeptide region)
UBI/7+6REW	ACCACCATTATCACCGTAAGGACCACCTCTTAGCCTTAGCAC (for generation of UBI/P-6 construct)
PRE7-F8-A/fw	CAAGCTAATCCTTACGGTG (for generation of UBI/Q-9 [F8A] construct)
PRE7-N7-A/fw	GCGCCTTACGGTGATAATG (for generation of UBI/Q-9 [N7A] construct)
Ubi/E7-F8-A/RE	CACCGTAAGGATTAGCTTGACCACCTCTTAGCCTTAGC (for generation of UBI/Q-9 [F8A] construct)
UBI/E7-A6RE	CACCATTATCACCGTACGCATTGAATTGACCACCTCTTAGC (for generation of UBI/Q-9 [P6A] construct)
UBI/E7-A7RE	CACCATTATCACCTGCAGGATTGAATTGACCACCTCTTAGC (for generation of UBI/Q-9 [Y5A] construct)
Ubi/E7-N7-A/RE	CATTATCACCGTAAGGCGCAATTGACCACCTCTTAGCC (for generation of UBI/Q-9 [N7A] construct)
Flag-Fw	GGCCGCGATTACAAGGATGACGACGATAAGATCTGAGC (FLAG epitope encoding region at NotI site in Pre7 C-terminis)
Flag-Rew	GGCCGCTCAGATCTTATCGTCGTCATCCTTGTAATCGC (FLAG epitope encoding region at NotI site in Pre7 C-terminis)
LoopFlag-Fw	GGCCGCGATTACAAGGATGACGACGATAAGATCTGCGGC (FLAG epitope encoding region at NotI site in Pre7 loop region)

LoopFlag-Rew	GGCCGCCGCAGATCTTATCGTCGTCATCCTTGTAATCGC (FLAG epitope encoding region at NotI site in Pre7 loop region)
PRE4Rew	GAACTCTCATTGCATTACG (for Pre4 subunit encoding region)
E7-IRS-FW	GCTAAAAAGAGATCGCTATATTCGATCGTAATGCATACATATC (to insert IRS epitope encoding region into Pre7 subunit)
E7-IRS-Rev	GATATGTATGCATTACGATCGAATATAGCGATCTCTTTTAGC (to insert IRS epitope encoding region into Pre7 subunit)
Prom-UMP1fw	GAAACAGCCTGCATACCAAC (for Ump1 promoter region)
Term-UMP1rew	CAATGGTTTACGTGACAGATG (for Ump1 terminator region)

3.1.9 Plasmid vectors

Vector	Application	Source
pBluescript II KS+	vector for <i>E.coli</i> (<i>amp^r</i>) T3, T7 promotor	Stratagene
pUC19	vector for <i>E.coli</i> (<i>amp^r</i>)	Biolabs
pGEM-T Easy	vector for <i>E.coli</i> (<i>amp^r</i>)	Promega
pTNT TM vector	vector for <i>E.coli</i> (<i>amp^r</i>)	Promega
pRS315	<i>CEN LEU2</i> vector for yeast and <i>E.coli</i> (<i>amp^r</i>)	Sikorski and Hieter, 1989
pRS316	<i>CEN URA3</i> vector for yeast and <i>E.coli</i> (<i>amp^r</i>)	Sikorski and Hieter, 1989
pRS415	<i>CEN LEU2</i> vector for yeast and <i>E.coli</i> (<i>amp^r</i>)	Mumberg et al., 1994
pRS406	<i>URA3</i> integrative vector for yeast and <i>E.coli</i> (<i>amp^r</i>)	Stratagene
pGEX-4T	vector for <i>E.coli</i> (<i>amp^r</i>) for fusions with GST	Pharmacia
pYES2	<i>2μ URA3 GAL1</i> vector for yeast and <i>E.coli</i> (<i>amp^r</i>)	Invitrogen

3.1.10 Plasmid constructs

Plasmid name (stock number)	Insert details	Vector	(Sites used)	Source
pTU2 (Ske 001)	PRE7	pRS315	(HindIII+SphI)	W. Heinemeyer
pP3 (Ske 011)	PRE4	pRS315	(HindIII+BamHI)	W. Heinemeyer
pP3 (Ske 011)	PUP3	pRS316	(Spe+XhoI)	W. Heinemeyer
pE3 (Ske 039)	PRE2	pRS315	(HindIII+BamHI)	W. Heinemeyer
pG1 (Ske 038)	UBI/mmpre7	pRS315	(HindIII+SphI)	W. Heinemeyer
pG1+pp (Ske 036)	PP+UBI/G1pre7	pRS315	(ApaI+XbaI & HindIII+SphI)	This work
pP3 Δ pp (Ske 028)	UBI/mmPUP3	pRS315	(SacI+XhoI)	This work
pE4 Δ pp (Ske 015)	UBI/mmPRE4	pRS315	(HindIII+BamHI)	S. Jäger
pI-E4 Δ pp (Ske 124)	UBI/mmPRE4	pRS406	(HindIII+BamHI)	This work
pE2 Δ pp (Ske 040)	UBI/mmPRE2	pRS315	(HindIII+BamHI)	W. Heinemeyer
pI-E2 Δ pp (Ske 123)	UBI/mmPRE2	pRS406	(HindIII+BamHI)	This work
pUC-E7 (Ske 032)	PRE7	pUC19	(SspI+XbaI)	This work
pGAL::E7 (Ske 149)	PRE7	pRS415	(HindIII+SphI)	This work
+9 (Ske 002)	UBI/Q-9pre7	pRS315	(HindIII+SphI)	This work
+7 (Ske 003)	UBI/N-7pre7	pRS315	(HindIII+SphI)	This work
+6 (Ske 088)	UBI/P-6pre7	pRS315	(HindIII+SphI)	This work
+5 (Ske 004)	UBI/Y-5pre7	pRS315	(HindIII+SphI)	This work
+3 (Ske 005)	UBI/D-3pre7	pRS315	(HindIII+SphI)	This work
+1 (Ske 006)	UBI/G-1pre7	pRS315	(HindIII+SphI)	This work
E3+9 (Ske 007)	UBI/E3-9pre7	pRS315	(HindIII+SphI)	This work

P3+8	(Ske 010)	UBI/P3-8pre7	pRS315 (HindIII+SphI)	This work
P3+8*	(Ske 034)	UBI/P3-8*pre7	pRS315 (HindIII+SphI)	This work
M+5	(Ske 008)	MetY-5pre7	pRS315 (HindIII+SphI)	This work
M+3	(Ske 009)	MetD-3pre7	pRS315 (HindIII+SphI)	This work
Gst-Ump1	(Ske 021)	GST-UMP1	pGEX4T (BamHI+NotI)	C. Enenkel
Sp6-E7	(Ske 055)	PRE7 (ORF)	pGEMT (EcoRI)	This work
Sp6-E4	(Ske 057)	PRE4 (ORF)	pGEMT (EcoRI)	This work
Sp6-E2	(Ske 059)	PRE2 (ORF)	pGEMT (EcoRI)	This work
T3-E7	(Ske 064)	PRE7 (ORF)	pB II KS+ (PstI+SacII)	This work
T3-E4	(Ske 066)	PRE4 (ORF)	pB II KS+ (PstI+SacII)	This work
T3-E2	(Ske 062)	PRE2 (ORF)	pB II KS+ (PstI+SacII)	This work
T7-E7	(Ske 050)	PRE7 (ORF)	pTNT (HindIII+SacI)	This work
T7-E4	(Ske 051)	PRE4 (ORF)	pTNT (HindIII+SacI)	This work
T7-E2	(Ske 049)	PRE2 (ORF)	pTNT (HindIII+SacI)	This work
E7-HA	(Ske 052)	PRE7-(C-HA)	pRS315 (HindIII+SphI)	W. Heinemeyer
E7-loopHA	(Ske 042)	PRE7-(I-HA)	pRS315 (HindIII+SphI)	This work
E7C-flag	(Ske 060)	PRE7-(C-FLAG)	pRS315 (HindIII+SphI)	This work
+9C-flag	(Ske 076)	UBI/Q-9pre7-(C-FLAG)	pRS315 (HindIII+SphI)	This work
+7-flag	(Ske 107)	UBI/N-7pre7-(C-FLAG)	pRS315 (HindIII+SphI)	This work
E7-loop-flag	(Ske 053)	PRE7-(I-FLAG)	pRS315 (HindIII+SphI)	This work
+9-loop-flag	(Ske 115)	UBI/Q-9pre7-(I-FLAG)	pRS315 (HindIII+SphI)	This work
+7-loop-flag	(Ske 117)	UBI/N-7pre7-(I-FLAG)	pRS315 (HindIII+SphI)	This work
E7C-IRS	(Ske 137)	PRE7-(C-IRS)	pRS315 (HindIII+SphI)	This work

+9C-IRS	(Ske 138)	UBI/Q-9pre7-(C-IRS)	pRS315 (HindIII+SphI)	This work
+7C-IRS	(Ske 139)	UBI/N-7pre7-(I-IRS)	pRS315 (HindIII+SphI)	This work
pI-Ump1-HA	(Ske 023)	ump1-5' Δ-HA	YIP5 (PstI+HindIII)	C. Enenkel
pCEN-Ump1-HA	(Ske 024)	UMP1-HA	pRS315 (SpeI+SacII)	This work
pGAL::Ump1-HA	(Ske 136)	GAL::UMP1-HA	pYES2 (HindIII+BamHI)	This work
E7 & Ump1-F	(Ske 153)	PRE7+UMP1-FLAG	pRS315 (SspI&XbaI+SpeI&BamHI)	This work
+9 & Ump1-F	(Ske 154)	UBI/Q-9pre7+UMP1-FLAG	pRS315 (SspI&XbaI+SpeI&BamHI)	This work
+7 & Ump1-F	(Ske 155)	UBI/N-7pre7+UMP1-FLAG	pRS315 (SspI&XbaI+SpeI&BamHI)	This work
+6 & Ump1-F	(Ske 156)	UBI/P-6pre7+UMP1-FLAG	pRS315 (SspI&XbaI+SpeI&BamHI)	This work
+5 & Ump1-F	(Ske 157)	UBI/Y-5pre7+UMP1-FLAG	pRS315 (SspI&XbaI+SpeI&BamHI)	This work
+3 & Ump1-F	(Ske 158)	UBI/D-3pre7+UMP1-FLAG	pRS315 (SspI&XbaI+SpeI&BamHI)	This work
M+5 & Ump1-F	(Ske 159)	Met Y5pre7 +UMP1-FLAG	pRS315 (SspI&XbaI+SpeI&BamHI)	This work
F8A	(Ske 120)	UBI/Q-9pre7 [-8F to A]	pRS315 (HindIII+SphI)	This work
N7A	(Ske 121)	UBI/Q-9pre7 [-7N to A]	pRS315 (HindIII+SphI)	This work
P6A	(Ske 085)	UBI/Q-9pre7 [-6P to A]	pRS315 (HindIII+SphI)	This work
Y5A	(Ske 086)	UBI/Q-9pre7 [-5Y to A]	pRS315 (HindIII+SphI)	This work
P6Y5AA	(Ske 087)	UBI/Q-9pre7 [-6P-5Y to AA]	pRS315 (HindIII+SphI)	This work
Y5F	(Ske 122)	UBI/Q-9pre7 [-5Y to F]	pRS315 (HindIII+SphI)	This work
HyFFAA	(Ske 126)	UBI/Q-9pre7 [93-94FF to AA]	pRS315 (HindIII+SphI)	This work
HyPA	(Ske 127)	UBI/Q-9pre7 [95P to A]	pRS315 (HindIII+SphI)	This work

-----Materials and methods

HyYYAA	(Ske 128)	UBI/Q-9pre7 [96-97YY to AA]	pRS315 (HindIII+SphI)	This work
Y5A+HyFFAA	(Ske 161)	UBI/Q-9pre7 [-5Y to A] [93-94FF to AA]	pRS315 (HindIII+SphI)	This work
Y5A+HyPA	(Ske 162)	UBI/Q-9pre7 [-5Y to A] [95P to A]	pRS315 (HindIII+SphI)	This work
Y5A+HyYYAA	(Ske 163)	UBI/Q-9pre7 [-5Y to A] [96-97YY to AA]	pRS315 (HindIII+SphI)	This work
Y5A+Hy5A	(Ske 164)	UBI/Q-9pre7 [-5Y to A] [93-97FFPYY to 5xA]	pRS315 (HindIII+SphI)	This work

Enzyme sites that are lost during triple ligation are underlined (see section 3.2.1.4 for details)

3.2 Methods

3.2.1 Molecular biological methods

3.2.1.1 Plasmid construction

Standard conditions were used to generate PCR fragments (White et al., 1993). Recombinant DNA-techniques and transformation of plasmids into *E.coli* were done as described (Ausubel et al., 1995; Sambrook et al., 1989). All new plasmid constructs were checked by sequencing (GATC, Konstanz, DE).

3.2.1.2 Site-directed mutagenesis by recombinant PCR

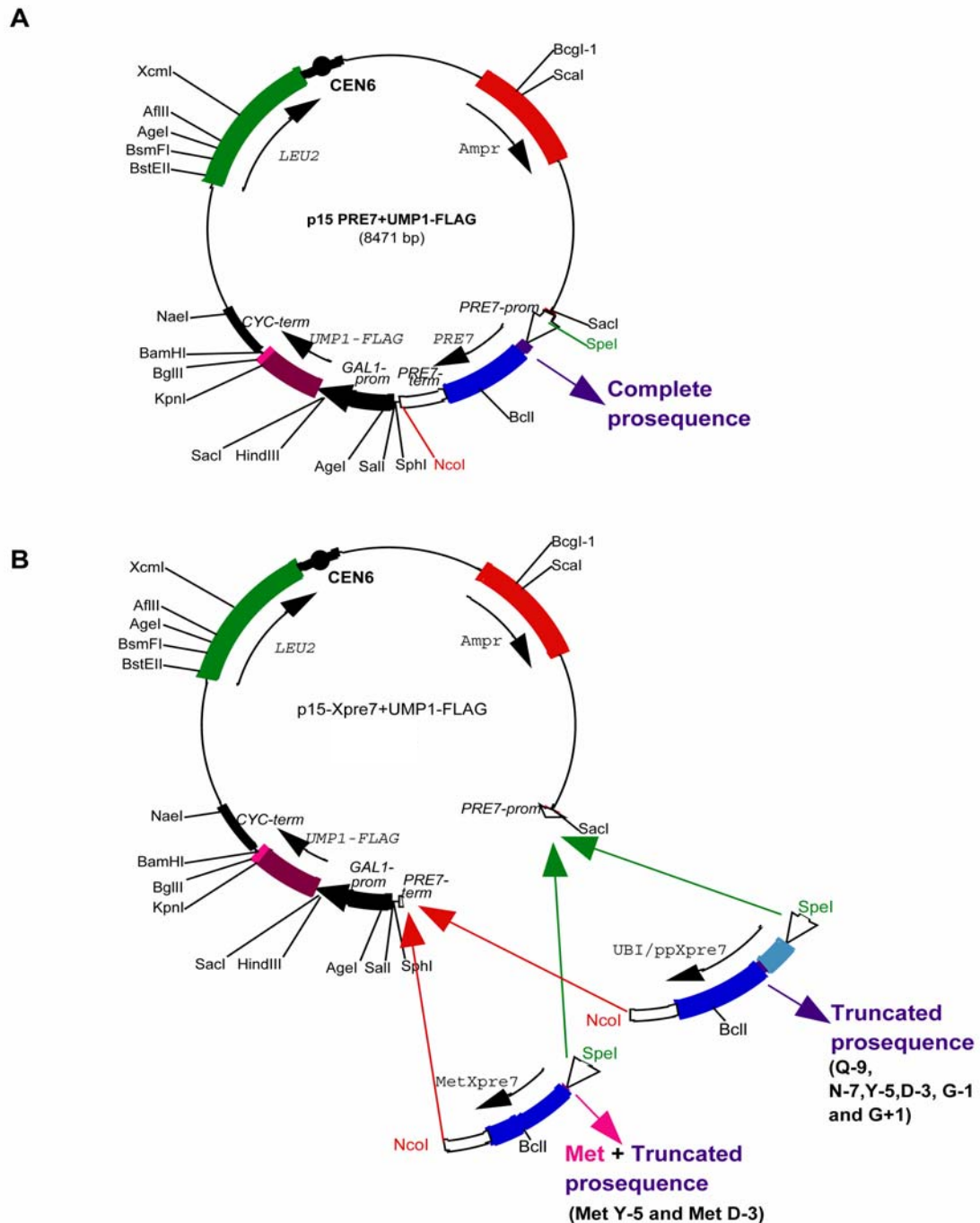
Two separate fragments were amplified from the plasmid pRS15 carrying a gene encoding the respective proteasomal subunit (*PRE7* or *PUP3*). The first fragment was created using a forward oligonucleotide containing the desired mutation and a universal reverse oligonucleotide (5/6Rprimer). The second fragment was generated by using the universal forward oligonucleotide (5/6Rprimer) with reverse an oligonucleotide carrying the mutation. Both fragments were purified and pooled. In the mixture, two overlapping regions obtained from the oligonucleotides with mutation sequence served as primers on one another to create the full-length PCR product in the presence of universal forward and reverse oligonucleotides (5/6Fprimer and 5/6Rprimer).

3.2.1.3 Site-directed mutagenesis by “Quick-Change” mutagenesis

Some of the mutations in *PRE7*, together with silent mutation(s) that either create or destroy a restriction site at or very near the codon-altering mutation(s), were generated starting from the UBI/Q-9 construct (see Fig 8 for details) using the QuickChange Site-Directed Mutagenesis Kit (Stratagene). Primer design and site-directed mutagenesis was performed according to the manufacturer’s instructions.

3.2.1.4 Construct maps

Most of the constructs were cloned into standard vectors (listed in table 3.1.9) using sites in the multi cloning sequence (see table 3.1.10). Construction and maps of the plasmids carrying the inducible *UMP1* gene in addition to different versions of the *PRE7* gene are anoted below. The sequence encoding FLAG epitope followed by a stop codon was introduced downstream of the *UMP1* gene. This construct was cloned under control of the *GALI* promoter in the pYES2 vector using HindIII and BamHI sites. The *PRE7* region was first cloned from pRS315-PRE7 into pUC19 using SspI and XbaI. Than the *PRE7* fragment was excised with SacI and XbaI from pUC19 and mixed with the SpeI/BamHI fragment carrying *UMP1-FLAG* under the *GAL* promoter from pYES2. These mixed fragments were subjected to “triple” ligation into SacI and BamHI digested pRS415 vector (see Fig 6). The ligation of the fragments leading to loss of XbaI and SpeI resulting in the p15PRE7+UMP1-FLAG construct ([A] PRE7 with complete propeptide coding region). The Pre7 truncated constructs (ubiquitin fusion or methionine fusion constructs) were introduced instead of wild type *PRE7* into the p15PRE7+UMP1-FLAG using the SpeI and NcoI sites at the *PRE7* promoter and terminator region respectively, resulting in p15UBI/pre7+UMP1-FLAG and p15METpre7+UMP1-FLAG constructs ([B] length of the propeptide remnant encoding region are indicated in parenthesis).

**Fig 6**

Maps of plasmids carrying the inducible *UMP1* gene in addition to different versions of the *PRE7* gene

A. The centromeric plasmid contains a gene encoding wild-type Pre7 with its own promoter and terminator, and in addition, the gene encoding Ump1-FLAG under control of the *GAL1* promoter and *CYC1* terminator (see text for details).

B. The sequences encoding different truncated Pre7 versions as ubiquitin fusions or starting with methionine are shown in general as UBI/ppXpre7 or MetXpre7, respectively. Different truncations in the propeptide region are shown in parenthesis (see Fig 8A for more details). These mutant constructs were inserted into the backbone derived from construct A using *SpeI* and *NcoI* in the Pre7 promoter and terminator, respectively.

3.2.1.5 Yeast colony PCR

Yeast colonies freshly grown on plates were picked with a pipetman tip and equal volumes of cells were suspended in 30 μ l of 0.2 % SDS solution. The cells were vortexed for ~ 30 seconds, heated for 4 min at 90 °C and centrifuged for 1 min at 14,000 rpm. The crude DNA in the supernatants was collected. 1 μ l of DNA was used as a template with respective primers in 50 μ l standard PCR mixture (Ausubel et al., 1995) with 2 μ l of 25 % Triton X-100.

3.2.2 Yeast techniques

3.2.2.1 Strain construction

For manipulation and generation of yeast strains, standard yeast genetic methods were used (Ausubel et al., 1995; Guthire and Fink, 1991; Sambrook et al., 1989).

3.2.2.2 Generation of *ump1 Δ ::HIS3* strains and verification by Southern blot analysis

After transformation with a linear fragment containing the *ump1 Δ ::HIS3* allele excised from pJD251 (Ramos et al., 1998), His⁺ colonies were checked for correct replacement of *UMP1* by *ump1 Δ ::HIS3* by using the Southern blot hybridization technique. A 603 base-pair BamHI + SpeI fragment upstream to the *UMP1* promoter region was used for preparation of a labeled DNA probe in accordance to the manufacture's instruction (Amersham - *Fluorescein gene images labelling and detection system, RPN 3340*). The chromosomal DNA was isolated from candidate yeast strains and digested with restriction enzyme ClaI. The digested DNA fragments were separated by agarose gel electrophoresis. The gel was soaked in depurination (250 mM HCl) solution for 8 min, denaturation (1.5 M NaCl and 500 mM NaOH) and neutralization (3M NaCl and 50 mM Tris/HCl) solution for each 10 min. A vacuum blotting unit (Midton acrylics ltd.) was used to transfer the DNA fragments from the agarose gel to a Nylon membrane (Hybond-N+ Amersham) using 20 x SSC buffer (3 M NaCl and 0.3 M Na₃ citrate pH 7.0) for 1 hr.

The dry membrane was exposed to UV light for 5 min. Hybridization and the luminescence detection procedure were carried out as described in the manufacturer's protocols.

3.2.3 Biochemical methods

3.2.3.1 Protein sample preparation and quantification

The yeast cells were harvested after reaching a given OD_{600} or at defined time points. The cells were lysed in lysis solution (0.25 M NaOH with 1% β -mercaptoethanol). The proteins were precipitated with 5.8 % trichloroacetic acid, sedimented and washed with acetone. The dried pellets were resuspended in Laemmli buffer (50 mM Tris-Cl pH 6.8, 2 % SDS, 0.1 % bromophenol blue, 10 % glycerol and 100 mM dithiothreitol or β -mercaptoethanol). Alternatively, the yeast cells were resuspended in 0.1 M potassium phosphate buffer pH 7.0 and lysed in lysis buffer (4.5 % SDS, 2.5 mM EDTA and 2.5 mM EGTA) with glass beads (Egner et al., 1993). The proteins were quantified using the Bradford assay (Bradford, 1976) or according to Lowry et al., 1951 with modifications (Ausubel et al., 1991).

3.2.3.2 Gel electrophoresis and immuno-blotting of proteins

Proteins were separated by SDS-PAGE (Laemmli, 1970) or using Tris-Tricine gel electrophoresis as described (Coligan et al., 2001) except that Tris/HCl, pH 6.8 was used for stacking gel preparation. The protein samples were electro-transferred to nitrocellulose or PVDF membrane (Towbin et al., 1979) by using either a semi-dry system or a wet-blotting system (Bio-Rad). The protein antigens on the membranes were probed with appropriate antibodies. The immunodetection procedure was carried out according to the manufacturer's protocol (ECL-Kit, Amersham Biosciences).

3.2.3.3 Stripping and re-probing of membranes

The antibodies bound to the proteins on the nitrocellulose or PVDF membranes were stripped by using either a harsh stripping buffer (88 mM 2-Mercaptoethanol, 1 % SDS and 62.5 mM Tris/HCl pH 6.7) for 30 min at 50 °C with occasional agitation, or a mild

stripping buffer (200 mM Glycine, 0.2 % SDS and 1 % Tween 20 pH 2.2) depending on the purpose. The antibodies bound to the membrane decorated with proteins derived from native gels are stripped with 0.2 N NaOH in PBS-T (80 mM Na₂HPO₄, 20 mM NaH₂PO₄, 100 mM NaCl and 0.1 % Tween-20) for 20 to 30 min. After stripping the membranes were washed with blotting buffer and treated as described above.

3.2.3.4 Antibody production against the Pre7 subunit and immuno-affinity purification of the anti Pre7 polyclonal antibody

3.2.3.4.1 Antibody production and analysis

The rabbit polyclonal antibody was raised against the synthetic peptide CNQVEPGTNG-KVKKPLKY. This peptide was chosen from a loop region in the Pre7 subunit due to its antigenic and hydrophilic capacity, and because it was expected to be freely accessible by the antibody in native conditions. The synthesized peptide antigen was conjugated with the carrier molecule Hemocyanin, injected into two different rabbits (SA681 and SA682) and the serums were collected periodically (Eurogenetic, Belgium). The received serum antibodies from rabbit SA681 did not show any specific signals against the Pre7 subunit in the western blot analysis, whereas rabbit SA682 serum from third and final bleeding showed specific signal against Pre7 in addition to non-specific signals. Therefore, the serum was subjected to affinity purification of the specific antibody.

3.2.3.4.2 Antigen column preparation

Epoxy-activated Sepharose™-6B medium was used to couple the peptide ligand through the cystine residue. 300 mg of the epoxy-activated sepharose-6B were swelled in 3 ml of H₂O and washed on sintered glass filter with 60 ml H₂O, transferred to 15 ml falcon tubes with 2 ml of the coupling buffer (20 mM disodium hydrogen phosphate and 1.6 % v/v DMF, pH 10.0) and subjected to centrifugation at 500 x g for 1 min. 4 mg of the peptide (CNQVEPGTNGKVKKPLKY) in 150 µl of water was added to the sepharose-6B medium with 1.6 ml of the coupling buffer and incubated for over night at room temperature.

The peptide bound epoxy-activated sepharose-6B medium was washed for five times with 1-2 ml of the coupling buffer by centrifugation at 500 x g for 1min (wash buffer was stored to quantify the coupling efficiency by the Bradford assay). The

remaining active groups on the gel were deactivated or blocked by washing with 2 ml of 1 M Ethanolamine (pH 8.0) and incubated for over night at 40 °C to 50 °C. The antigen bound sepharose-6B medium was washed five cycles of alternating pH. Each cycle consist of a wash with 2 ml of acetate buffer pH 4.0 (0.1 M sodium acetate containing 0.5 M NaCl) followed by a wash with 2 ml of acetate buffer pH 8.0.

The antigen bound epoxy-activated sepharose 6B slurry was filled in to the column (BioRad, #737-1007) carefully without any air bubbles, and immediately 10 ml of PBS pH 7.5 (50 mM Na₂HPO₄, 15 mM NaH₂PO₄ and 75 mM NaCl) containing 30 mM sodium azide were added. The column was stored at 4 °C.

3.2.3.4.3 Antibody purification

The crude rabbit serum was equilibrated at room temperature, centrifuged at 20,000 g for 4 min and subjected to the column, prepared as described above (binding efficiency was quantified by the Bradford method). The column was washed with 30-50 ml PBS pH 7.5 and the antibodies were eluted with 15 ml of 0.1 M glycine pH 2.8. The antibodies were collected as 1 ml aliquots in 1.5 ml tubes containing 80 µl of 1 M Tris-Cl pH 8.0. Eluted antibodies were concentrated by centrifugation in macrosepTM centrifugal concentrators (Filtron, 30K) at 3000 g for 60 min in a swinging bucket rotor and the concentrated antibodies were stored with 20 % Glycerol at -80 °C.

3.2.3.5 Fractionation of whole-cell extracts by gel-filtration

Yeast cells were grown at 30 °C in YPD to OD₆₀₀ = 1.4 (± 0.1), harvested at 3000 g, washed with cold water, frozen in liquid nitrogen, and stored at -80 °C. 1000 mg of yeast pellets as dissolved in 1 ml of extraction buffer (50 mM Tris-HCl (pH 7.5), 2 mM ATP, 5 mM MgCl₂, 1 mM DTT and 15 % glycerol). The cell paste was ground to a powder in a mortar in the presence of liquid nitrogen. The cell extracts were centrifuged at 31,000 g for 10 min at 2 °C and the supernatant was subjected to a second centrifugation at 60,000 g for 30 min. The extracts yielded the protein concentration of ~ ±5 mg/ml, which was adjusted with extraction buffer. By using the FPLC system (Pharmacia), 200 µl samples of the extract were chromatographed on a Superose-6 column with extraction buffer. The flow rate was 0.3 ml/min and fractions of 0.6 ml were collected. The Superose-6 column

was calibrated using the following standards: thyroglobulin (669 kDa), ferritin (443 kDa) and bovine serum albumin (66 kDa). The dextran blue was used to monitor the void volume.

3.2.3.6 Pulse-chase analysis and immuno-precipitation analysis

Cells were grown at 30 °C until an OD₆₀₀ of 0.8 and pulse labeled with ³⁵S-methionine (Redivue promix, Amersham) for 5 min at 30 °C in synthetic medium lacking methionine (Bartel et al., 1990), followed by a chase in synthetic medium containing cold 40 mM methionine (unlabelled) and 0.2 % BSA. The cells were precipitated with 10 % TCA and the pellets were washed once with cold acetone. The pellets were resuspended in 100 µl Di-buffer (90 mM Na-HEPES pH 7.5, 30 mM dithiothreitol and 2 % SDS) and incubated at 100 °C for 3 min. 1 ml of LZ5 Buffer (50 mM Na-HEPES pH 7.5, 150 mM NaCl, 5 mM EDTA, 5 % Glycerol and 1 % Triton X100) with protease inhibitor (Complete™ Inhibitor-Cocktail, Roche) was added to the lysate, which was then centrifuged at 12,000 x g for 10 min. Immuno-precipitation was carried out with the supernatants by adding ascetic fluid containing the anti-Pre4 antibody for 1-4 hrs at 4 °C. The samples were then incubated with 7 % sepharose ProA beads for 1 hr at 4 °C. The beads were washed for 3-4 times with 0.9 ml of LZ5 buffer, resuspended in electrophoresis sample buffer and heat-denatured at 95 °C for 3 min. The proteins samples were separated on SDS-PAGE and subjected to fluorography.

3.2.3.7 Non-denaturing PAGE and an in-gel protease assay

Non-denaturing PAGE and an in-gel assay using the fluorogenic substrate Suc-LLVY-AMC were carried out as described (Glickman et al., 1998a), with following modifications. The native-polyacrymaid gels were prepared by mixing 3.5 % acrylamide, 0.01 % APS, 0.01 % TEMED and 2.5 % sucrose in native-gel buffer (90 mM Tris, 2.5 mM MgCl₂, 0.5 mM EDTA, 1 mM ATP and 1 mM DTT, pH 8.35). Xylene cyanol was added to the protein samples prior to loading. Native protein extracts were separated in the gel using native-gel buffer at 4 °C for 2 hrs. To visualize proteolytic activity in the proteasome complexes, the gel was overlayed with 0.1 mM Suc-LLVY-AMC in buffer A

(30 mM Tris-HCl (pH 7.8), 5 mM MgCl₂, 10mM KCl, 0.5mM DTT and 2 mM ATP) for 10-20 min at 37 °C.

3.2.3.8 Non-denaturing PAGE and immuno-blotting analysis

Proteins in crude extracts were fractionated in non-denaturing gels as described above. The gels were incubated with transfer buffer (Towbin, 1979) containing 2 % SDS for 20 min at room temperature. The proteins in the gel were transferred onto nitrocellulose membrane by the semi-dry blotting method (Bio-rad). Transfer was carried out for 2-3 hrs at 80 mA with transfer buffer containing 0.1 % SDS. The membrane was incubated with 0.025 N NaOH for ~ 30 min at room temperature and optionally boiled for 2-3 min. Protein antigens were probed with the appropriate antibody and immuno-detection was done according to manufacturer's instruction (ECL-Kit, Amersham).

3.2.3.9 Assays for proteolytic activities with fluorogenic peptide substrates

To determine the chymotrypsin-like activity, 50 µl of the protein fraction and 10 µl of 1.5 mM succinyl-Leu-Leu-Val-Tyr-7-amido-4- methylcoumarin in 75 mM Tris-HCl (pH 7.8), 2 mM ATP, 15 mM MgCl₂ were mixed and incubated for 15 min at 37 °C. The reaction was stopped by adding of 960 ml 99 % ice-cold ethanol, and the fluorescence was measured at 460 nm, using an excitation wavelength of 380 nm. The trypsin-like activity and the peptidylglutamyl peptide-hydrolyzing activity were determined using Cbz-Ala-Ala-Arg-4MeO-β-naphthylamide and Cbz-Leu-Leu-Glu-β-naphthylamide, respectively as fluorogenic peptide substrates (Fischer et al., 1994). The volume of the protein fraction was 150 µl and 75 µl for trypsin-like and PGPH activity respectively. The reactions were stopped after 270 min incubation at 37 °C by adding 200 µl of 0.2 M citrate buffer with 4 % Tween-20, pH 6.4. The fluorescence emission was measured at 425 nm, using an excitation at 340 nm for trypsin-like activity and PGPH activity was measured at 410 nm using an excitation at 340 nm.

3.2.3.10 Induction of Ump1 protein expression and immunoblot analysis

Strains expressing Ump1-FLAG under control of the *GALI* promoter were grown in SR medium (synthetic medium with 2 % raffinose) until $OD_{600} \sim 0.7$ and 2 % galactose were added to the culture, defining the zero time point. Cells were collected at the different time points of proceeding incubations, frozen in liquid nitrogen and stored at -80°C . The cells were lysed in extraction buffer with complete protease inhibitors (Complete™ EDTA-free, Roche). The extracts were centrifuged at 20,000 g for 10 min at 4°C and the supernatant was subjected to a second centrifugation at 31,000 g for 10 min at 4°C . The protein concentration of extracts was normalised with extraction buffer and subjected to non-denaturing PAGE. The gels were incubated with 2 % SDS in blotting buffer and transferred to nitrocellulose membrane with blotting buffer containing 0.2 % SDS by using a semi-dry blotting system. The membrane was boiled for 3 min and processed as described above. Alternatively, the cells were lysed in denaturing conditions using lysis solution or glass beads as described above. The standard immunoblotting procedure was used to detect protein antigen using the appropriate antibody.

3.2.3.11 Fusion protein expression in *E. coli*

The expression plasmid pGEX-4T (Pharmacia) containing the *GST-UMPI* hybrid gene under an inducible promoter was introduced into *E. coli* BL21-Codon Plus. Cells were grown until $OD_{550} = 0.4$ in LB ampicillin (75 $\mu\text{g/ml}$) medium at 37°C . The protein expression was induced by addition of 0.1 mM IPTG and followed by growth for 3-4 hr at 30°C . The cells were collected by centrifugation at 5,000 g for 10 min at 4°C and resuspended in 10 ml of ice-cold PBS (140 mM NaCl, 2.7 mM KCl, 10 mM Na_2HPO_4 and 1.8 mM KH_2HPO_4 , pH 7.3) with complete protease inhibitors (Complete™ EDTA-free, Roche). The cells were lysed by sonication. 1 % Triton X 100 was added to the lysate and incubated for 30 min at room temperature in an overhead shaker. The lysate was centrifuged at 10,000 g for 10 min at 4°C and the supernatant was subjected to pull-down or binding assay.

3.2.3.12 Binding of proteasome complexes to immobilized GST-Ump1

The GST-Ump1p fusion proteins were expressed in *Escherichia coli*, as described above and incubated with Sepharose 4B in PBS-T pH 7.3 (PBS with 0.5 % Triton X-100) for ~ 3 hrs at 4 °C. The column was washed with PBS-T for three times. Yeast cells were lysed as described above to obtain native cell extracts. The native protein extracts were added to the column coupled with GST-Ump1 and incubated for over-night at 4 °C. The column was washed 4-5 times with PBS containing protease inhibitors (Complete™ Inhibitor-Cocktail, antipain, pepstatin, chymostatin, leupeptin and PMSF). The proteins residing in the column were eluted using urea buffer (10 M Tris, 8 M urea, 5 % SDS and 1.5 % DTT) and denatured for 5-10 min at 95 °C. Samples were separated in SDS-PAGE and subjected to immunoblot analysis.

3.2.3.13 *In vitro* transcription/translation and interaction assay

The open reading frames encoding the proteasomal subunits Pre7, Pre2 and Pre4 were amplified under standard PCR conditions and cloned into the pGEMT easy vector (Promega). For convenient *in vitro* expression of the cloned genes they are subsequently inserted into the pTNT™ vector (Promega) under control of the T7 promoter. 0.5 µg plasmid DNA was added to 25 µl of a coupled T7 transcription /translation mixture (rabbit reticulocyte lysates (TNT kit, Promega), with 1 µl (0.37 mbq) of ³⁵S methionine (Redivue promix, Amersham) and appropriate RNase inhibitors (20 µg of recombinant RNasein, Promega). The lysate mixture was incubated at 30 °C for 90 min. The translated proteins were analysed by SDS-PAGE and autoradiography. Equal amounts of labeled proteins were used to study the interaction using GST-pull down or binding assay.

The *E. coli* expressed GST-Ump1 was added to the Sepharose-4B column that is equilibrated with PBS-B1 buffer (PBS with 1 % BSA) and incubated for 3-4 hrs. The column was washed for two times with PBS-B1 buffer and once with PBS-B5 buffer (500 mM NaCl in PBS-B1 buffer). The *in vitro* translated proteins were added to the GST-Ump1 bound Sepharose-4B column in PBS-B1 buffer and incubated for 3-4 hrs. The column was washed two times with each PBS-B1, B2, B3 and B5 buffer (PBS buffer containing 140 mM, 260 mM, 380 mM and 500 mM NaCl, respectively). The bound

proteins were eluted using Laemmli buffer and denatured for 5-10 min at 95 °C. Proteins were fractionated in SDS-PAGE and subjected to fluorography analysis to detect the labeled proteins.

4 Results

4.1 Genetic analysis of the requirements of proteasomal β -subunit propeptides

4.1.1 The β 6/Pre7 propeptide is essential for yeast cell viability, in contrast to the propeptides of other inactive β -type proteasome subunits

An inspection of the yeast 20S proteasome crystal structure exhibits the partially processed propeptide remnants of the inactive subunits β 7/Pre4 and β 6/Pre7 as well as the short unprocessed β 3/Pup3 propeptide to be located at the restrictions separating the central cavity from the antechambers (Fig 6) (Groll et al., 1997). In the case of the Pre4 subunit, genetic deletion of the propeptide including the remnant piece has been shown to allow normal growth of the cells (Jäger et al., 1999). This elucidated that the entire propeptide was not required for the proteasome assembly and that even the eight residue Pre4 propeptide remnant was dispensable for proteasomal function. In order to complete the studies on the propeptide functions in the proteasome, the analysis was extended to the other two inactive β -type subunits Pre7 and Pup3. To create a Pre7- Δ pp strain, the *mmPRE7* allele encoding only the “mature moiety” (abbreviated mmPre7) of the subunit was created using the same approach as for the Pre4 truncation (Jäger et al., 1999), by replacing the propeptide encoding portions with the ubiquitin (*UBI*) gene (Fig 7A). The resulting fusion protein was expected to be split co-translationally into the “mature moiety” of the Pre7 subunit and free ubiquitin by ubiquitin C-terminal hydrolases (Bachmair et al., 1986), thus exposing a N-terminal glycine of the β 6/Pre7 subunit that corresponds to Thr1 of the active subunits. A different approach was used to create a Pup3- Δ pp strain expressing the Pup3 subunit without propeptide region (*mmPUP3* allele). Here, the prosequence region in the *PUP3* gene was deleted and a start codon was introduced instead (Fig 7A). The constructs were cloned into a centromeric, *LEU2*-marked yeast/*Escherichia coli* shuttle plasmid and introduced into haploid yeast cells carrying the respective chromosomal gene deletion complemented by the wild-type gene on a *URA3*-marked centromeric plasmid. The strains possessing only the modified gene variants in the *LEU2*-marked centromeric plasmid were obtained on solid synthetic media

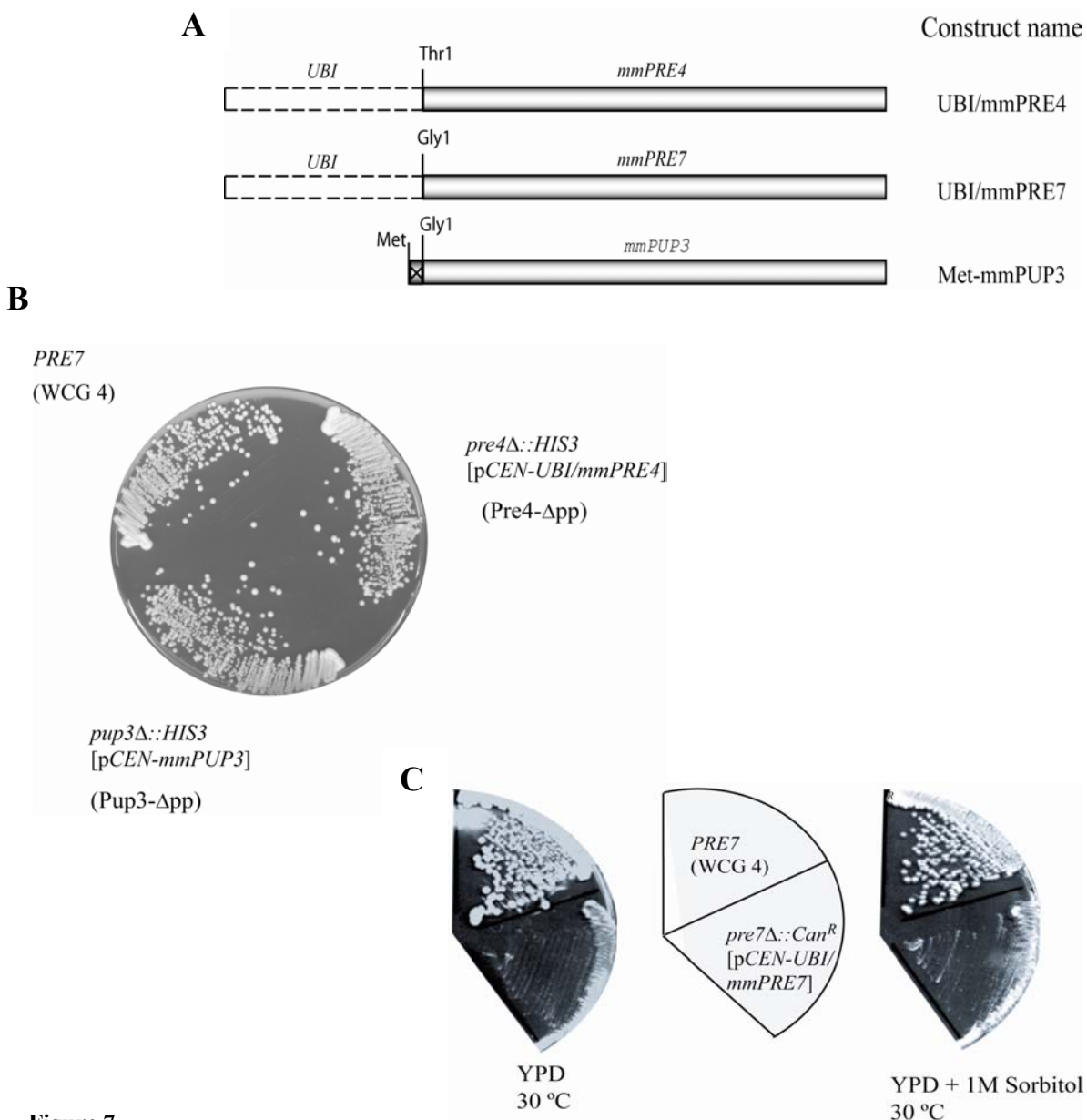


Figure 7
Deletion analysis of propeptides of inactive β -type subunits

A. Schematic representation of constructs encoding inactive β -type subunits without propeptides. In the *PRE4* and *PRE7* genes the propeptide encoding regions were replaced by the ubiquitin gene (*UBI*, dotted box) resulting in hybrid genes under control of their original proteasomal promoters encoding N-terminal fusions of ubiquitin to the “mature moiety” (mm, closed box) of the proteasomal subunits (see text for more details). The propeptide encoding region of *PUP3* was replaced by a start codon (Met, crossed box) resulting in a mutant allele of *PUP3* expressing the Pup3 subunit lacking the 8 residue propeptide region. B, C. Colony growth of yeast strains harbouring mutant constructs UBI/mmPRE4, Met-mmPUP3 (B) and UBI/mmPRE7 (C). Mutant alleles in *LEU2*-marked centromeric plasmids were introduced by plasmid shuffling into haploid yeast strains containing a deletion of the respective wild-type gene on the chromosome. Transformants were streaked on solid YPD plates and grown at 30 °C for two days to compare the colony growth with a wild-type strain (WCG4). Strains carrying plasmids with Met-mmPUP3 or UBI/mmPRE4 were able to produce colonies as the wild-type cells (B). Cells possessing the UBI/mmPRE7 plasmid rarely survived on 5-FOA plates, which resulted in few slow growing colonies (see text for more details). The strong growth defect of one such exception is shown in streaks on YPD and YPD-Sorbitol plates (C).

lacking leucine and containing 5-fluoro-orotic acid (5-FOA) for counter-selection against *URA3* (“plasmid shuffling”). The appropriate control strains were obtained in the same manner by introducing *LEU2*-marked plasmids containing the respective wild-type gene.

The Pup3- Δ pp strain expressing the Pup3 subunit without propeptide region grew on 5-FOA plates as fast as the *PUP3* wild-type control strain. On solid YPD, it produced colonies similar to the wild-type (WCG4) cells (Fig 7B), suggesting that these eight Pup3 propeptide residues are not required for yeast cell viability and do not contribute to any function of the proteasome.

Surprisingly, the strain transformed with the plasmid carrying the *UBI/mmPRE7* allele did not yield any visible colonies on the 5-FOA plate after 3 days, although some small heterogeneous colonies appeared after longer incubation with low frequency. This effect is likely to depend on the spontaneous background mutations that eventually lead to production of suppressor clones (Fig 7C). Hence, the propeptide of the Pre7 subunit apparently is essential for yeast cell viability. It might be required during proteasome assembly or for other functions in the mature 20S proteasome.

4.1.2 The propeptide remnant in the Pre7 subunit is necessary for proteasome function

In order to know whether the entire 28 residue propeptide of the Pre7 subunit is essential or the short nine residue propeptide region that remains attached in the mature particle is sufficient for yeast cell viability, the *UBI/Q-9PRE7* allele was created. The sequence encoding the N-terminal 19 residues (Fig 8A: -28→ -9) in the Pre7 propeptide, which are cleaved off upon proteasome maturation, was removed and replaced by the ubiquitin gene. The resulting construct, named UBI/Q-9 (or Q-9) expresses a hybrid protein from the *PRE7* promoter that will be split into ubiquitin and the β 6/Pre7 subunit containing the natural propeptide remnant starting from the Q-9 residue (Fig 8A). Strains bearing the UBI/Q-9 construct were able to grow as wild-type cells (Fig 8B), showing that the propeptide remnant of the Pre7 subunit is sufficient for normal yeast cell viability and accommodates a crucial role for the proteasome.

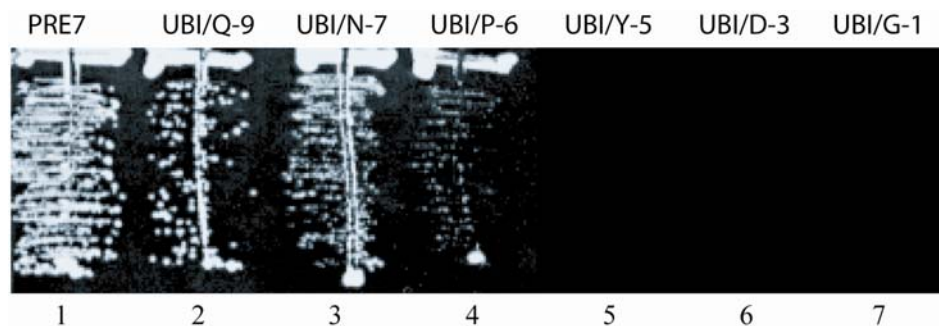
In order to determine the length of the Pre7 propeptide remnant that would be sufficient for the proteasome function, the plasmid containing the *UBI/Q-9PRE7* allele was exploited to truncate the amino acids in the N-terminus of the Pre7 propeptide remnant stepwise by using site-directed mutagenesis techniques. The resulting constructs expressing different lengths of the propeptide remnant region are *UBI/N-7*, *UBI/P-6*, *UBI/Y-5*, *UBI/D-3* and *UBI/G-1* (Fig 8A). These constructs were introduced into yeast as described above. Only the strains possessing the *UBI/N-7* or *UBI/P-6* constructs were able to produce colonies on the 5-FOA plate, whereas the other constructs failed to confer growth on 5-FOA plates (Fig 8A, indicated as (+/-) symbols). Furthermore, the strains expressing the truncated Pre7 subunits starting with N-7 and P-6 (*UBI/N-7*, *UBI/P-6*) showed gradually increased growth defects (Fig 8B 3 and 4) as compared to *UBI/Q-9* or wild-type strains (Fig 8B 1 and 2). Therefore, at least six residues in the propeptide remnant of the Pre7 subunit are necessary for yeast cell viability, and the nine propeptide residues that remain attached in the mature subunit are required for normal cell growth.

It is known that the *in vivo* half-life of a protein can depend on the identity of its N-terminal residue, according to the N-end rule (Varshavsky, 1995). Since two of the alleles, *UBI/Y-5PRE7* and *UBI/D-3PRE7*, that did not yield any viable strains (see above), code for truncated Pre7 subunits with destabilizing tyrosine and aspartic acid residues at their N-termini, respectively, limiting amounts of these mutant Pre7 variants could not be excluded to cause the lethal effect. To clarify this question and to avoid the fusion protein approach, the ubiquitin gene from the respective constructs was exchanged against a start codon, resulting in the Met Y-5 and Met D-3 constructs (Fig 8C). Surprisingly, the strain expressing the Met Y-5 construct was viable, but showed a growth phenotype (not shown) similar to that of strains carrying *UBI/P-6* (Fig 8B 4). However, the strain possessing Met D-3 was not able to produce any viable clones on the 5-FOA plate. These results confirm the requirement of the six residues in the propeptide of the Pre7 subunit for survival and show that a proline at position -6 is not essential for their function. Nevertheless, lethality caused by instability of the *UBI-Y5Pre7* mutant variant formally cannot be ruled out by these results. However, the steady state level of this variant in the cell disputes this possibility (see chapter 4.2.5).

A

Constructs	Pre7 propeptide truncations	Viability
PRE7	⁻²⁸ MATIASEYSSEASNTPIEH QFN PYGDNG G1::: ⁻⁹ <i>proc-pp</i>	+++
UBI/Q-9	:::GG QFN PYGDNG G1:::	+++
UBI/N-7	:::GG NP YGDNG G1::: ⁻⁷	++
UBI/P-6	:::GG P YGDNG G1::: ⁻⁶	+
UBI/Y-5	:::GG Y GDNG G1::: ⁻⁵	-
UBI/D-3	:::GG D NG G1::: ⁻³	-
UBI/G-1	:::GG G G1::: ⁻¹	-

B



C

Construct	Amino acid alterations in Pre7 propeptide	Viability
Met Y-5	MY GDNG G1:::	+
Met D-3	MD NG G1:::	-
UBI/E3-9	:::GG VNKGEVSLG G1:::	-
UBI/P3-8	:::GG SDPSSINGG G1:::	-
UBI/P3-8*	:::GG SDP <u>R</u> SINGG G1:::	-

Figure 8

Analysis of truncations and replacements of the β 6/Pre7 propeptide

A. Truncated Pre7 constructs and their growth behaviours are represented schematically. Amino acid sequences and their positions in the Pre7 propeptide region are indicated. The region with bold letters represents the remnant residues, which stay in the mature proteasome (see text for more details). The G1 (Gly1) corresponds to T1 (Thr1) of the active subunits and the three colons (:::) represent the continuation of the wild-type Pre7 protein sequence after G1. The UBI/Q-9 construct expressing Pre7 in the processed form with propeptide remnant (position -9 \rightarrow -1) and N-terminally fused ubiquitin (===GG) (for more details see Fig 1) was used to make further truncations of the propeptide remnant (highlighted regions). The respective N-termini of the mature subunits (N-7, P-6, Y-5, D-3 and G-1) are indicated on the top of each construct. Strains transformed with these constructs were checked for viability after counterselection against the *URA3*-marked *PRE7* wild-type plasmid (see text for details). Their growth behaviours are represented as follows: strains producing colonies of the same size as the wild type (+++), strains with impaired growth (++) , strains with strong growth defect (+) and non-viable strains (-) (compare with B). Continue to next page for B and C

B. Growth of strains expressing different Pre7 mutant versions (see A) is shown in streaks. The 5-FOA resistant clones were streaked on solid YPD and incubated at 30° C for 2 days. At lane 5 to 7 no streaks were made, indicating that no viable strains were obtained on the 5-FOA plate.

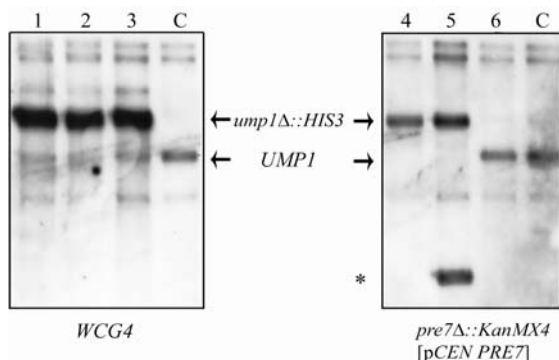
C. The hybrid constructs UBI/Y-5 and UBI/D-3 (see A) were modified to express the truncated Pre7 subunit alone by removing the ubiquitin coding region and introducing a methionine (M/Met) codon resulting in constructs Met Y-5 and Met D-3 respectively. In addition, the propeptide remnant in the construct UBI/Q-9 was replaced by respective propeptide sequences from Pre3 and Pup3, resulting in the hybrid subunits UBI/E3-9, UBI/P3-8 and UBI/P3-8* (* denotes a point mutation, see underlined amino acid).

These constructs were introduced into the haploid yeast strain containing the *pre7Δ::KanMX4* gene deletion on the chromosome, complemented by the *PRE7* allele on a *URA3* marked centromeric plasmid. Viability (+/-) was checked after 5-FOA counterselection.

Proteasome subunits of a given species share ~ 20 to 40 % identical residues, although the prosequences of the subunits do not show any similarity. In the case of Pre7, the six amino acids in the propeptide remnant were found to be essential and the replacement of the proline at the -6 position to methionine was functional. Therefore, to examine whether the function of the propeptide remnant would be sequence specific it was replaced by corresponding prosequence stretches of similar length from the active β 1/Pre3 and the inactive β 3/Pup3 subunit, resulting in constructs UBI/E3-9 and UBI/P3-8, respectively (Fig 8C). These coding regions were introduced by PCR-based mutagenesis, which resulted in an additional variant carrying a point mutation in the Pup3 prosequence region (UBI/P3-8*, (Fig 8C)). This construct was also subjected to further studies. The strains expressing these hybrid constructs were not able to grow on the 5-FOA plate, suggesting that the amino acid sequence in the propeptide remnant of the Pre7 subunit is crucial for its function and replacement of this region by corresponding regions from other β -type subunits results in production of mal-functional subunits.

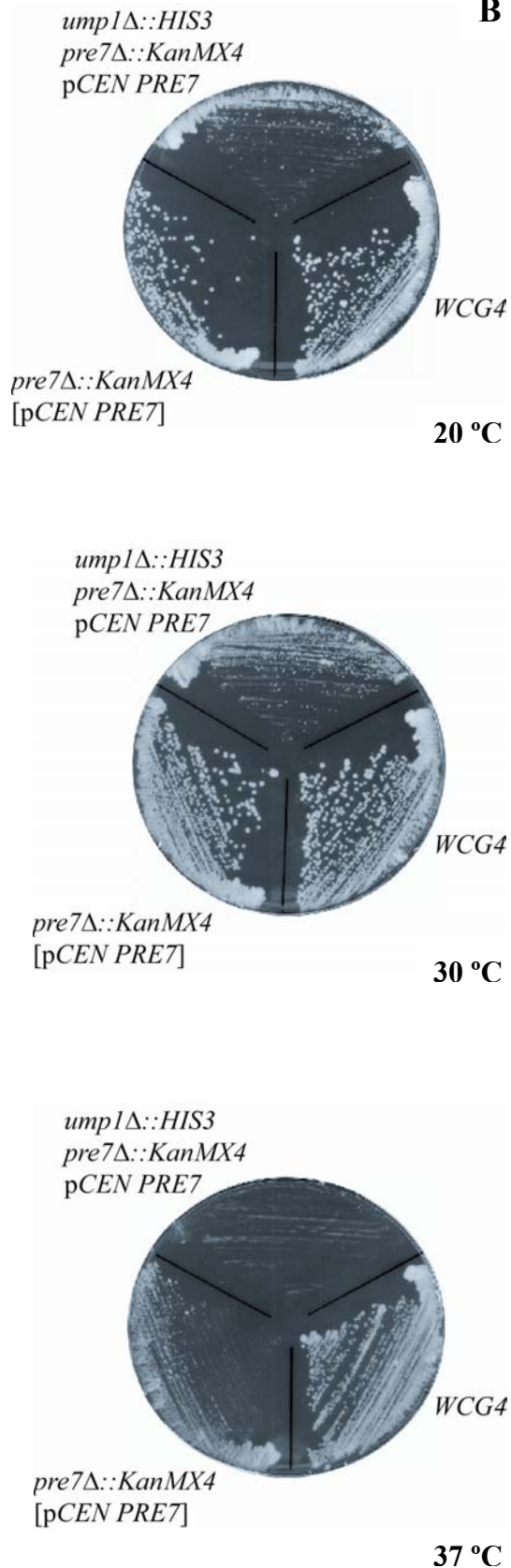
4.1.3 Deletion of *Ump1* suppresses lethality caused by the Pre7 propeptide deletion

Similar to the Pre7 propeptide deletion effect, the propeptide of Pre2 was found to be essential for yeast cell viability (Chen and Hochstrasser, 1996). Remarkably, this lethal effect was suppressed by deleting the *UMPI* gene, which encodes a chaperone-like factor involved in the proteasome assembly process (Ramos et al., 1998). In order to examine

A**Figure 9**Chromosomal disruption of the *UMP1* gene

A. Strains transformed with an *ump1Δ::HIS3* fragment were analyzed by Southern blot to demonstrate that the *UMP1* locus on the chromosome is converted to the *ump1Δ::HIS3* allele. A DNA fragment upstream to the *UMP1* promoter was labeled and probed against the total DNA of candidate transformants that was digested by a specific restriction enzyme (see methods). Each 3 transformants of wild-type strain WCG4 and of a strain carrying *pre7Δ::KanMX4* on the chromosome (complemented by a plasmid encoding *PRE7*) were compelled for *UMP1* disruption. Bands diagnostic for *UMP1* and the disrupted *ump1Δ::HIS3* locus are marked in transformed candidates (1 to 3 and 4 to 6) and in untransformed control strains (C). One of the *PRE7 ump1Δ* strains (lane 1 to 3) and the *pre7Δ::KanMX4* shuffle strain with *ump1Δ* (lane 4) were chosen for further analysis. The * symbol marks an additional hybridizing fragment resulting from further chromosomal alterations.

B. Growth comparison of the *ump1Δ pre7Δ::Δ KanMX4* shuffle strain with the wild type strain and the *pre7Δ::KanMX4* shuffle strain. The strains were streaked on YPD plates and incubated for 2 days at 20 °C, 30 °C and 37 °C, as indicated.

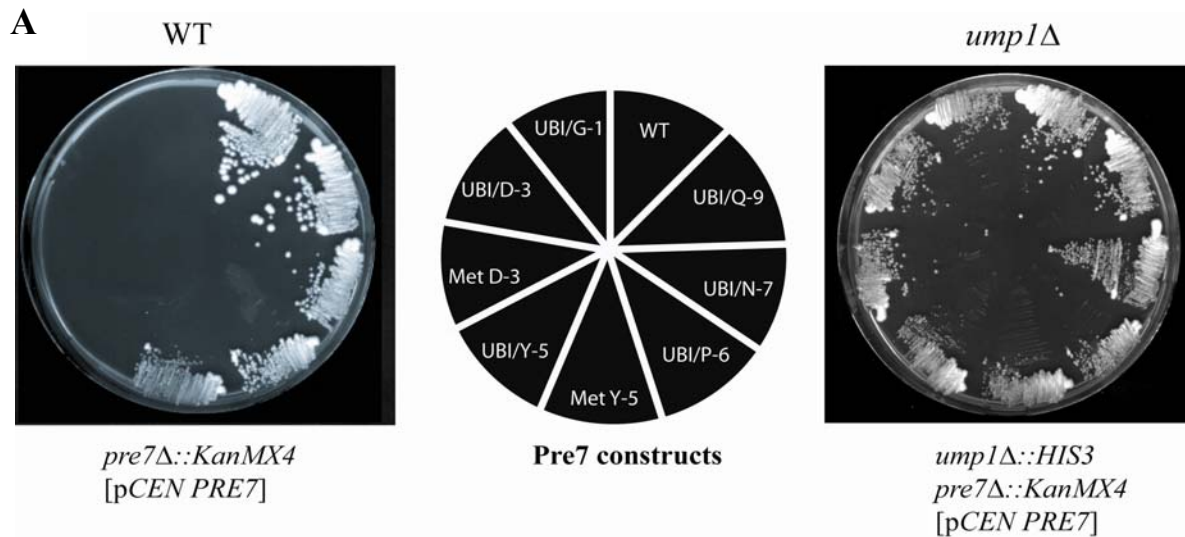
B

the effect of the propeptide deletion in the Pre7 subunit in the absence of Ump1, *ump1Δ* strains were created, as described in Ramos et al., 1998. The gene disruption was carried out in haploid yeast cells carrying the *pre7* deletion on the chromosome complemented by *PRE7* on a *URA3*-marked centromeric plasmid (shuffle strain), into which the mutant constructs can be introduced as described above. In addition, the *UMPI* gene was disrupted in the wild-type strain.

The chromosomal *UMPI* gene disruption was confirmed by Southern blot analysis using appropriate wild-type controls (Fig 9A). The resulting WCG4-derived *ump1Δ* strain grew slower than the wild type at 30 °C and was severely impaired in growth at higher temperatures (data not shown), which corresponds to the reported growth behaviour of *ump1Δ* strains (Ramos et al., 1998). Accordingly, the *pre7Δ::KanMX4* shuffle strain with *ump1Δ* grew slower than its *UMPI* counterpart at 20 °C or 30 °C and failed to grow at 37 °C (Fig 9B).

To examine the Pre7 propeptide deletion effect in the *ump1Δ* background, the truncated Pre7 constructs (Fig 8A & 8C) were introduced as described above into the Pre7 shuffle strain carrying *ump1Δ*. Surprisingly all constructs expressing truncated Pre7 variants (Fig 8A & 8C) allowed survival on 5-FOA plates with almost similar growth rate of the cells (Fig 10A and B) in contrast to the situation in the wild-type background, where the growth phenotype of the viable mutants was strengthened gradually along with the propeptide remnant truncation (Fig 10A). However, for the 3 variants of Pre7 carrying heterologous replacements of the propeptide remnant only the *ump1Δ* strain possessing the mutant hybrid construct UBI/P3-8* was able to produce colonies on 5-FOA plate (Fig 10B).

These results elucidate that the propeptide deletion effects observed in wild type can be suppressed by *ump1Δ*, but not the defects caused by hybrid Pre7 subunits carrying heterologous propeptide remnants. The growth of *ump1Δ* cells carrying the Pup3/Pre7 hybrid subunit with a point mutation at the -5 position already points to a putative function of this position in the subunit (see chapter 4.3).

**B**

Construct	Replaced propeptide sequence	Viability and strain background	
		<i>WT</i>	<i>ump1Δ</i>
UBI/E3-9	:::GG VNKGEVSLG G1:::	-	-
UBI/P3-8	:::GG SDPSSINGG G1:::	-	-
UBI/P3-8*	:::GG SD <u>P</u> RSINGG G1:::	-	++

Figure 10

Growth comparison of the *pre7* mutants in *UMP1* and in *ump1Δ* background

A. Strains expressing different Pre7 mutant constructs (see Fig 8) in wild type (*UMP1*) and in *ump1* deletion (*ump1Δ*) background were streaked on YPD plates (non-viable strains were not streaked), as indicated in the cartoon. The plates were incubated for 2 days at 30 °C.

B. The viability of strains carrying the hybrid subunits (see Fig 8C) is represented schematically (+/-, as in Fig 8).

4.1.4 The Pre7 propeptide does not function as separate component

The propeptide of Pre2 is indispensable for cell viability in yeast (Chen and Hochstrasser, 1996). However, this propeptide was shown to operate *in trans* as a chaperone-like component allowing proteasome assembly in the presence of Ump1 (Chen and Hochstrasser, 1996; Ramos et al., 1998). In order to analyze whether the Pre7 propeptide can

function as a separate peptide, the entire propeptide coding region was cloned under the constitutive *TDH3* promoter and sequences encoding an epitope derived from the influenza hemagglutinin (HA) were introduced to the 3' end, followed by a stop codon and the *PHO5* terminator. This synthetic gene was inserted upstream of the *UBI/mmPRE7* construct resulting in construct PP+*UBI/G1* (Fig 11).

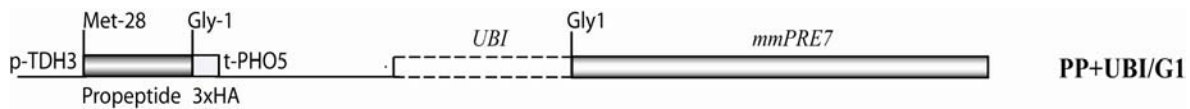


Figure 11

Functional analysis of the Pre7 propeptide as separate peptide

A cartoon showing the PP+*UBI/G* construct that expresses the Pre7 propeptide as a HA-tagged, individual polypeptide (see text for more details).

This construct was not able to confer the viability to a strain carrying *UBI/mmPRE7* allele (data not shown). However, the conclusion that the propeptide cannot serve as separate factor cannot be drawn. Due to its short length and lack of any folding, it might be rapidly degraded. In addition, interference of the epitope tag with a putative Pre7 propeptide function *in trans* cannot be excluded.

4.1.5 The *pre1-1* mutation does not suppress the Pre7 truncation phenotype

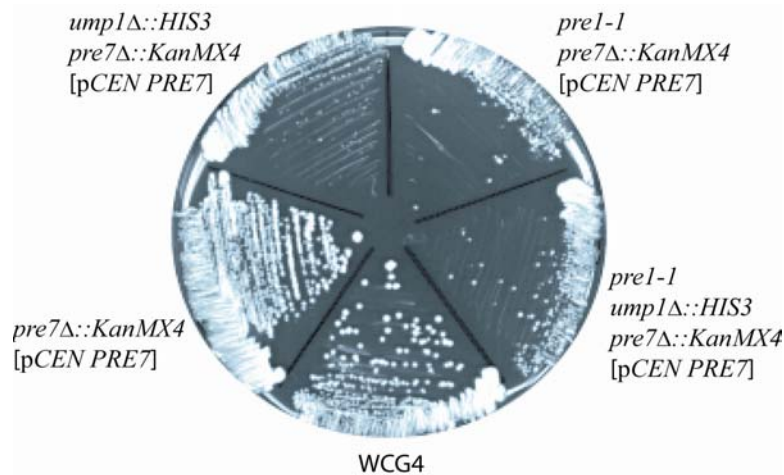
During the proteasome assembly process, the Ump1 protein serves two functions: It was found to promote the dimerization of two half proteasomes and to trigger in addition the maturation of β -subunit precursors (Ramos et al., 1998). The lethal effect of the Pre7 propeptide deletion was suppressed by *ump1 Δ* (Fig 10B). An important question was whether the suppression effect was specific for *ump1 Δ* or whether other mutations in the

proteasome that affect its assembly or maturation could also act as suppressors. One could imagine that for example any retardation of the halfproteasome dimerization could allow incorporation or correct folding of the truncated Pre7 subunit that in the normally proceeding process is too inefficient and becomes rate-limiting. Therefore, the fast dimerization of assembly intermediates could lead into dead-end assembly products.

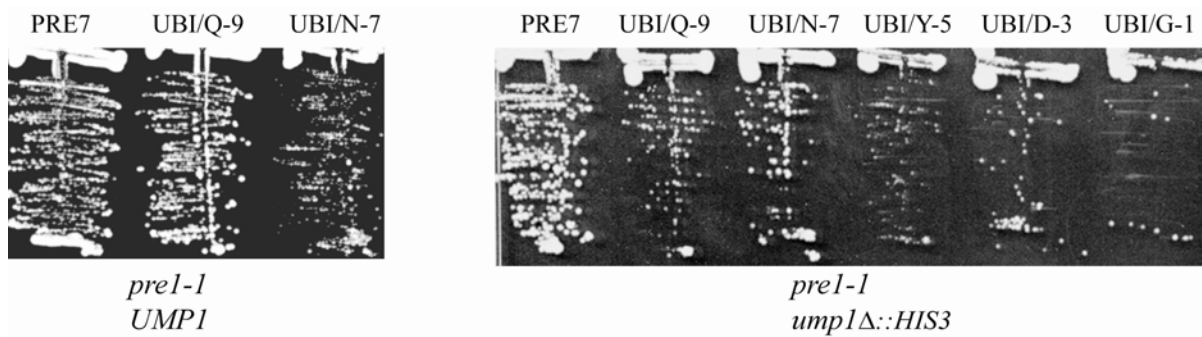
A mutation in the H3 helix of the proteasomal subunit β 4/Pre1 (*pre1-1*) was found to interfere with the contacts between β 4/Pre1 and the β 5/Pre2 subunit in the opposite ring. Hence, processing of the Pre2 subunit was impaired in the *pre1-1* strains and even processed Pre2 did not gain chymotrypsin-like activity (Chen and Hochstrasser, 1996). However, a conceivable effect of this *pre1-1* mutation on half proteasome dimerization has not been reported, but cannot be excluded. To test the effect of Pre7 truncations in the *pre1-1* background, a *pre1-1* strain (Heinemeyer et al., 1993) was crossed with Pre7 shuffle strains (*pre7 Δ ::KanMX4* and *pre7 Δ ::KanMX4 ump1 Δ* , see Fig 9B) and the diploids were sporulated to isolate *pre1-1* and *pre1-1 ump1 Δ* Pre7 shuffle strains. The *pre1-1* Pre7 shuffle strain grew slower, but the *pre1-1 ump1 Δ* Pre7 shuffle strain produced slightly bigger colonies, when compared to their *PRE1* counterparts, respectively (Fig 12A). The constructs (see Fig 8A & 8C) carrying truncated Pre7 versions were introduced into the single and double mutant shuffle strains, as described above. Apparently, the *pre1-1* mutation was unable to suppress the effect of the Pre7 propeptide deletion. Interestingly, the mutation in Pre1 further strengthened the phenotype of strains harboring the UBI/N-7 construct (Fig 12B). Moreover, *UMPI* strains possessing UBI/P-6 or Met Y-5 were unable to grow on 5-FOA plates (not shown). However, all of the Pre7 mutant constructs (see Fig 8A & 8C) were able to produce viable clones in the double mutant background which showed a similar growth rate (Fig 12B).

These results reveal that the defects in proteasome maturation caused by *pre1-1* do not suppress the defects originating from Pre7 propeptide truncations. However, they do not rule out that other mutations specifically affecting half proteasome dimerization can act as suppressor similar to *ump1 Δ* .

A



B

**Figure 12**

The effect of the *pre1-1* mutation in *pre7* mutant strains

A. Growth of *pre7::KanMX4* and *ump1Δ::HIS3 pre7::KanMX4* shuffle strains with or without *pre1-1* mutation was compared with a wild-type strain on a YPD plate.

B. *pre7* mutant constructs (as in cartoon of Fig 4) were introduced into Pre7 shuffle strains carrying *pre1-1* and either *UMP1* or *ump1Δ*. 5-FOA resistant clones were streaked on YPD plate to show the growth phenotypes. The plates were incubated at 30 °C for 2 days.

4.1.6 Genetic evidence for Ump1 independent propeptide functions in proteasome assembly intermediates

The propeptides of β -type precursor subunits are likely to play a role in the interaction of Ump1 with the half-proteasome complex. This is indicated by the finding that the essential Pre7 and Pre2 propeptides become dispensable in the *ump1 Δ* background. The propeptides of Pup1, Pre3 and Pre4, on the other hand, are not essential in a wild-type (*UMPI*) background and only the propeptide of Pup1 is required for normal cell proliferation (Jäger et al., 1999). However, the requirement or dispensability of the Pup1, Pre3 and Pre4 propeptides in an *ump1 Δ* strain has not been determined. Therefore, these propeptide deletions were combined with *ump1 Δ* .

The Pre4- Δ pp, Pre3- Δ pp and Pup1- Δ pp strains expressing the mature moiety (abbreviated as “mm”) of the respective subunits (Jäger et al., 1999) were crossed with an *ump1 Δ* strain and the resulting diploids were sporulated to isolate the double mutants *ump1 Δ pre4- Δ pp*, *ump1 Δ pre3- Δ pp* and *ump1 Δ pup1- Δ pp*, respectively. Surprisingly, the deletion of the Ump1 protein causes a severe growth defect for the strain possessing the Pre4 subunit without propeptide (Fig 13B) and for the strain lacking the propeptide of the Pre3 subunit (Fig 13D). In the case of the Pup1 propeptide deletion the growth defect, which already exists in the *pup1- Δ pp* single mutant was further strengthened by the combination with *ump1 Δ* (Fig 13C). These results are contrary to the results acquired for the Pre7 propeptide deletion in this study and to the effect of the Pre2 propeptide deletion (Ramos et al., 1998) (Fig 13A). They suggest that the suppression by *ump1 Δ* found for the Pre2 or Pre7 propeptide deletions is specific and not applicable for other propeptide deletions, which even show a synthetic effect in combination with *ump1 Δ* . Obviously, the function of the propeptides of Pre4, Pre3, and Pup1 in proteasome biogenesis does not depend on Ump1. However, this does not exclude that these propeptides contribute the binding of Ump1 to early proteasomal assembly intermediates.

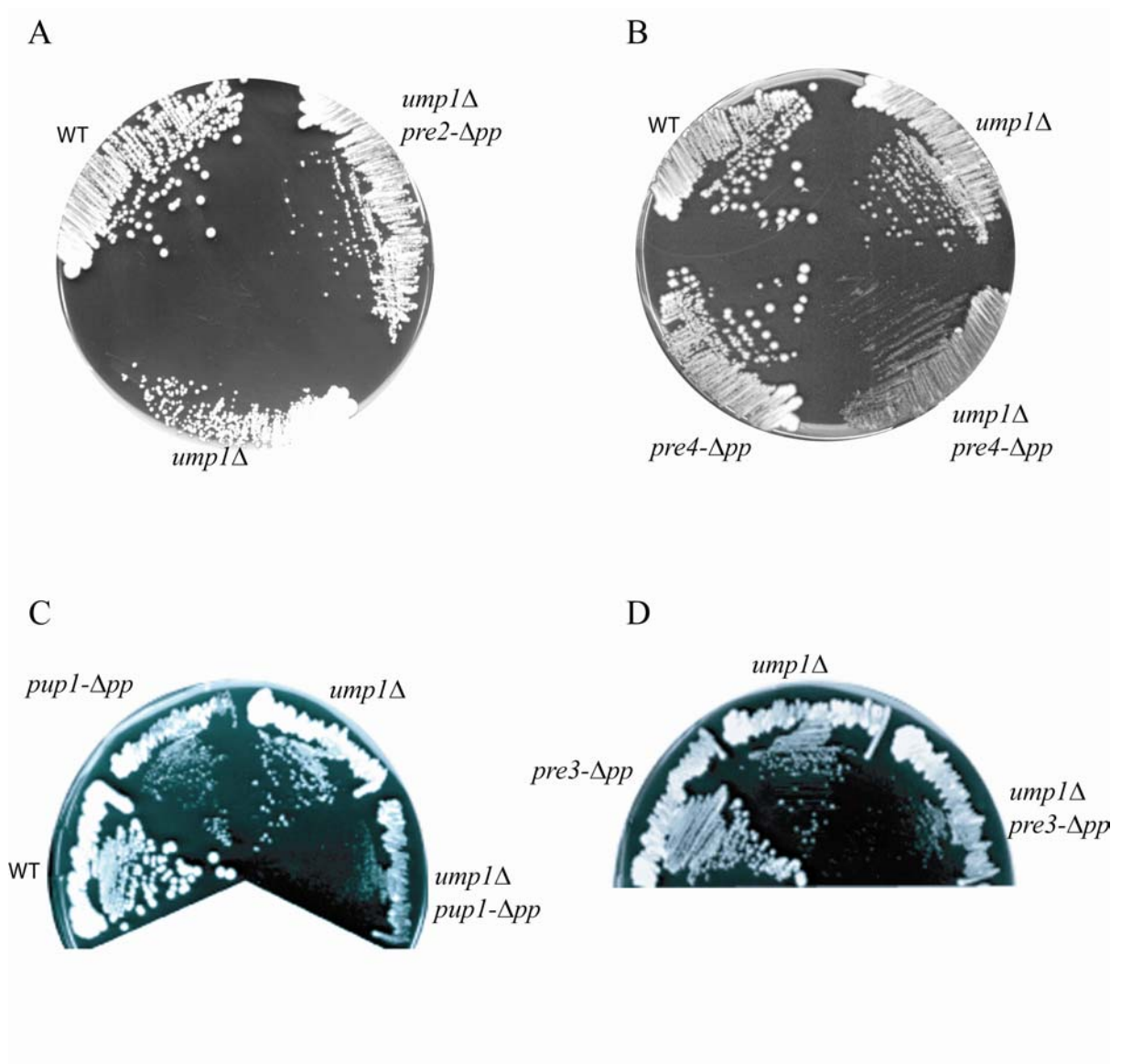


Figure 13

Genetic analysis to determine the necessity of β -type subunit propeptides in proteasome assembly in the absence of the Ump1 protein

The growth behavior on YPD plates of respective *ump1Δ* strains expressing Pre2 (A), Pre4 (B), Pup1 (C) or Pre3 (D) β -type subunits without propeptide is compared with wild type, *ump1Δ* and single mutant strains expressing Pre4 (B), Pup1 (C) and Pre3 (D) subunits lacking the propeptide region. The plates were incubated for 2 days at 30 °C.

4.2 Biochemical analysis of proteasome biogenesis

4.2.1 The Ump1 protein interacts with proteasome assembly intermediates

Ump1 was found in proteasome precursor complexes, where it functions to promote the half-proteasome assembly (Burri et al., 2000; Ramos et al., 1998). In order to study the interactions of Ump1 with precursor complexes containing wild type or truncated Pre7 subunits, GST-pull down experiments were performed. A plasmid based on pGEX-4T, expressing a *GST-UMP1* allele was applied to produce the fusion protein in *E. coli* cells with a yield of ~ 25 % of total *E. coli* protein (Fig 14A).

Native crude cell extracts were prepared from strains bearing wild-type and truncated Pre7 subunits, either in the wild-type or in the *ump1Δ* background. The cell extracts were loaded onto a glutathione sepharose column coupled with GST-Ump1 fusion protein. The bound proteins were eluted and subjected to SDS-PAGE and immunoblot analysis using a polyclonal anti-20S proteasome antibody that detects a subset of proteasome subunits.

From the wild type extracts, the fusion protein GST-Ump1 bound only traces of proteasome subunits, detectable by the anti-20S proteasome antiserum (Fig 14B lane 1 to 4). In the case of extracts from the *ump1Δ* background, considerably more proteasomal material was pulled down by GST-Ump1 (Fig 14B lane 5 to 8). These results may be explained by the fact that the Ump1 protein in the wild-type background immediately occupies its place in early assembly intermediates or in the half-proteasomes and competes for binding of the GST-bound Ump1 protein. Remarkably, the amount of material bound to GST-Ump1 in *ump1Δ* is not affected by the truncations of the Pre7 subunit (Fig 14B 5 to 8) indicating, that residues -9 to -7 in the propeptide are not crucial for binding of Ump1 to precursor complexes. However, the interaction of Ump1 with assembly intermediates in cells harbouring longer truncations of Pre7 than until position -6 was not analysed.

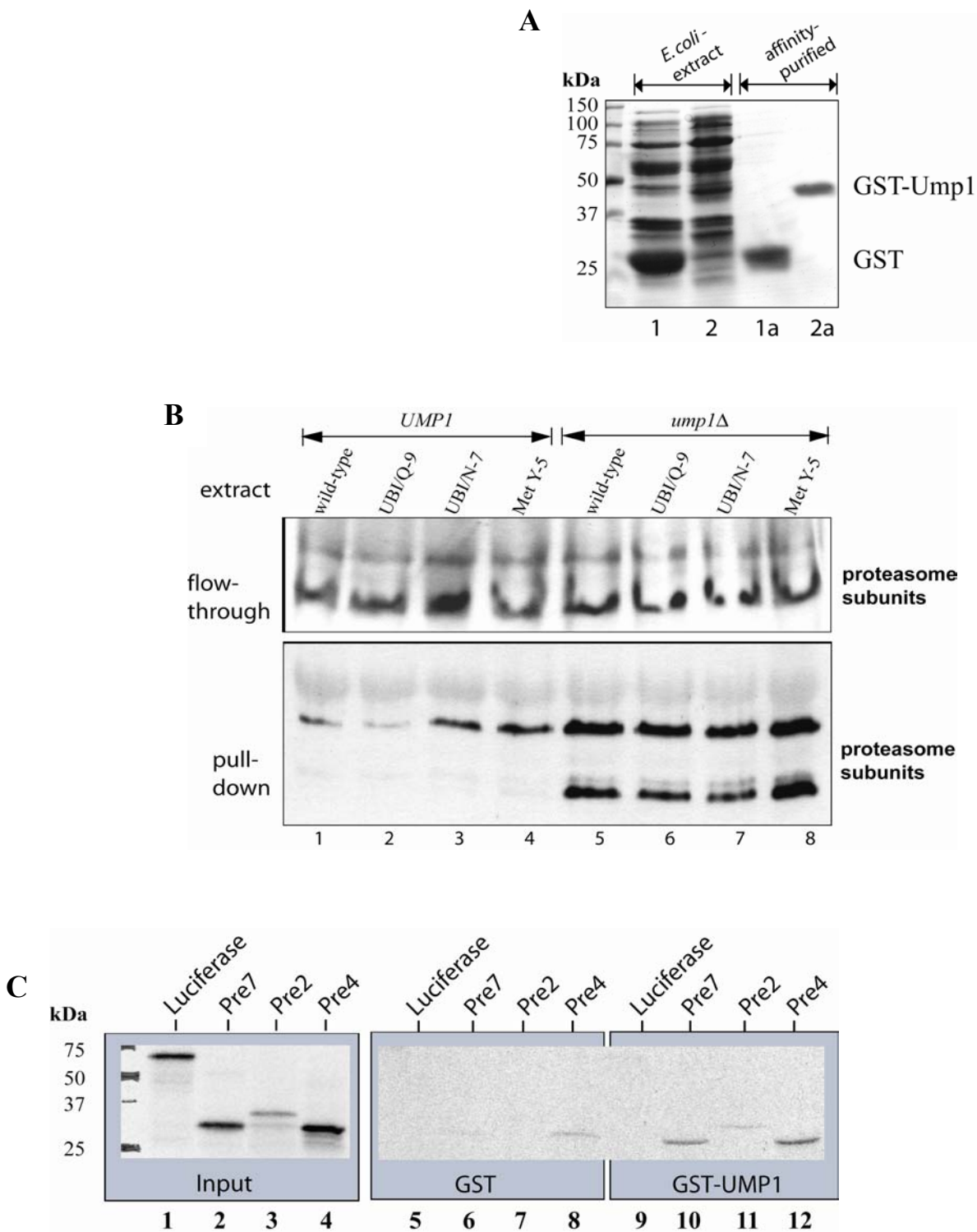


Figure 14
Ump1-proteasome interactions studied by GST pull-down experiments

A. Expression of the GST-Ump1 fusion protein in *E. coli* cells

The plasmids encoding GST or GST-Ump1 were transformed into *E. coli* and induced to express the proteins (see methods). The fusion protein from cell extracts (lane 1 and 2) was purified by a glutathione sepharose column (lane 1a and 2a) and fractionated by SDS-PAGE. The gel was stained with Coomassie blue. Continue to next page for B and C

B. Proteasomal subunits interact with Ump1

Protein extracts were prepared under native conditions from selected Pre7 mutant strains (wild type, UBI/Q-9, UBI/N-7 and MY-5) with *UMP1* (lane 1 to 4) and *ump1Δ* background (lane 5 to 8). These extracts were incubated with GST-Ump1 (for pull-down) or GST (for control, not shown) bound to glutathione-sepharose beads. Unbound proteins in the column were collected (flow through) and precipitated, as an input control. Proteins retained in the column were eluted (pull-down) and subjected to SDS-PAGE and immunoblot analysis. An anti-proteasome antibody was used to detect proteasomal subunits.

C. Study of Ump1 interaction with *in vitro* translated proteasomal subunits

The plasmids containing *LUC* (Luciferase), *PRE7*, *PRE2* and *PRE4* genes under the T7 promoter (see methods) were translated *in vitro* with ³⁵S methionine, using a rabbit reticulocyte system (lane 1 to 4). The labeled proteins were subjected to GST column (lane 9 to 12) or to GST-Ump1 column (lane 5 to 8). Bound proteins were eluted as described in (B). The samples were separated by SDS-PAGE and analysed by fluorography.

4.2.2 The Ump1 protein interacts with proteasomal β -type subunits *in vitro*

The results of the GST-pull down experiments presented in the last chapter as well as immunoprecipitation experiments (Burri et al., 2000) revealed an interaction of Ump1 with proteasomal subunits (Fig 14B lane 5 to 8), but did not specify the interactions with individual subunits. To clarify whether the Ump1 interaction requires the assembled half-proteasome complex or whether interactions with individual β -subunit precursors can be detected, some late incorporating subunits, Pre7, Pre2 and Pre4 were chosen for *in vitro* binding studies. The open reading frames of these subunits were cloned under the control of the T7 promoter, the genes were transcribed and translated *in vitro* in a reticulocyte lysate system in the presence of ³⁵S methionine (Fig 14C lane 1 to 4) and the translation products were applied to glutathione-agarose beads coupled with GST-Ump1. Bound proteins were eluted, separated by the SDS-PAGE and visualized by autoradiography. All the proteasomal subunits Pre7, Pre2 and Pre4 were pulled down by the GST-Ump1 protein (Fig 14C lane 10 to 12). These results suggest that the interaction of Ump1 with assembly intermediates is mediated by multiple contacts to individual β -subunit precursors. However, the mature subunits without propeptide region were not analysed, which would allow conclusions about the regions that interact with the Ump1 protein.

4.2.3 Epitope tagging of the Pre7 subunit causes impaired cell growth

In order to allow immunological detection of the Pre7 subunit during proteasome biogenesis, a triple HA epitope was added to the C-terminus of Pre7. The strains expressing Pre7-HA tagged subunits showed a strong growth phenotype (Fig 15 lane 2, symbols are as in Fig 8). Furthermore, the triple HA epitope tag was introduced in frame into an internal loop region of the Pre7 subunit (Fig 15 lane 3). However, strains expressing this subunit version were not able to grow like wild type yeast cells either.

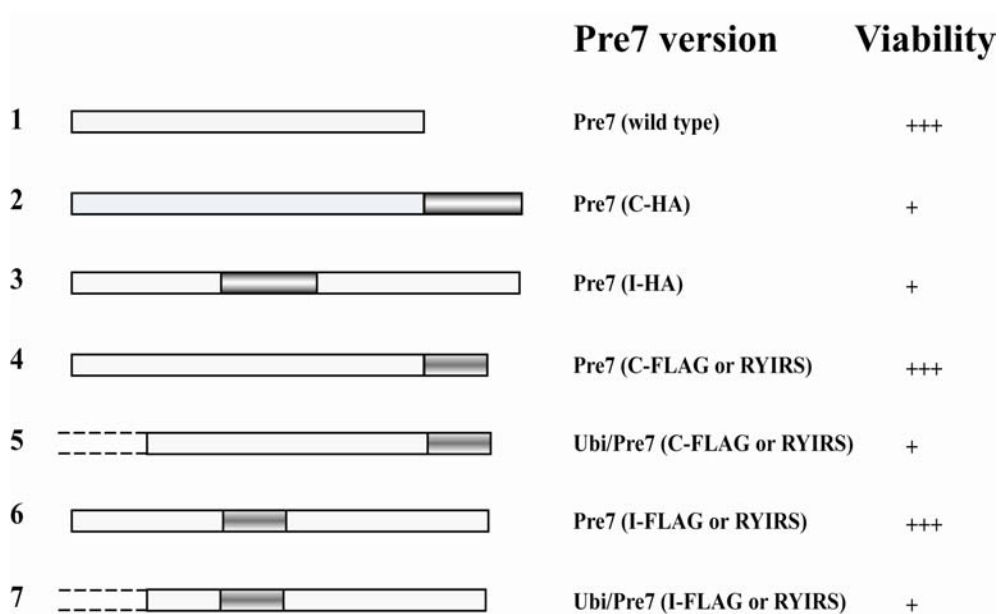


Figure 15

Schematic diagram representing approaches to create the Pre7 subunit with an epitope tag and resulting growth behaviours

The sequence encoding the wild type Pre7 subunit is depicted as closed white box. Epitope tags (dark boxes) were introduced at the C-termini or into an internal loop region of different Pre7 constructs (see Fig 8). The different Pre7 versions (wild-type or truncated subunit) carrying the respective epitope tags (shown in parentheses as C for C-terminal or I for internal) are indicated as Pre7 version. Growth phenotypes of strains are indicated as symbols (+ or +++), as described in Figure 8.

In order to avoid the putative interference of the long triple HA (3xHA) epitope with the Pre7 subunit structure, a single FLAG or a short RYIRS epitope was introduced at the C-terminus or into the internal loop region of the Pre7 subunit (Fig 15 lane 4 to 7). The

strains carrying these hybrid subunits grew like wild type cells, but strains expressing the truncated Pre7 subunits with these epitope tags grew worse than respective strains synthesizing the untagged variants (as indicated with + symbol). All these results show that even minor modifications in the Pre7 subunit structure lead to malfunction of the subunit.

4.2.4 Polyclonal antibody production against the Pre7 subunit

To produce polyclonal antibodies against the $\beta 6$ /Pre7 subunit, a peptide region was chosen as antigen, which was derived from a loop region of the Pre7 subunit (Fig 16). This loop is situated on the outer surface of the subunit in the mature particle and should be easily accessible by the antibody even under native conditions. A rabbit was immunized with the peptide CNQVEPGTNGKVKKPLKY and the serum was collected periodically (by Eurogenetic, Belgium).

Figure 16

An approach used to produce antibody against the Pre7 subunit.

The peptide used to produce antibody is shown in single letter amino acid code in red color on top of a ribbon diagram illustrating its location in a loop region (red) of the Pre7 subunit.



By immunoblot analysis, the specificity of the antibodies against the Pre7 protein was investigated. Unfortunately, many other proteins migrating close to Pre7 were also detected by the antibody (not shown). In order to solve this problem the antibodies were purified by affinity chromatography using the peptide applied for the immunization

experiment. The peptide was coupled with epoxy-activated sepharose-6B column, crude serum was subjected to the column and antibodies specifically bound to the peptide were collected as purified antibody (see methods). The purified antibody bound specifically to all forms of the Pre7 subunit (Fig 17). Most of the nonspecific reactions were eliminated except one cross-reacting band, which migrates close to the precursor form of Pre7 (Fig 17, marked with *symbol).

4.2.5 Precursor subunits accumulate in Pre7 truncation mutants

To visualize the steady state level of the Pre7 subunits in different mutant strains, the strains carrying different Pre7 versions in wild type background and in *ump1Δ* background were grown to stationary phase. The cells were lysed and equal amounts of protein were separated by SDS-PAGE. The proteins in the gel were transferred to nitrocellulose or PVDF membrane and probed with the affinity purified anti-Pre7 antibody. Evidently, the stepwise truncated Pre7 versions showed a gradual decrease in the size of the subunit. Interestingly, the truncated Pre7 subunits (N-7 to MY-5) were found to accumulate in the wild type background compared to the wild type or Q-9 Pre7 proteins (Fig 17 *UMPI*). In the *ump1Δ* background, all mutant Pre7 subunits showed up in higher concentration except P-6 and Y-5 Pre7, when compared to wild type Pre7 (Fig 17, upper panel). In order to observe the influence of Pre7 truncations for other proteasome subunits, the blot was stripped and re-probed by using polyclonal antibodies against Pre4 or Rpt5 subunits.

Surprisingly, in the wild type background the strains carrying truncated Pre7 subunits (N-7 to MY-5) showed a strong accumulation of the precursor form of Pre4 subunit (Fig 17, middle panel). In the *ump1Δ* background, such an accumulation is found for all Pre7 versions, including wild type. This material represents either the free form of the precursor Pre4 subunit or species bound to early assembly intermediates. This result strongly indicates that the strains expressing mutant Pre7 versions (N-7 to MY-5) in the wild type background are impaired in the proteasome maturation. This might explain the lethality of strains possessing shorter versions of Pre7 (Y-5 to G-1), because here the capacity to synthesize mature proteasome might be further reduced. Accumulation of the

Pre4 precursor subunit in the *ump1Δ* background (WT to G-1) is due to the known impaired ability of proteasome formation (Ramos et al., 1998). Nevertheless, sufficient amounts of mature β -type subunits must be produced in all Pre7 mutant strains lacking Ump1.

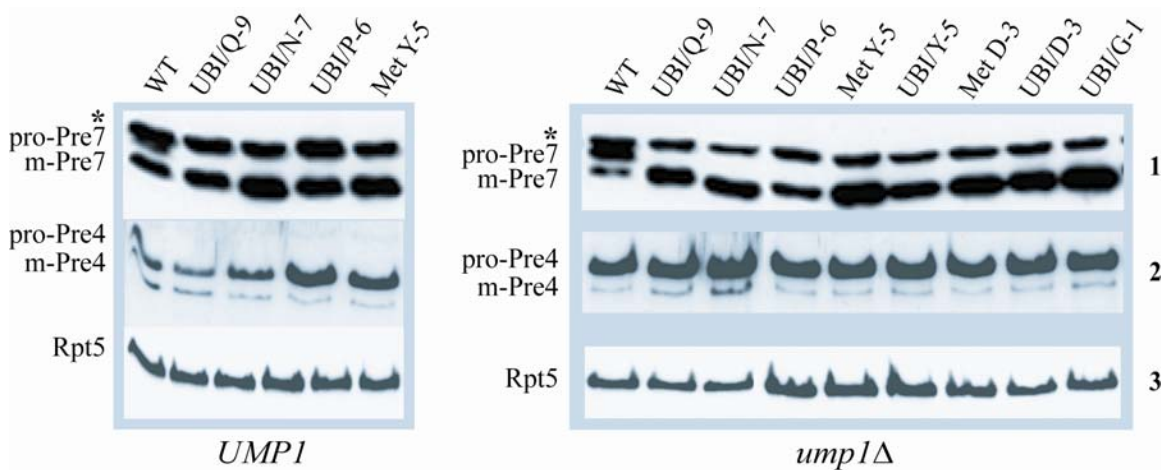


Figure 17
Immunoblot analysis of proteasome subunits in crude extracts of Pre7 mutants.

The respective Pre7 mutants in wild type (*UMP1*) and in *ump1Δ* background were grown to stationary phase and equal volumes of cells were collected. The cell pellets were lysed and equal amounts of proteins were subjected to SDS-PAGE and immunoblot analysis. An affinity-purified antibody against Pre7 (see text) was used to detect the different forms of Pre7 (top panel, precursors (pro-Pre7) and mature (m-Pre7) Pre7 subunit). The * symbol represents a non-specific reaction of the affinity-purified antibody. The precursor (pro-Pre4) and mature (m-Pre4) forms of the Pre4 subunit were detected by anti-Pre4 antibody (middle panel). As a control, the proteasome subunit Rpt5 was detected using anti-Rpt5 antibodies (lower panel).

4.2.6 Pre7 mutant strains are impaired in the proteasome assembly

Most proteasomal β -type subunits are synthesized as precursors with N-terminal propeptides. After incorporation into nascent 20S proteasomes, they are finally processed in a multi-step reaction. In order to follow the influence of truncations of the Pre7 subunit on proteasome biogenesis, either on the formation of assembly intermediates leading to half-proteasomes or on late assembly and maturation stages, gel filtration by a Superose-6

column was used to separate different forms of assembly intermediates and mature proteasome complexes. The viable strains expressing different Pre7 versions (wild-type PRE7, UBI/Q-9, UBI/N-7 and MY-5) in both wild-type and *ump1Δ* background (see Fig 10) were chosen for this study. In order to follow the autocatalytic processing of the active subunit Pre2 and subsequent proteasome maturation, an integration allele encoding the Pre2 subunit with double HA epitope at the C-terminus (a gift from C. Enenkel, Berlin) was used for chromosomal integration. This *PRE2-HA* allele was integrated into the chromosomal *PRE2* locus to each of the strains chosen above. All the strains (wild-type PRE7, UBI/Q-9, UBI/N-7 and MY-5) with Pre2-HA grew slightly slower than the untagged strains (not shown). The strains were grown until OD₆₀₀ of 1.4, the cell pellet was frozen in liquid nitrogen and lysed by grinding with extraction buffer in presence of liquid nitrogen (see methods). The resulting native crude protein samples were subjected to fractionation by gel filtration on Superose-6, the fractions were then separated by SDS-PAGE and transferred to PVDF membrane for immunodetection analysis.

The monoclonal anti-HA antibody was used to follow the autocatalytic processing of Pre2-HA, the polyclonal rabbit antibody against Pre4 was used to detect the processing of the Pre4 precursor by the neighboring Pup1 subunit and an antibody against Pre6 was used to follow the proteasome assembly from free subunits to fully assembled proteasome.

In the *UMP1* strain producing wild-type Pre7, only the mature Pre2 and Pre4 subunits are detected in the earlier fractions (Fig 18 A1 fraction #15 to 19) containing the mature 20S proteasome with or without regulatory particle. The middle fractions (#20 to 24), where 20S proteasome formation occurs by dimerization of two half-proteasome precursors, contain both precursor and processed forms of the Pre2 and Pre4 subunits. Moreover, the precursors of Pre2 are not detectable in later fractions (#25 to 30), but the precursors of the Pre4 subunit are detectable in those fractions containing early assembly intermediates and probably some of the free precursor subunits. In contrast to the situation found for this wild-type strain, the strain expressing Q-9 Pre7 shows a slight increase in the amount of Pre4 and Pre2 subunit precursors in the middle fractions (#20 to 24). However, the earlier fractions (#15 to 19) with 20S or 26S proteasomes contain only the mature subunits (Fig 18A panel 2).

The strain expressing N-7 Pre7 shows a strong accumulation of the precursor Pre2 and Pre4 subunits, when compared to the wild-type or Q-9 strains. The Pre2 and Pre4 subunit precursors are clearly detectable in the fractions #18 to 30. In the earlier fractions and the middle fractions (#15 to 24), considerable amounts of mature Pre2 and Pre4 subunits are also found (Fig 18A panel 3). This appearance of equal amounts of precursor and mature Pre2 subunit in the fractions #19 to 21 is due to the defect of the Pre2 autocatalytic processing in the 20S proteasome. The appearance of precursor Pre2 subunit in the later fractions #25 to 30 might be a consequence of the proteasome maturation defects, which lead to up-regulation of proteasome subunit synthesis.

Even stronger maturation defects in the proteasome and a dramatic up-regulation of proteasome subunits are found in the strains expressing the MY-5 Pre7 version (Fig 18A panel 4). The precursor Pre2 and Pre4 subunits are found almost in all fractions. However, the fact that most of them are accumulating in the fractions #18 to 21 suggests defects in the proteasome maturation. Nevertheless, some material of the mature subunits is also detectable in the earlier fractions (#15 to 24) containing 20S and 26S proteasomes, suggesting the availability of functional proteasomes required for the cell viability. This result illustrates, that the Pre2 autocatalytic processing is dramatically reduced in this last viable Pre7 truncation version, which leads to accumulation of a bulk of immature proteasomes. The appearance of the intermediately processed Pre2 subunit in the earlier fractions (#16 to 22) indicates that in the fraction of proteasomes that has lost the ability to process the Pre2 propeptide autocatalytically, at least some proteolytically active Pup1 and/or Pre3 subunits, are capable of intermediately processing the Pre2 subunit.

In the *ump1Δ* background, defects in the Pre2 and Pre4 precursor processing, similar to those seen for the latter two strains, are already detectable even in the strains expressing wild-type or Q-9 Pre7 subunit (Fig 18B panels 1 and 2). However, in both strains more of the mature forms of Pre2 and Pre4 can be detected relative to the precursor subunits. Interestingly, the early and middle fractions #15 to 24 contain intermediately processed Pre2 subunit but the unprocessed Pre4 subunit is only detectable in the middle fractions #20 to 22 and in the later fractions #26 to 30 (Fig 18B panel 1).

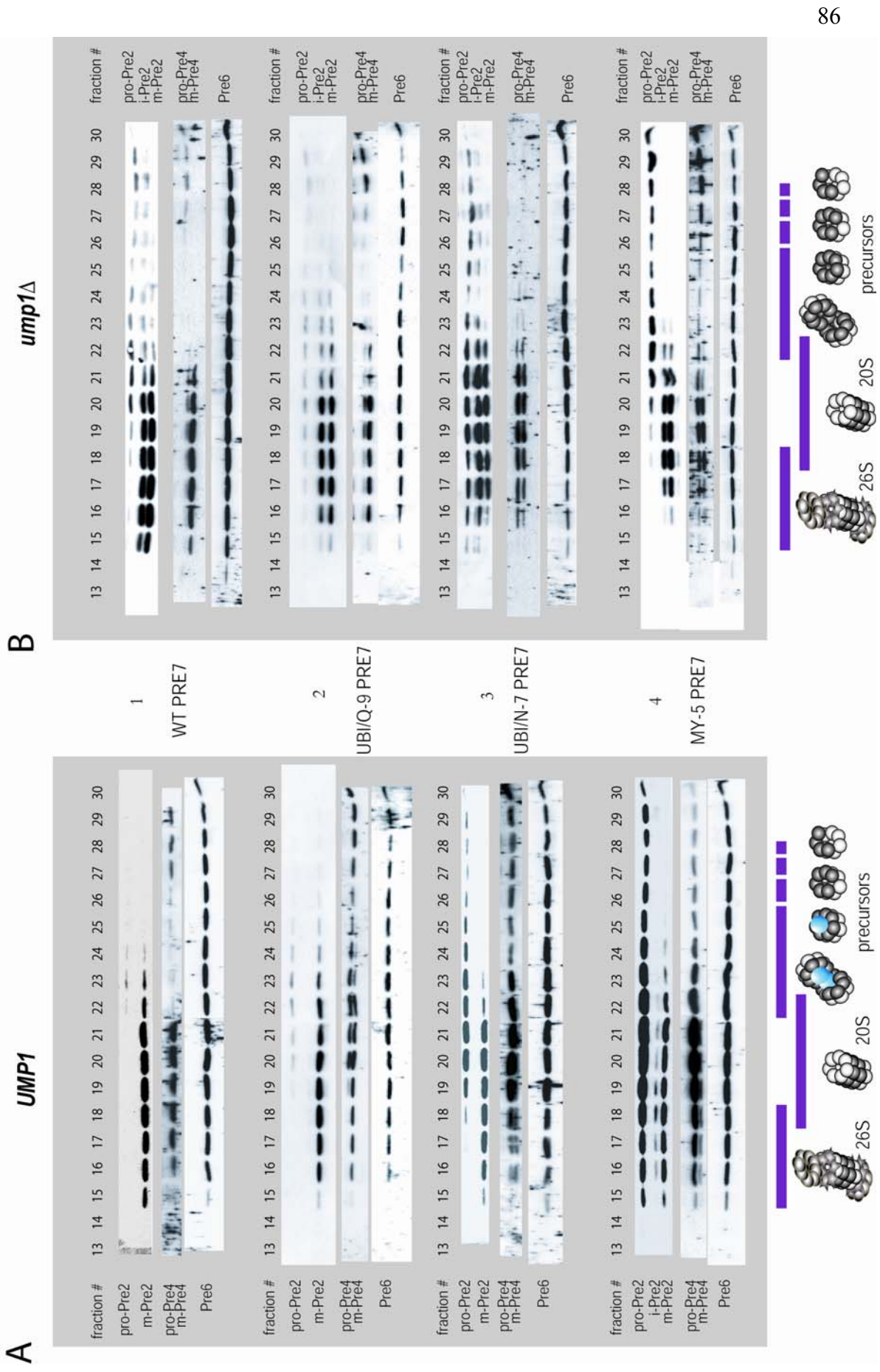


Figure 18 The Pre7 propeptide is essential for normal proteasome assembly and maturation (see next page for legend)

Figure 18

The Pre7 propeptide is essential for normal proteasome assembly and maturation

Native protein extracts from selected Pre7 mutants (WT, UBI/Q-9, UBI/N-7 and MY-5) in *UMPI* (A) or *ump1Δ* background (B) were fractionated on a Superose-6 column.

The fractions (fraction #13 to 30) were separated by SDS-PAGE and transferred to PVDF membrane for immunoblot analysis. Precursor (pro-Pre2), intermediately processed (i-Pre2) and mature (m-Pre2) forms of the Pre2 subunit were detected by anti-HA antibody. An anti-Pre4 antibody was used to detect unprocessed (pro-Pre4) and processed (m-Pre4) forms of the Pre4 subunit. Pre6 was detected to follow the assembly processes, as control, by an anti-Pre6 antibody. The fractions containing early assembly intermediates (precursors), assembled 20S proteasome (20S) or the core particle with regulatory complexes (26S) are represented as cartoons at the bottom of the respective pictures (A and B) and their distribution is indicated by the gray bars.

These results indicate that the other two active sites are matured to a large extent and capable to process Pre2 and Pre4 partially. The appearance of the intermediately processed Pre2 subunit in the later fractions #24 to 28 could be explained by 20S proteasomes that fell apart, either *in vivo* or *in vitro* (Fig 18B panel 1 and 2). Similarly, the strain possessing the N-7 Pre7 subunit also shows the mature and intermediately processed Pre2 subunit in the early and middle fractions (#15 to 24) (Fig 18B panel 3). However, increased amounts of the Pre2 and Pre4 precursor forms in fractions #16 to 23 can be found relative to the wild-type and Q-9 Pre7 strains without Ump1.

In the strain carrying the MY-5 Pre7 subunit, the Pre2 precursor material is detectable from the fractions #18 to 30 and the unprocessed Pre4 subunit is present in the fractions #16 to 30 (Fig 18B panel 4), which corresponds to their distribution in the *ump1Δ* strain carrying wild-type Pre7 (Fig 18B panel 1). A still higher amount of the mature forms of Pre2 and Pre4 compared to the abundance of the precursor forms is detectable in the fractions #16 to 23, indicating the availability of functional proteasomes. Remarkably, when compared to the profiles found for MY-5 Pre7 in the *UMPI* background, the *ump1Δ* strain containing the MY-5 Pre7 subunit is able to process the Pre2 and Pre4 subunits with higher efficiency (compare Fig 18 panels A4 and B4). This processing ability might apply also to the lethal Pre7 versions, which cannot produce functional proteasomes in the wild-type background but do produce functional particles in the *ump1Δ* background.

4.2.7 The Pre7 mutant strains show reduced proteasomal activity

The autocatalytic processing defect of the Pre2 subunit in the Pre7 mutant strains is expected to be reflected by reduced proteolytic activity of the particle. In order to clarify this question, the proteasome fractions from the strains expressing wild-type, N-7 and MY-5 Pre7 in either wild-type or *ump1Δ* background were measured for peptidase activities. To assay the chymotrypsin-like activity and peptidylglutamyl peptide-hydrolyzing (PGPH) activities, the substrates succinyl-Leu-Leu-Val-Tyr-7-amido-4-methylcoumarin and Cbz-Leu-Leu-Glu- β -naphthylamide were used, respectively.

In the wild-type background, the stepwise Pre7 truncations show a slight decrease in the chymotrypsin-like activity for the fractions #15 to 22, where the 20S and 26S proteasomes are detectable (Fig 19A). The chymotrypsin-like activity peak in the fractions #24 to 27 (Fig 19 A) cannot be caused by prematuration since there was no mature Pre2 subunit found in those fractions (see Fig 18A panel 4). In contrast, the PGPH activity is dramatically reduced in the fractions #15 to 22 from extracts of Pre7 truncated strains (Fig 19 A), whereas the trypsin-like activity is only slightly reduced in mutant Pre7 strains compared to wild-type Pre7 strains in both backgrounds (data not shown). The reduced chymotrypsin-like activity in the truncated Pre7 versions correlates with the impaired autocatalytic processing of the Pre2 subunit, as detected in the fractionation experiment (Fig 18A, panels 2 to 4). The dramatically reduced PGPH activity in the Pre7 mutant stains can only be explained by an almost complete loss of autocatalytic processing ability of the Pre3 subunit in the 20S proteasome.

In the *ump1Δ* background, the chymotrypsin-like activity is strongly decreased in the fractions #15 to 22, showing that strains expressing the wild-type and all truncated Pre7 subunits form less mature proteasome (Fig 19B). In the N-7 strain, appearance of an activity peak in the fractions #24 to 27 may correspond to assembly intermediates bearing prematurely processed forms of Pre2 (Fig 19B). Alternatively, this might be caused by disintegration of late assembly intermediates, either *in vivo* or *in vitro*.

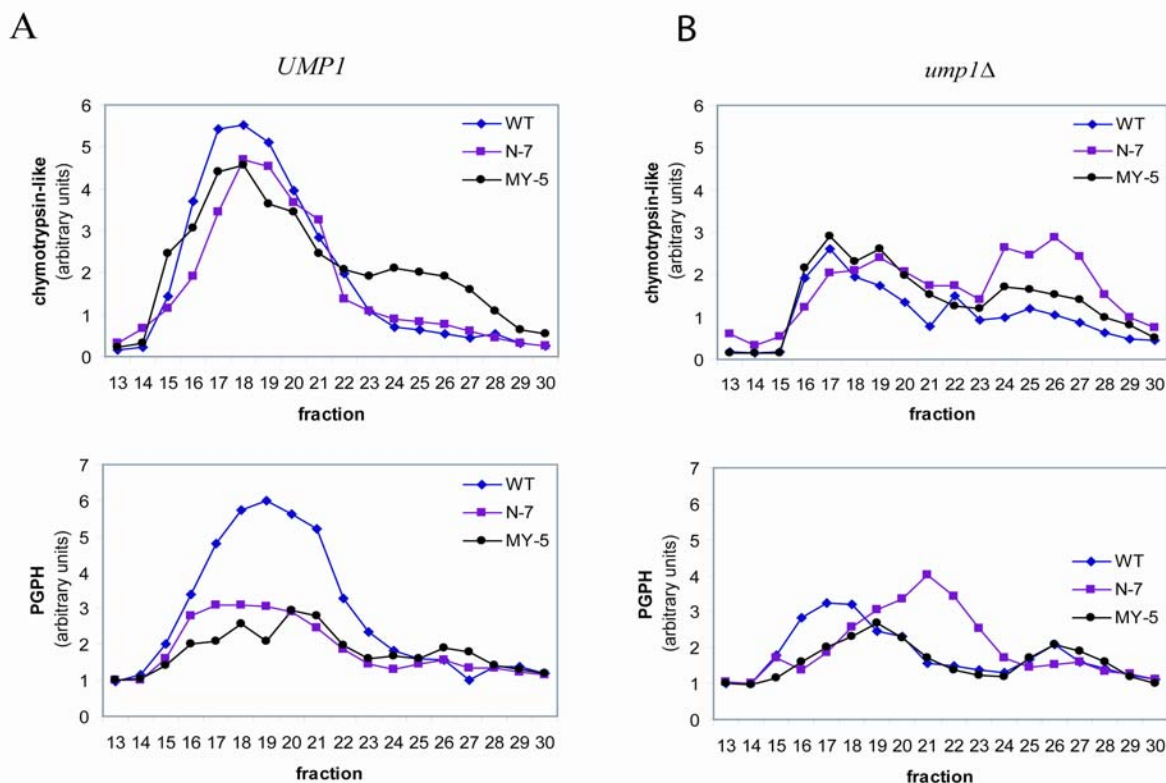


Figure 19
Comparison of peptidase activities in extracts of Pre7 mutants

Equal amounts of total protein from selected Pre7 mutants in *UMP1* (A) or *ump1Δ* (B) background (as in Fig 18) were fractionated by gel filtration on Superose-6 and the fractions were subjected to peptidase activity assays. The chymotrypsin-like and PGPH activities were measured using respective substrates (see text) and plotted in arbitrary units.

Similar to chymotrypsin-like activity, the PGPH activity is notably reduced strains expressing the wild-type and all truncated Pre7 subunits (Fig 19B). The shift of the PGPH activity from fractions #15 to 20 to the 20S region (fractions #20 to 23) for the strain carrying the N-7 Pre7 subunit might be caused by dissociation of the 26S to 20S proteasome during *in vitro* handling.

In summary, in accordance with the known reduction of proteasome assembly and maturation in the *ump1Δ* strains (Ramos et al., 1998), the activity profiles show similarly reduced peptidase activities for all strains with different Pre7 versions in the *ump1Δ* background.

4.2.8 Proteasome maturation is diminished in mutant Pre7 strains

In order to analyse the processing kinetics of β -type subunits in the Pre7 mutant strains, the Pre4 subunit was chosen, because the polyclonal antibodies against Pre4 were capable to immunoprecipitate the precursor and the processed form of the Pre4 subunit (Jäger et al., 1999). All the viable stains in either *UMP1* or *ump1 Δ* background were grown to $OD_{600} = 1.0$, pulse labelled with ^{35}S methionine and grown in the presence of unlabelled methionine (chase) for additional time periods. The cells were lysed and the extracts were subjected to immunoprecipitation with anti-Pre4 antibody. Precipitated material was subsequently separated by SDS-PAGE and subjected to fluorography.

In the wild type Pre7 cells, most of the precursor form (with propeptide) of the Pre4 subunit was converted into mature Pre4 during the 60 min chase (Fig 20A 1). Similar processing kinetics were also found in the Q-9 strain (Fig 20A 2). In the strain expressing the N-7 Pre7 subunit, most of the Pre4 subunit precursors remained unprocessed during this time and only few mature material was found even after a 120 min chase (Fig 20A 3). Furthermore, the precursor Pre4 subunit was converted even slower in the P-6 and MY-5 strains where only traces of mature Pre4 subunits were detectable after a 120 min chase (Fig 20A panels 4 and 5). These findings are consistent with the results from the fractionation analysis and further confirm the defect of Pre7 mutant strains in the processing of β -type subunits during proteasome maturation.

In the *ump1 Δ* mutant background, the conversion of precursor Pre4 into mature form was dramatically decreased in all Pre7 truncated strains. However, some mature Pre4 subunits were detectable after the 120 min chase time (Fig 20B). These results further confirm the results obtained in the fractionation studies, where Pre2 and Pre4 subunit processing in the *ump1 Δ* background was almost similar for all Pre7 truncated versions. The maturation kinetics of Pre4 in the UBI/Y-5, MD-3, UBI/D-3 and UBI/G-1 Pre7 strains with *ump1 Δ* background exhibited the same stabilisation of the unprocessed Pre4 subunit and only little mature Pre4 subunit appeared after 120 min of chase time (Fig 20B, see right square).

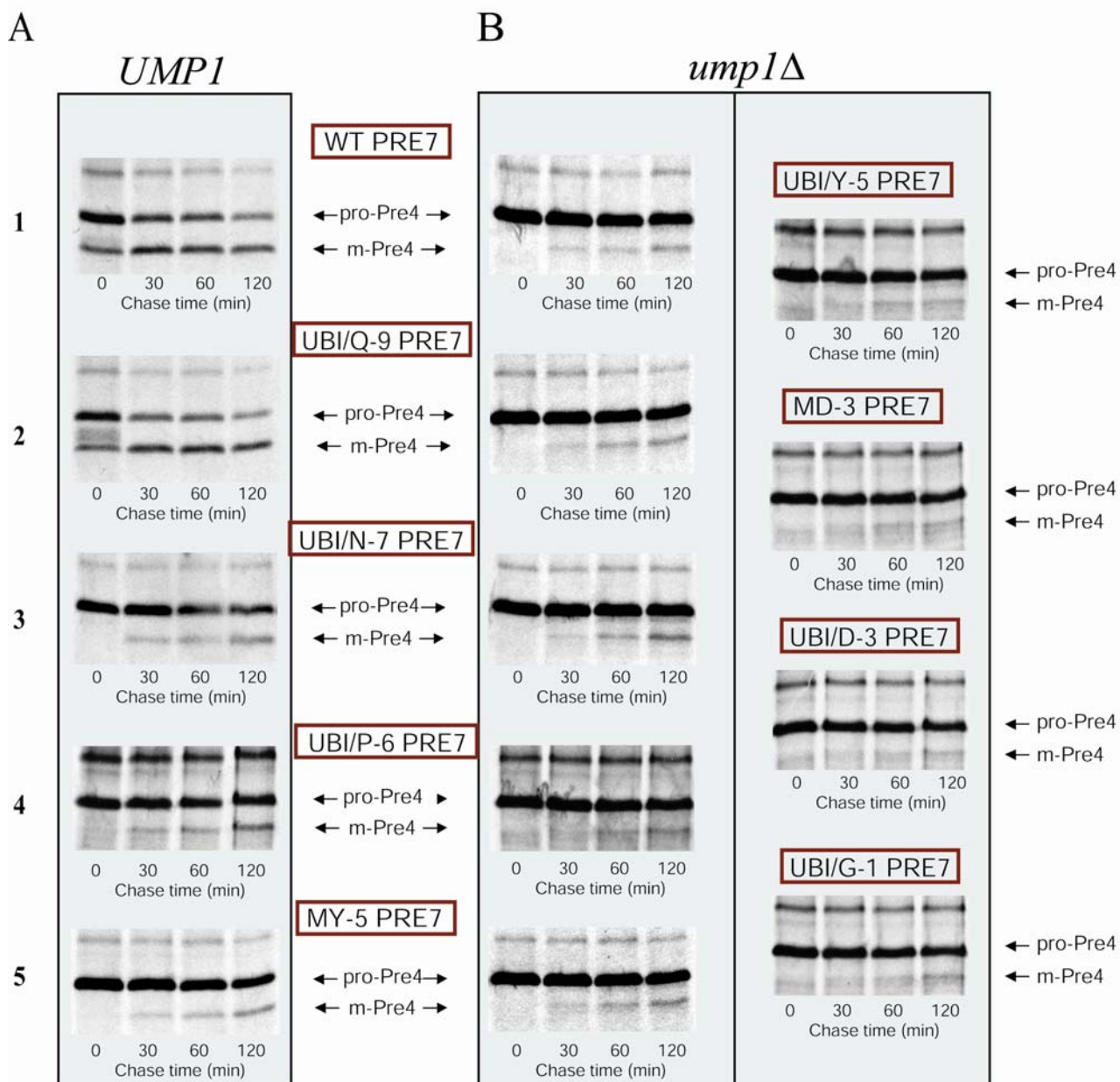


Figure 20
Pulse chase analysis of Pre4 processing in Pre7 truncated strains

Indicated Pre7 mutants (in boxes) in *UMP1* (A) or *ump1Δ* (B) background were pulse-labeled with ^{35}S methionine for 10 min, followed by chase periods of increasing length (chase time in minutes). Immunoprecipitation was carried using anti-Pre4 antibody (see methods). The samples were separated on tris-tricine gels and analysed by fluorography. Those Pre7 mutants viable only in *ump1Δ* background are shown in the right column in B.

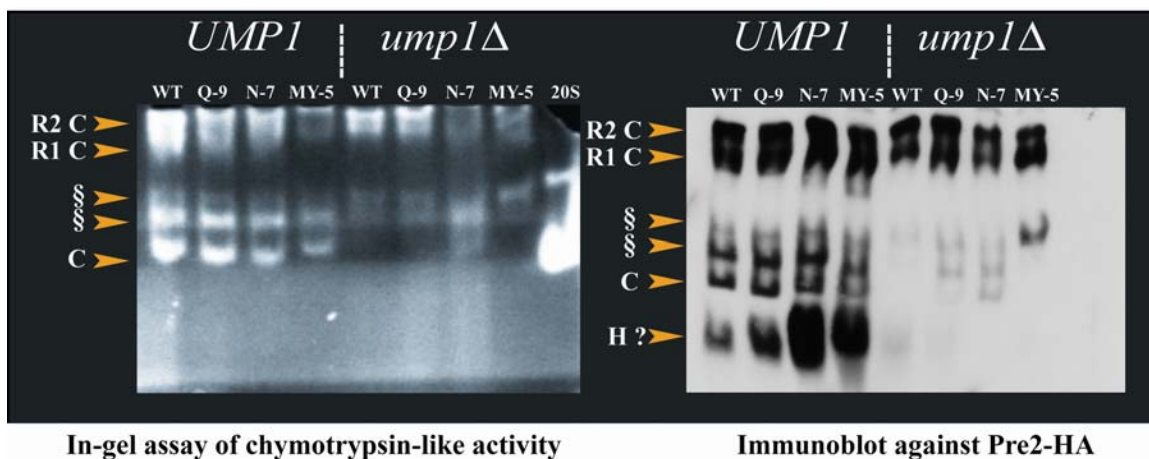
4.2.9 Visualization of proteasome assembly intermediates accumulating in Pre7 mutant strains

To visualize the different assembly intermediates in the proteasome biogenesis, total cell extracts and fractions from gel-filtration containing proteasome complexes were resolved by non-denaturing gel electrophoresis (native-PAGE). The crude samples from the wild-type, UBI/Q-9, UBI/N-7 and MY-5 Pre7 strains in both genetic backgrounds (as in Fig 18) were subjected to native-PAGE. Purified 20S proteasome was used to identify the location of the 20S core particle in the gel (21 A, in-gel assay).

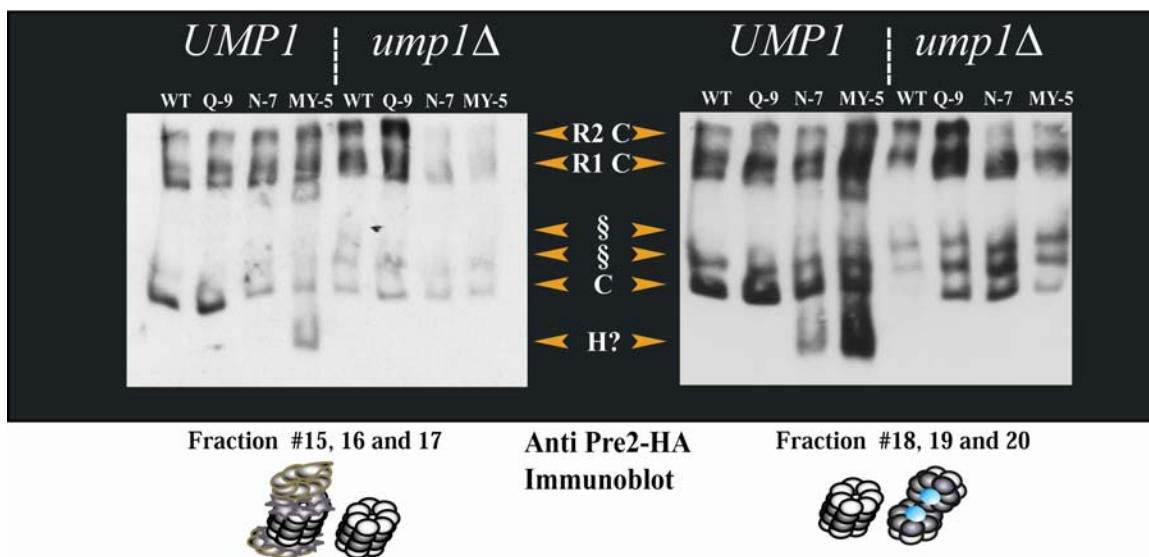
An in-gel activity assay was performed using the fluorogenic substrate for chymotrypsin-like activity. Activity of the core particle (C) was found for all strains in wild type background but was hardly detectable in the *ump1Δ* background (Fig 21A [C]), in accordance with the activity profiles of the fractionation studies. In addition to the core particle, two other slower migrating complexes were also detected (Fig 21 A [§]) in all strains and in the both backgrounds. Since the position of 26S proteasomes with one or two regulatory particle (Fig 21A [R2C and R1C]) is clearly defined in this gel system, these complexes (§) may contain 20S proteasome with some other putative regulatory complex on one or both ends. These putative complexes migrate at positions, where Blm3 containing proteasome complexes have been found in this native-gel system (Fehlker et al., 2003).

Furthermore, to detect proteolytically inactive early proteasome assembly intermediates, protein complexes separated in the native gel were transferred to nitrocellulose membrane under denaturing conditions. The membrane was probed with anti-proteasome polyclonal antibody to identify the purified core particle (data not shown) and an anti-HA monoclonal antibody was used to detect the complexes containing the Pre2-HA subunit (Fig 21A immunoblot). The 26S proteasomes are detectable in all Pre7 mutant strains in both backgrounds (R2C, R1C), but interestingly, the 20S forms are found only in the wild-type background and are hardly visible in the *ump1Δ* background. However, the putative 20S proteasome/Blm3 complexes are clearly detectable in the wild-type and in *ump1Δ* background, and this complex is enriched in the *ump1Δ* strain carrying the MY-5 Pre7 subunit (Fig 21A immunoblot). Interestingly, a distinct fast migrating complex is detected only in the wild type background (*UMPI*) accumulating

A



B

**Figure 21**

Detection of proteasome assembly intermediates in Pre7 mutants using native-gel analysis

A. Crude extracts were prepared under native conditions from selected Pre7 mutants (indicated at the top of each lane) in *UMP1* and *ump1Δ* background, as in figure 18. The native proteins were resolved on non-denaturing PAGE in the presence of ATP and $MgCl_2$ (see methods). The proteasome complexes were visualized in the gel by an in-gel activity assay using the fluorogenic substrate suc-LLVY-AMC (A, in-gel assay). Purified 20S proteasome was used to locate the particle in the gel system. Free 20S proteasome (C) and putative complexes of 20S proteasome with Blm3 (§) or with 19S regulatory particles (R1 C, R2 C) are labeled. Alternatively, the protein complexes were transferred from the gel to nitrocellulose membrane under denaturing conditions and analysed by immunoblotting (A, immunoblot). The proteasome assembly products containing Pre2-HA subunit were detected by anti-HA antibody. H? represents a proteasome assembly intermediate (15S or 13S).

B. Detection of proteasome complexes from fractions (same as Fig 18)

Early fractions containing 26S and 20S proteasomes (fraction #15 to 17) were pooled and the middle fractions (#18 to 20) containing 20S core particle and half-proteasomes were combined (see Fig 18 and cartoon). Mixed fractions were subjected to native-PAGE immunoblot analysis using anti-HA antibody. Labelling of distinct Pre2-HA containing complexes is as in A.

especially in the Pre7 mutant strains (Fig 21A immunoblot (H?)). Due to its fast migration behavior, this complex is considered as early assembly intermediate, probably a half-proteasome. Increased amounts of these complexes in the Pre7 mutant strains suggest that the 20S proteasome formation from the two half-proteasome precursors is diminished in the presence of the Ump1 protein.

To detail these results and to identify the obstruction stage in the assembly process, the earlier fractions from the fractionation studies (#15, 16 and 17) containing 26 and 20S forms were pooled (see Fig 18). In addition, the middle fractions (#18, 19 and 20) were pooled to get 20S and half proteasomes. These early and middle fractions from truncated Pre7 versions in both genetic backgrounds were analysed by native-PAGE and immunoblotting. In the early fractions (#15, 16 and 17), mostly assembled 20S proteasome is detected alone or in association with respective regulatory complexes (Fig 21B). In the middle fractions (#18, 19 and 20) the 20S particles with 19S complexes are detectable in similar amounts in wild type and in *ump1Δ* background. However, the abundance of the 20S particle with Blm3 is increased in the *ump1Δ* background (Fig 21B) which correlates with the results obtained above. The early assembly intermediates or half-proteasomes are clearly detectable in the wild-type (*UMPI*) strains containing the N-7 or MY-5 Pre7 subunit. These results further demonstrate that the stepwise truncations in the Pre7 subunit lead to accumulation of half-proteasomes due to difficulties in their dimerization to form the stable mature particle. The absence of Ump1 may allow faster assembly and thus abolishes the accumulation of intermediates in the Pre7 truncation versions.

4.2.10 The effect of Ump1 induction in Pre7 truncation mutants

The experiments described above demonstrated, that the Ump1 protein is not compatible with N-terminal truncations of Pre7 subunit beyond position -6. Therefore, to analyse the influence of Ump1 in the assembly and maturation process in the Pre7 mutant strains, an Ump1 inducible system was created. The region encoding the C-terminus of Ump1 with HA epitope was excised from plasmid YIP5-ump1-5'Δ-HA (a gift from C. Enenkel, Berlin) and introduced into the *UMPI* gene in a pCEN-UMPI plasmid resulting in the pCEN-UMPI-HA construct. This *UMPI-HA* region was subsequently cloned into a

URA3-marked high-copy number (2 μ) plasmid under the control of the GAL promoter (see methods and Fig 6). The resulting construct (pGAL::*UMP1-HA*) was introduced into *ump1 Δ* strains possessing the wild-type, UBI/N-7, Met Y-5 or UBI/Y-5 version of Pre7. This system allowed to follow by biochemical analysis of the fate of the Ump1 protein in proteasome assembly including those strain synthesizing a mutant Pre7 subunit with propeptide remnants shorter than 6 residues (for example UBI/Y-5 Pre7). In these strains, induction of Ump1 was expected to arrest cell proliferation eventually.

Growth of *ump1 Δ* strains transformed with the construct (pGAL::*UMP1-HA*) on solid synthetic medium containing glucose (Fig 22A Glu) was similar to untransformed strains expressing respective Pre7 mutant versions (not shown). As expected, when these cells were transferred to solid synthetic medium containing galactose, the strain carrying the wild-type Pre7 subunit (WT) grew faster than the strains expressing N-7 or Met Y-5 Pre7 subunits (Fig 22B Gal). However, growth of the strain possessing the Y-5 Pre7 subunit was obstructed after few cell division cycles and thus no visible colonies were formed (Fig 22B Gal). This indicates that overexpression of Ump1-HA results in the same growth behaviour as chromosomal expression of wild-type Ump1. The appearance of Ump1-HA in *ump1 Δ* strains innovates the wild type situation in the presence of non-mutated Pre7 and causes lethality if the Y-5 Pre7 subunit is expressed.

To follow the influence of Ump1-HA expression in proteasome assembly in *ump1 Δ* strains with mutant Pre7 subunits, Ump1-HA induction experiments were performed (see methods). The Pre7 mutant strains (wild-type, UBI/N-7, Met Y-5 or UBI/Y-5) in *ump1 Δ* background carrying the construct (pGAL::*UMP1-HA*) were grown to OD₆₀₀ = 0.7 in liquid synthetic medium with raffinose and Ump1-HA expression was induced by the addition of galactose to the medium (zero time point). Equal volumes of cultures were then collected after increasing time of incubation. The cell pellets were lysed and the proteins were subjected to SDS-PAGE and immunoblot analysis. The monoclonal anti-HA antibody was used to follow the expression of the Ump1-HA and an anti-Pre4 antibody was used to follow the maturation kinetics of the Pre4 subunit.

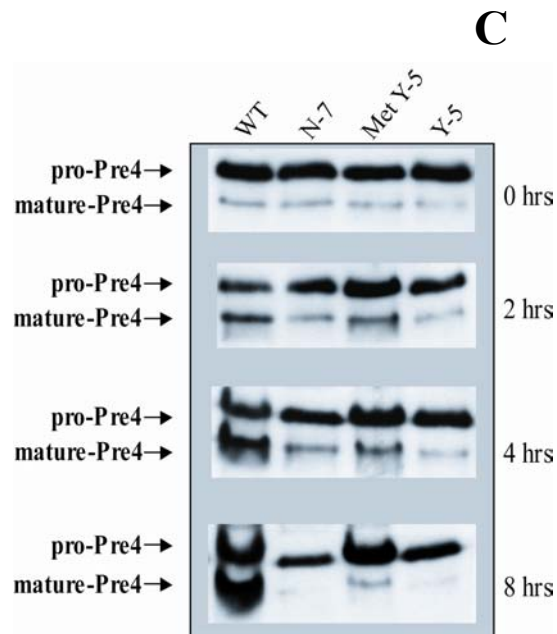
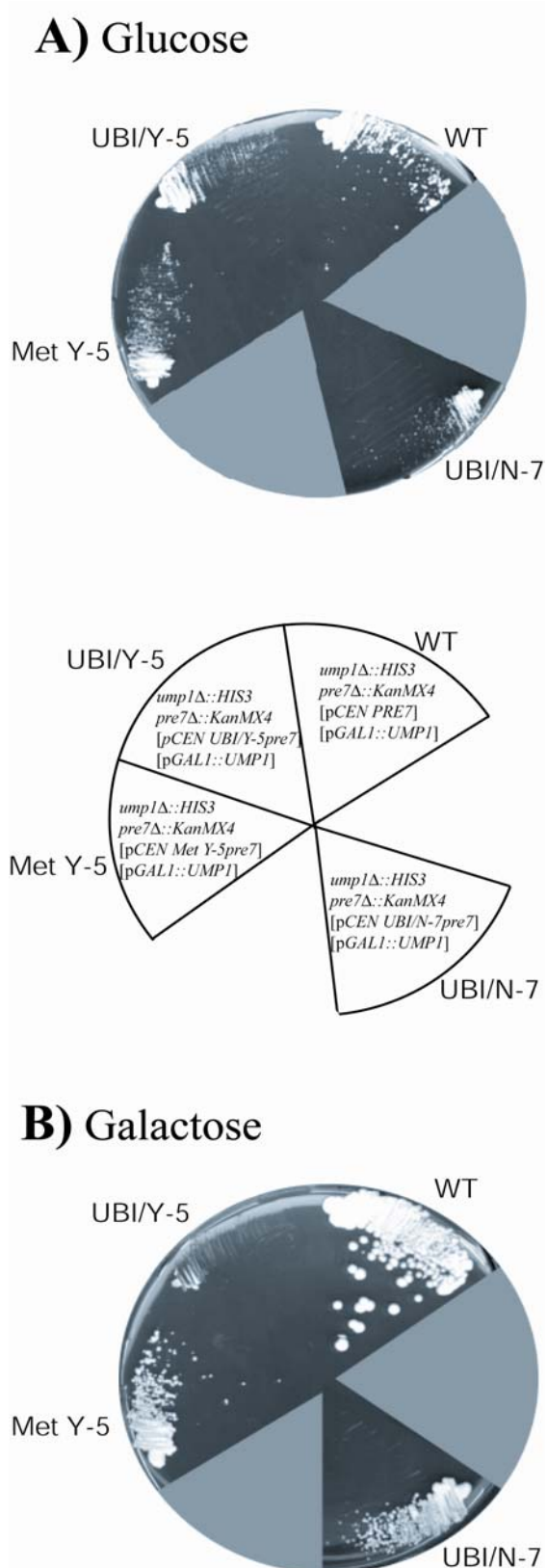


Figure 22

The impact of Ump1 induction in Pre7 truncation mutants

A, B. Strains expressing wild-type (WT) and truncated Pre7 versions (UBI/N-7, Met Y-5 and UBI/Y-5) in *ump1Δ* background transformed with a plasmid carrying an *UMP1* gene under control of the inducible *GAL* promoter (see schematic drawing) were grown at 30 °C for 2 days on solid synthetic medium containing glucose (A) or galactose (B).

C. Immunoblot analysis of indicated strains that were grown until log phase in liquid synthetic medium containing raffinose (see text) and shifted to synthetic medium containing galactose to induce Ump1 expression. Equal volumes of cultures were collected at different time points (hrs). Maturation of Pre4 was monitored using anti-Pre4 antibody.

The Ump1-HA protein appeared in the induced cells after 2 hrs (not shown). In the next hours, the Ump1-HA amount increased only in strains expressing the WT, N-7 or Met Y-5 Pre7 subunit, but not in the strain containing the Y-5 subunit (data not shown). At the 0-time point more precursor form of Pre4 than mature form was detectable in all strains (Fig 22C [0 hrs]). However, in samples of later time points the conversion of the precursor Pre4 subunit to mature form was only detectable in the strain expressing wild-type Pre7, but not in the Pre7 mutants (Fig 22C 4 to 8 hrs). These results are in accordance with the growth behavior detected on galactose plates and further confirmed that Ump1 can function properly only in the wild-type cells, but not in strains with mutated Pre7.

The results described above reveal that appearance of Ump1 in the Pre7 mutant strains cause defects in proteasome formation accompanied by accumulation of precursor β -type subunits. In order to follow the fate of Ump1 in the proteasome assembly intermediates, extracts from mutant strains (WT, UBI/N-7, Met Y-5 and UBI/Y-5) were analysed by native-PAGE. Native cell extracts were prepared from cultures after transfer to galactose, subjected to non-denaturing PAGE and the separated proteasome complexes were transferred to nitrocellulose membrane. Ump1-HA was detected after 2 hrs in two faster migrating assembly intermediates in the wild-type strain (Fig 23 2 hrs lane 1 [* and ☼]). The location of these assembly products was compared with the complexes containing Pre2-HA detected in native-PAGE immunoblot analysis shown in Fig 21A. These complexes (* and ☼) might represent an assembly intermediate and half-proteasome, respectively. In contrast, in the UBI/N-7 and Met Y-5 strains Ump1 was detectable only in the region containing 15S proteasome (Fig 23 2 hrs lane 2 and 3). No Ump1 was detectable in UBI/Y-5 strains after 2 hrs of induction, but it was appearing after 4 and 8 hrs only at the half proteasome region (Fig 23 lane 4). In the other strains (WT, UBI/N-7 and MY-5) Ump1 containing half proteasome increased with time (Fig 23 4 to 8 hrs lane 1 to 3), however the lower band corresponding to the putative early assembly intermediate was gradually increased during the induction time only in the wild-type strain (Fig 23 4 to 8 hrs, lane 1). These results may imply that in the mutant Pre7 strains Ump1 was able to bind only with the half-proteasome but not to the early assembly intermediates.

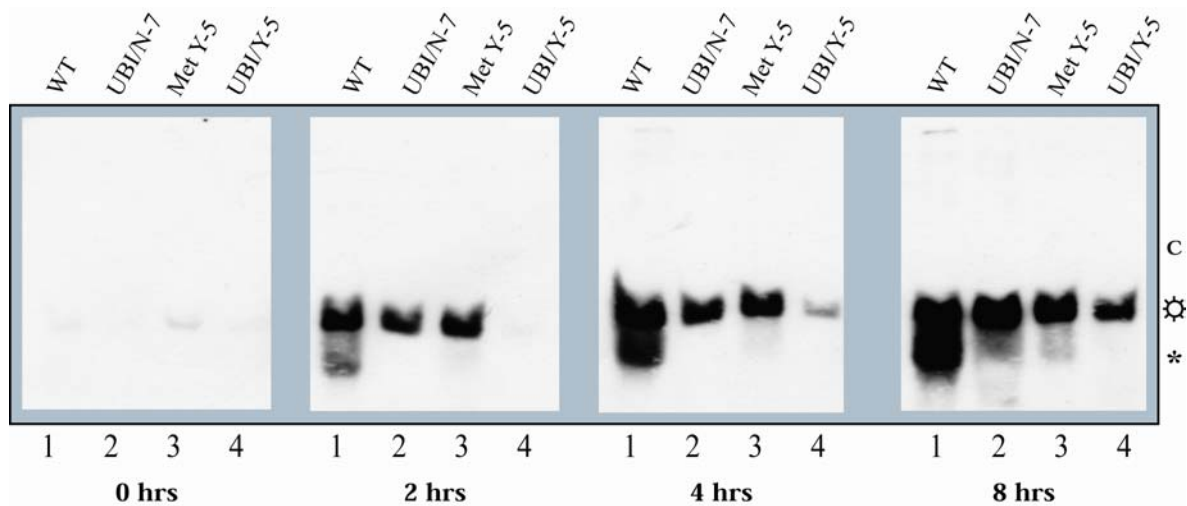


Figure 23

Detection of proteasome assembly intermediates containing Ump1 in Pre7 mutant strains

Expression of Ump1 was induced in respective *ump1Δ* cells carrying truncated Pre7 as described as in Fig 22C, but extracts were prepared under native conditions. The native proteins were separated on a native-gel and subjected to immunoblot analysis. Proteasome assembly complexes containing Ump1 were detected using anti-HA antibody. A fast migrating complex in the 15S half-proteasome region (⊙) and a putative early assembly intermediate (*) are marked according to their migration relative to purified 20S proteasome (C) and to known assembly intermediates (see Fig 21).

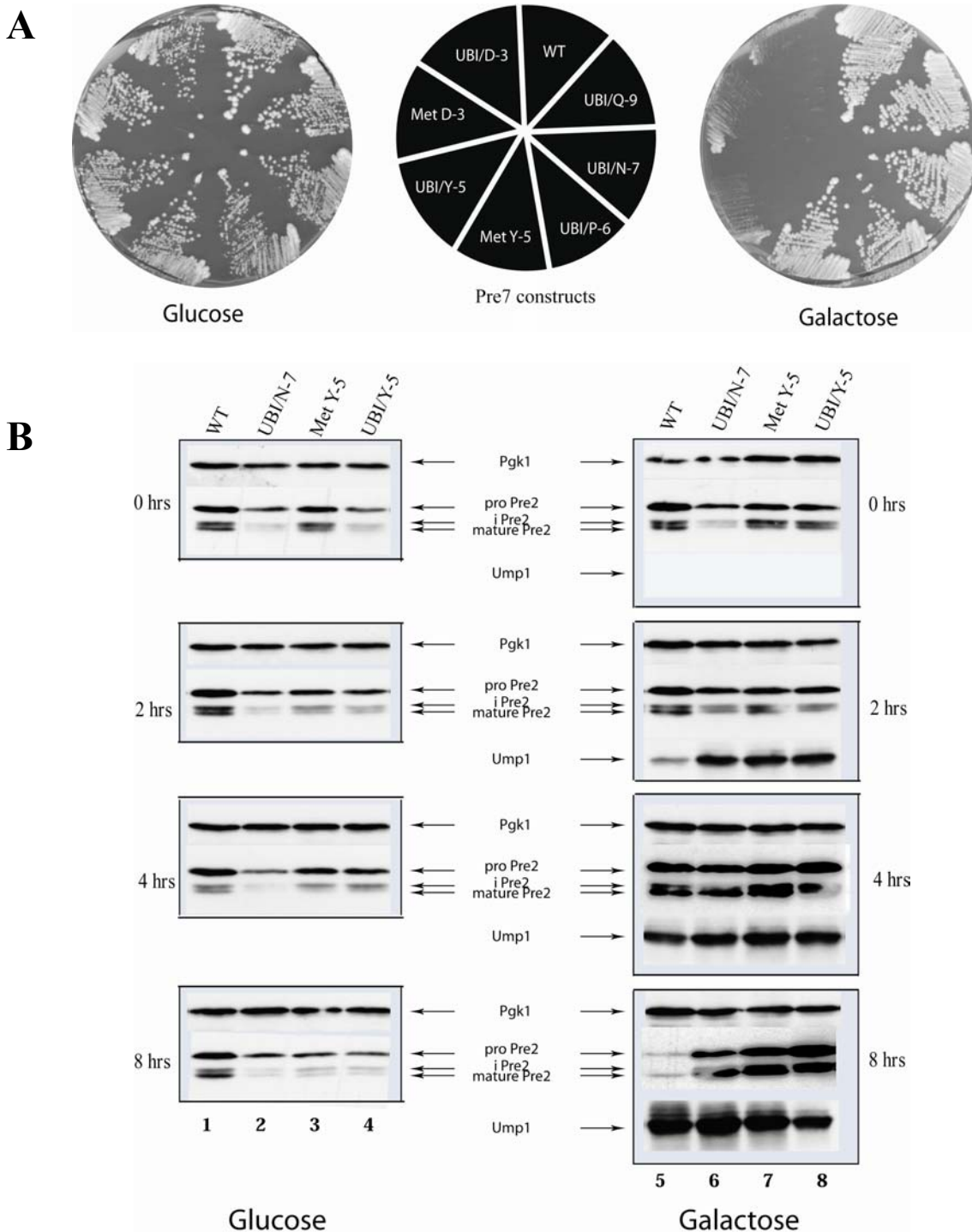
The induction experiments shown above imply that the induction of Ump1-HA in *ump1Δ* strains leads to accumulation of the proteasome assembly intermediates and the 15S proteasome. Strikingly, appearance of the early assembly intermediate is obstructed in strains expressing the mutant Pre7 subunits. The disadvantage of this experimental setup was that no proteasome subunit was tagged with epitope for immunodetection. Therefore, a different approach was used to construct strains in which Ump1 and a proteasome subunit were detectable.

An open reading frame of *UMP1* was cloned behind the *GAL* promoter. The sequence encoding the FLAG epitope tag was introduced at the 3' end of the *UMP1* gene followed by a stop codon and the *CYC1* terminator sequence. The resulting construct was inserted upstream of each Pre7 mutant construct in the *LEU2*-marked centromeric plasmids (see Fig 6 for construct details). These plasmids were introduced into the

ump1Δ Pre7 shuffle strain and the Pre7 mutants were selected as described before. In selected Pre7 mutant strains (UMP1+PRE7 to UMP1+UBI/D-3) the Pre2 subunit was tagged individually at the C-terminus with the HA epitope, as described in Fig 18. The resulting strains express Pre2-HA and Ump1-FLAG in the respective Pre7 mutants (Fig 24 cartoon, WT to UBI/D-3). All these strains showed similar growth on solid synthetic medium with glucose (Fig 24A glucose), whereas on synthetic medium with galactose, only the strains carrying the WT, Q-9, N-7, P-6 and MY-5 Pre7 subunits were able to grow (Fig 24A galactose). As expected, the strains expressing Y-5, MD-3, D-3 Pre7 subunits were halted in cell proliferation after few cycles which is comparable to the results obtained in the previous Ump1 induction studies (as in Fig 22).

To follow the fate of Ump1 in the proteasome assembly intermediates and its involvement in the proteasomal subunit maturation kinetics, selected strains (WT, UBI/N-7, Met Y-5 and UBI/Y-5) were grown in liquid YP-raffinose medium until $OD_{600} = 0.7$ and the cells were then split into halves (0-time point). One half of the cells was inoculated into liquid YP-medium with glucose, as control. The other half of the cells was transferred to YP-medium with galactose to induce the Ump1 expression. Equal amounts of cells were collected at different time points (0 to 8 hrs). The cell pellets were lysed and samples with equal amounts of protein were subjected to SDS-PAGE and immunoblot analysis. Monoclonal anti-HA and anti-FLAG antibodies were used to detect Pre2 and Ump1, respectively, and anti-Pgk1 antiserum was used for a loading control.

All Pre7 mutant strains grown on YP-glucose medium showed more Pre2 precursors and intermediately processed form than the mature Pre2 subunit (Fig 24B glucose 0 to 8 hrs) comparable with the Pre4 maturation defect detected by pulse chase analysis in Pre7 mutants with *ump1Δ*. Evidently, no Ump1 signal was detectable in these strains (not shown). Furthermore, the ratio of precursors to mature subunit is similar in all strains (Fig 24B glucose lane 1 to 4). At zero time point the strains grown on YP-galactose medium did not produce an Ump1 signal as well, but after 2 hrs the expression of Ump1 was clearly detectable in all mutant strains (Fig 24B 2 hrs). However, the wild-type strain showed a lower amount of Ump1 than the UBI/N-7, Met Y-5 and UBI/Y-5 strains (Fig 24B lane 5-8). Thus, the appearance of Ump1 in the WT strain obviously

**Figure 24**

Growth phenotypes and Pre2 maturation after induction of Ump1 in Pre7 mutants

A. Strains expressing different Pre7 mutant constructs that carry a galactose inducible *UMPI* gene in *ump1Δ* background (see text) were streaked on solid YP-glucose or YP-galactose plates and grown for 2 days at 30 °C.

B. Immunoblot analysis of indicated strains (WT, UBI/N-7, MY-5 and UBI/-5) grown in liquid YP-glucose or YP-galactose for indicated time-periods (0 to 8 hrs). The 0-time point represents the point when the cells were shifted from YP-raffinose to YP-glucose or YP-galactose medium (see text). Equal amounts of proteins were loaded on SDS-PAGE. Precursor (pro-Pre2), intermediately processed (i-Pre2) and the mature Pre2 subunit were detected using anti-HA antibody. An anti-FLAG antibody was used to detect Ump1. As a loading control, phosphoglycerate kinase was detected by anti-Pgk1 antibody.

enhances the proteasome assembly and leads to its rapid turnover upon maturation in contrast to the Pre7 mutants (UBI/N-7, Met Y-5 and UBI/Y-5), where it accumulates due to impaired proteasome maturation. The steady state level of Ump1 was increased in WT strain at 4 and 8 hrs (Fig 24B 4 and 8 hrs) but it was accumulating more in UBI/N-7 and Met Y-5 strains. Interestingly, the amounts of Ump1 remain constant after 4 hrs to 8 hrs in the UBI/Y-5 strain (Fig 24B 4 to 8 hrs, lane 8). This effect can be correlated with the growth arrest of the UBI/Y-5 strain, in galactose medium after 4 hrs $OD_{600} = 1.3 \pm 0.2$ and after 8 hrs $OD_{600} = 1.6 \pm 0.2$.

The conversion of precursor to mature Pre2 subunit was slightly enhanced in WT strain during time points (Fig 24B 2 to 8 hrs) along with the appearance of Ump1 (Fig 24B lane 5). In strains UBI/N-7 and Met Y-5 equal amounts of precursor and mature Pre2 subunits were detectable after 8 hrs of induction (Fig 24B lane 6 and 7). As expected, in the UBI/Y-5 strain the precursor Pre2 subunit was accumulating in the cell after 4 to 8 hrs (Fig 24B lane 8). These results show again that Ump1 expression in the Pre7 mutants causes defects in proteasome assembly and maturation. Therefore, to analyse the fate of Ump1 in the proteasome and in its assembly intermediates, the cell pellets from the induction experiment described above were lysed under native conditions and subjected to native-gel immunoblot analysis as described in section 4.2.9. The complexes containing Pre2, Ump1 and 20S proteasome were detected using anti-HA, anti-FLAG and anti-proteasome antibody, respectively.

The selected strains grown on YP-glucose showed similar “steady state” amounts of 20S proteasome and proteasome with different regulatory complexes (Fig 25A lane 1 to 4), as detected in the earlier native gel analysis (Fig 21B *ump1Δ*). Some amounts of faster migrating assembly intermediates (*) were detectable in this system but this pattern remains constant during time (Fig 25A 0 to 8 hrs). Since Ump1 is absent in these strains (WT, UBI/N-7, Met Y-5 and UBI/Y-5) they all are capable to assemble functional proteasomes, albeit with reduced efficiency.

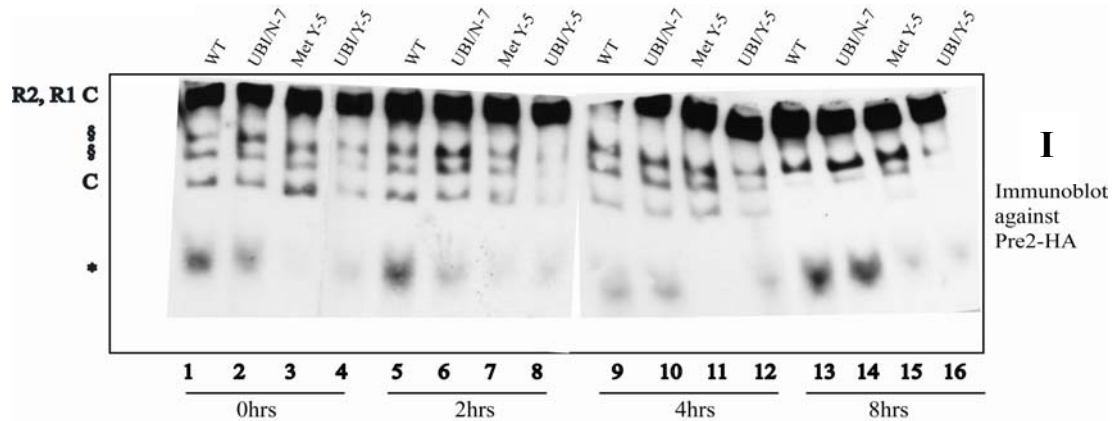
The anti-proteasome antibody detected only the purified 20S proteasome in the native gel system but failed to produce any proteasome signals in the given crude extracts (not shown). Therefore, by using this as an advantage, the location of purified 20S proteasome was detected (shown as a control “C” in Fig 25B) on the membrane, which

was then re-probed to detect Ump1 by anti-FLAG antibody. In the induced cells, Ump1 appeared after 2 hrs in a faster migrating complex (☼), which migrated in between 20S proteasome and early assembly intermediates (Fig 25B lane 5 to 8 and lane 9 to 12). These Ump1 containing complexes might be 15S or half-proteasomes with considerable half-life as in wild-type cells. However, the putative early assembly intermediates (faster migrating complex *) with Ump1 were only detected after 8 hrs (Fig 25B lane 13 to 15). Interestingly, binding of Ump1 was restricted only to the half-proteasome complex in the UBI/Y-5 strain (Fig 25B lane 16). This might be explained by the inability of Ump1 to bind to the proteasome assembly intermediates containing the Y-5 Pre7 subunit, whereas its binding is not affected when other Pre7 versions with longer propeptide remnant residue in this complex (Fig 25B lane 13 to 15).

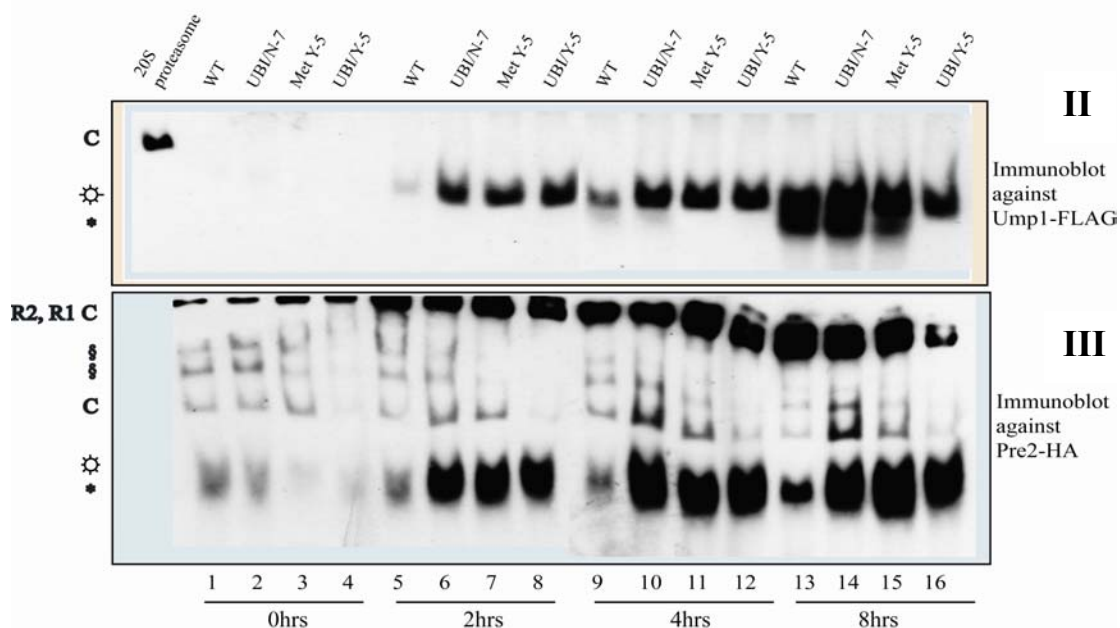
In the wild-type strain the early proteasome assembly complex (*) containing the Pre2 subunit remains in similar concentration after 2 hrs of Ump1 induction (Fig 25B lane 1 and 5), and increased only slightly in later time points (2 to 8 hrs lane 5, 9 and 13). Strikingly, a bulk of faster migrating complex (☼) is accumulated in between 20S proteasome and the early assembly intermediates (*) in Pre7 mutants after 2hrs of induction (Fig 25B 2hrs lane 6 to 8). This complex (☼) might represent the complete half-proteasome. Unexpectedly, increase or decrease of early assembly intermediate (*) in Pre7 mutants cannot be explained at this stage because of dramatic increase of the half-proteasome accumulates in this region. After 4 hrs of induction these complexes (☼ with or without *) were further increased (Fig 25B lane 10 to 12). Interestingly, these assembly intermediates accumulated most in the Met Y-5 strain at 8 hrs than 4 hrs of Ump1 induction (Fig 25B, compare lane 11 and 15), but they remain constant in UBI/Y-5 strain, in agreement with the detected growth arrest as well as the precursor accumulation (see Fig 24 A and B lane 8). As expected the amount of 20S (C) and 20S proteasomes with regulatory particles (R1, R2 and §) are noticeably reduced in the UBI/Y-5 strain at 8 hrs when compared to 4 hrs (compare R1, R2 in lane 12 and 16).

These results further indicate that the Pre7 mutants (UBI/N-7 and Met Y-5) accumulate proteasome assembly intermediates in the presence of Ump1 due to their impaired ability to dimerize 2 half-proteasomes into 20S proteasome, but in the UBI/Y-5 strain binding of Ump1 to the half-proteasomes causes a dead-end assembly product.

A. Glucose



B. Galactose

**Figure 25**

Non-denaturing PAGE and immuno-blot analysis of early proteasome assembly intermediates

Ump1 deletion strains possessing different Pre7 mutant constructs (WT, UBI/N-7, MY-5 and UBI/-5) carrying the *UMPI* gene under the inducible *GAL* promoter (see text) were grown in YP-glucose (A) or YP-galactose (B) (as described in Figure 24) and cells were collected at different time points (hrs). Cells was lysed under native conditions and subjected to native-gel immunoblot analysis.

I. Immunodetection of assembly intermediates and proteasome complexes containing Pre2-HA in non-induced cells (A). The early assembly intermediates (*) and the 20S core particle (C) with Blm3 complexes (§) or with 19S regulatory particle (R1, R2) are labelled.

II. Proteasome assembly intermediates containing Ump1 protein in induced cells were detected using anti-FLAG antibody. The ☼ and * symbol represents the 15S half-proteasome and a putative early assembly intermediate, respectively. By using anti-proteasome antibody the purified 20S proteasome (C) signal was detected (see text for details).

III. Proteasome complexes containing the Pre2 subunit were detected in Ump1 induced cells. The Pre2 subunit is found in 20S proteasome (C), core particle with different regulatory complexes (§ or R1, R2) and in early assembly intermediates (☼ + *). The content and distribution of Pre2-HA is followed at the start of Ump1 induction (0 hrs) and at later time points (2, 4 and 8 hrs).

4.3 Structure-based mutation analysis of the β 6/Pre7 subunit

4.3.1 The Pre7 propeptide remnant adheres to the Pre7 surface via a hydrophobic pocket

The results from genetic and biochemical studies presented so far revealed that the remnant of the Pre7 propeptide is essential for assembly of functional proteasomes in yeast. In addition, the function of the Pre7 propeptide remnant was found to be sequence specific. Surprisingly, comparison of the Pre7 amino acid sequence with available sequences of β 6-subunit orthologues from other species uncovers that the proline and tyrosine, respectively, at position -6 and -5 in the β 6/Pre7 propeptide region are absolutely conserved (Fig 26). In addition to this, a region containing a small stretch of hydrophobic amino acids (FFPYY) at position 93 to 97 in the Pre7 subunit is also absolutely conserved among species as well (Fig 26).

	+1	77	90	105
		oooooooooooooooooooo		=====>
		H2		S5
<i>Saccharomyces cerevisiae</i>	QFN PY GDN GG	INSAARNIQHLL YGKRFFFPYY VHTIIAGL		
<i>Schizosaccharomyces pombe</i>	QFD PYVQ N GG	AQSCACMVRTL LYGKRFFFPYY VYTTVAGI		
<i>Caenorhabditis elegans</i>	RWN PYSME GG	VDLCAELLSRN LYRFFFPYY TGAILAGI		
<i>Drosophila melanogaster</i>	F S PYES N GG	TEAVAQMLSIAM YNRFFFPYY VSNILAGI		
<i>Mus musculus</i>	R F S PYAF N GG	TGAI A AMLSTIL YSRFFFPYY VYNI I GG L		
<i>Homo sapiens</i>	R F S PYVF N GG	TGAI A AMLSTIL YSRFFFPYY VYNI I GG L		
<i>Rattus norvegicus</i>	R F S PYAF N GG	TGAI A AMLSTIL YSRFFFPYY VYNI I EG L		
<i>Arabidopsis thaliana</i>	N W S PYDN N GG	CPAMAQLLSNT LYFKRFFFPYY AFNVL GG L		
<i>Nicotiana tabacum</i>	S PYDN N GG	CPAMGQLLSNT LYKRFFFPYY SFNVL GG L		
<i>Carassius auratus</i>	K F S PYAF N GG	SGAI A AMLSTIL YGRFFFPYY VYNI I GG L		
<i>Trypanosoma brucei</i>	H W S PYTD N GG	TKAI A AKLTSTML YQRFFFPYY TFNMIV G I		

Figure 26

Sequence alignment of parts of the β 6/Pre7 subunit with corresponding parts of β 6 orthologues from different species

Conserved amino acid residues in the propeptide remnant and in the region comprising the H2 helix and the S5 strand are highlighted.

By exploring the available crystal structure of the yeast 20S proteasome (Groll et al., 1997), the location of these conserved hydrophobic amino acids in the mature Pre7 subunit was analysed. Interestingly, the amino acids FFPYY located in a loop connecting

helix H2 and β -strand S5 form a hydrophobic pocket on the inner surface of the Pre7 subunit that accommodates the side chain of tyrosine -5 from the propeptide region (Fig 27).

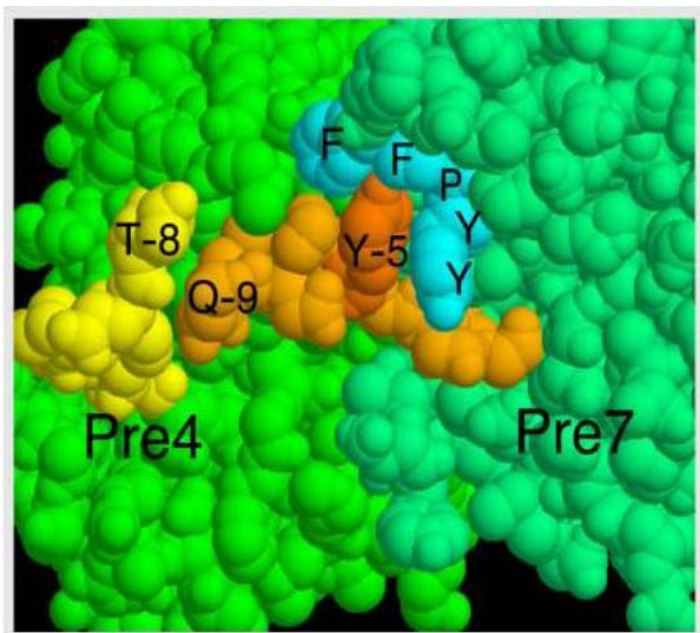


Figure 27

Space-filling presentation of the structure of the Pre7 subunit surface with the propeptide remnant bound to a hydrophobic pocket.

The residues FFPYY forming a hydrophobic pocket in the Pre7 subunit surface (spring green) and the Pre7 propeptide remnant are coloured in aqua blue and orange, respectively. The tyrosine (Y-5) in the Pre7 propeptide remnant is highlighted by dark orange colouring. The neighboring Pre4 subunit (lime green) and its propeptide remnant (yellow) are presented as well. The N-terminal residues of Pre7 and Pre4 are labelled.

4.3.2 Conserved amino acids in the Pre7 subunit are essential for proteasome biogenesis

In order to determine the requirement or dispensability of these conserved residues in the Pre7 subunit for proteasome function, a site-directed mutagenic analysis was performed. At first proline (at position -6) and tyrosine (at position -5) in the propeptide remnant region were replaced by alanine individually (-6P to A and -5Y to A) (Fig 28A, 2 and 3). In addition, both proline and tyrosine were mutually mutated to alanines (Fig 28A, 4). The constructs encoding these mutant Pre7 subunits were introduced into yeast strains in both wild type and *ump1Δ* background, as described above. Interestingly, in *UMP1* wild-type strains possessing the construct encoding Pre7 with a point mutation at -5 position (-5Y to A) or with double mutation (-6P, -5Y to A) failed to produce viable colonies on 5-FOA (Fig 28A shown as - symbol). In contrast, strains expressing the Pre7 subunits

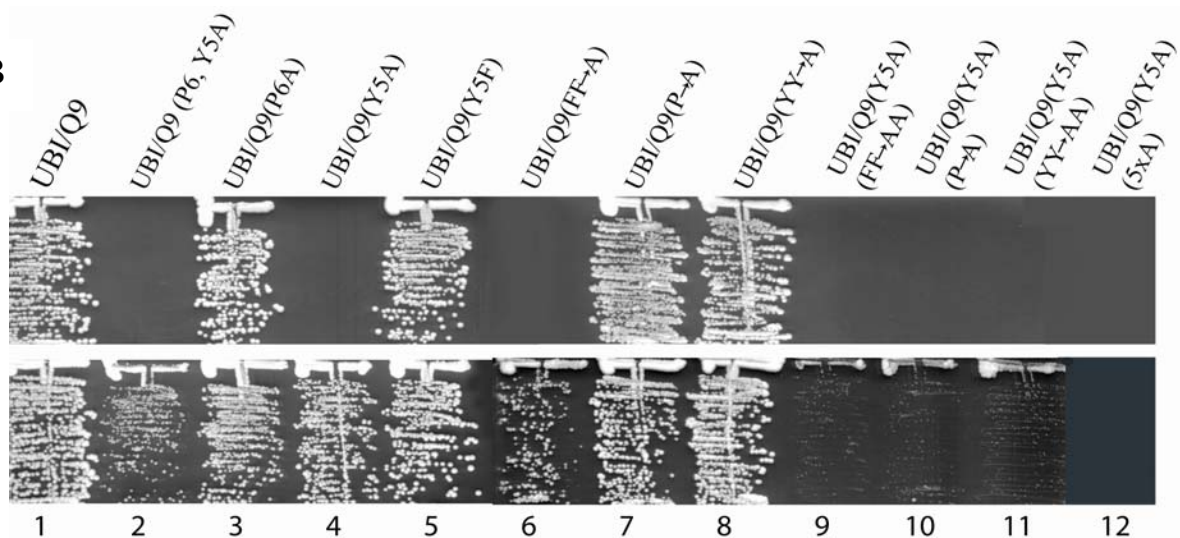
carrying a mutation at -6 position (-6P to A) produced colonies comparable to *PRE7* wild-type cells (Fig 28A shown as +++ symbol). However, in the *ump1Δ* background, all strains expressing different point mutant versions of the Pre7 propeptide region produced viable colonies on 5-FOA (Fig 28A ++). To examine the structural requirement of the side chain of tyrosine at position -5 in the Pre7 propeptide remnant region, a phenylalanine was introduced instead (-5Y to F) (Fig 28A, 5). Surprisingly, this construct was able to confer viability to cells both with wild type and with *ump1Δ* background (Fig 28A and B). This result revealed that the hydroxyl group of tyrosine is not required for its function, whereas presence of its aromatic structure at position -5 in the Pre7 propeptide is sufficient.

Next, to explore the necessity of the amino acids FFPYY that form the hydrophobic pocket in the Pre7 subunit, alanines were introduced instead of these amino acids in different combinations (Fig 28B, 6 to 8). In *UMPI* background, cells possessing the Pre7 subunit with mutation of FF to AA in the hydrophobic pocket did not produce colonies on 5-FOA plates (Fig 28A lane 6, shown as - symbol) but strains expressing mutant subunits with P replaced by A or YY replaced by AA grew as wild type strains (Fig 28A and B, lanes 7 and 8, +++ symbol). However, in the *ump1Δ* background the effect of the FF→AA mutation was suppressed again. Thus, in the absence of Ump1 all Pre7 mutants altered in the hydrophobic pocket produced viable clones (Fig 28A and B lanes 6 to 8).

The mutation analysis described above implicated that a tyrosine in the Pre7 propeptide region and the two phenylalanines in the FFPYY region are sufficient to admit the propeptide at the hydrophobic pocket. However, this contact seems to be dispensable in the absence of Ump1 suggesting that the appearance of this hydrophobic surface region in Pre7 is incompatible with the function of the Ump1 protein. If this is true, the tyrosine from the propeptide should be dispensable when the hydrophobic pocket is demolished by mutations. To verify this prediction residues of the FFPYY sequence were exchanged to alanines in different combinations in addition the -5Y to Y mutation in the Pre7 propeptide remnant region (Fig 28A and B, lanes 9 to 12). Strikingly, conversion of all five amino acids from the FFPYY region and the tyrosine in the propeptide region to alanines was lethal both to *UMPI* and *ump1Δ* cells (Fig 28A, 12).

Construct	Amino acid replacements in Pre7	Viability and strain background	
		WT	<i>ump1Δ</i>
1 UBI/Q-9	===GG QFN <u>P</u> YGDNG G1::: : FFP <u>Y</u> Y::	+++	++
2 UBI/Q-9 (P6A)	===GG QFN <u>A</u> YGDNG G1:::	+++	++
3 UBI/Q-9 (Y5A)	===GG QFN <u>P</u> <u>A</u> GDNG G1:::	-	++
4 UBI/Q-9 (P6A, Y5A)	===GG QFN <u>A</u> <u>A</u> GDNG G1:::	-	+
5 UBI/Q-9 (Y5F)	===GG QFN <u>P</u> <u>F</u> GDNG G1:::	+++	++
6 UBI/Q-9 (FF→AA)	===GG QFN <u>P</u> YGDNG G1::: : <u>A</u> AP <u>Y</u> Y::	-	+
7 UBI/Q-9 (P→A)	===GG QFN <u>P</u> YGDNG G1::: : <u>F</u> F <u>A</u> Y <u>Y</u> ::	+++	++
8 UBI/Q-9 (YY→AA)	===GG QFN <u>P</u> YGDNG G1::: : <u>F</u> FP <u>A</u> <u>A</u> ::	+++	++
9 UBI/Q-9 (Y5A, FF→AA)	===GG QFN <u>P</u> <u>A</u> GDNG G1::: : <u>A</u> AP <u>Y</u> Y::	-	[+]
10 UBI/Q-9 (Y5A, P→A)	===GG QFN <u>P</u> <u>A</u> GDNG G1::: : <u>F</u> F <u>A</u> Y <u>Y</u> ::	-	[+]
11 UBI/Q-9 (Y5A, YY→AA)	===GG QFN <u>P</u> <u>A</u> GDNG G1::: : <u>F</u> FP <u>A</u> <u>A</u> ::	-	[+]
12 UBI/Q-9 (Y5A, 5xA)	===GG QFN <u>P</u> <u>A</u> GDNG G1::: : <u>A</u> A <u>A</u> <u>A</u> <u>A</u> <u>A</u> ::	-	-

B

**Figure 28**

Constructs encoding mutant Pre7 subunits with point mutations in highly conserved regions and growth behaviour of the mutant strains

A. The growth of *UMP1* and *ump1Δ* strains transformed with the UBI/Q-9 based constructs is shown by +/- symbols (same as in Fig 8A). A ubiquitin encoding sequence (= = = GG) is fused to the G1 (Gly1) codon that corresponds to T1 (Thr1) of active subunits. The dotted line (: : : :) represents the continuation of the wild type Pre7 protein sequence from G1 up to the loop connecting the H2 helix and the S5 strand (see Fig 26). Different point mutations created in the conserved amino acids in the propeptide remnant and in the hydrophobic pocket in the β 6/Pre7 subunit are underlined. The mutant constructs were introduced into yeast strain with *UMP1* or *ump1Δ* background and the cell viability was checked on 5-FOA plate as described in Fig 10. The [+] symbol represents a very strong growth defect of the strain (compare with streaks in B).

B. Colony growth of strains expressing different Pre7 mutant versions (see A) is shown in streaks for comparison. Viable strains (+/[+]symbol in A) were streaked on solid YPD and incubated at 30 °C for 2 days for *UMP1* and 3 days for *ump1Δ*. Non-viable strains were not streaked.

This can be explained by the fact that FFPYY motif is essential for the structural integrity of the Pre7 subunit. Unexpectedly, all individual mutations of these amino acids when combined with the -5Y to A mutation, did not allow survival of cells in the presence of Ump1 protein (Fig 28A, lanes 9 to 11). In addition, these combined mutations caused a severe growth phenotype even in the *ump1Δ* background (Fig 28A and B, lanes 9 to 11).

In summary, all conserved amino acids under consideration contribute substantially to the structural functionality of the Pre7 subunit. Interactions between propeptide and hydrophobic pocket seem to be mediated by multiple contacts, in which the tyrosine in the propeptide remnant region and the phenylalanines in the FFPYY region are essential for this function. Finally, the appearance of the hydrophobic surface in Pre7 appears to disrupt the function of Ump1 in the biogenesis of the proteasome.

5 Discussion

5.1 The role of propeptides in proteasome biogenesis

The 14 different subunits constituting the eukaryotic 20S proteasome must be assembled into an ordered structure with an invariable subunit topology (Groll et al., 1997; Unno et al., 2002b) through a multi-step reaction requiring a host of specific interactions. The order of events at early assembly stages collecting free non-assembled subunits into precursor complexes still is unexplained (Heinemeyer et al., 2004). In the late assembly stages the conversion of β -subunit precursors of β 1/Pre3, β 2/Pup1 and β 5/Pre2 to their mature active forms is an essential step in order to acquire active 20S core particles (Chen and Hochstrasser, 1996; Heinemeyer et al., 1997; Schmidt et al., 1997). Many studies elucidated that the activation of these subunits occurs through intramolecular autolysis of the precursor subunits, resulting in removal of their N-terminal propeptides (Chen and Hochstrasser, 1996; Ditzel et al., 1998a; Frentzel et al., 1994; Heinemeyer et al., 1997; Schmidtke et al., 1997). Extensive studies on the 20S core particle biogenesis disclosed the requirement of propeptides in the different active β -type subunit precursors. One general function of these propeptides was found to protect against an irreversible modification of the amino group of the catalytic Thr1 by N- α -acetylation (Arendt and Hochstrasser, 1999; Jäger et al., 1999). In addition, unequal contributions of the β 1/Pre3, β 2/Pup1 and β 5/Pre2 propeptides in the proteasome assembly process were reported (Arendt and Hochstrasser, 1999; Chen and Hochstrasser, 1996; Jäger et al., 1999). Interestingly, the propeptide of Pre2 was found to be essential for yeast cell viability (Chen and Hochstrasser, 1996) and therefore must be indispensable for generation of functional proteasome in sufficient amount.

Three of the four inactive β -type subunits; β 7/Pre4, β 3/Pup3 and β 6/Pre7 are synthesized with prosequence, of which β 3/Pup3 stays unprocessed, whereas the β 7/Pre4 and β 6/Pre7 precursors are partially processed by an active neighbor subunit in the mature particle (Groll et al., 1997; Jäger et al., 1999). Putative functions of these propeptides during particle assembly or functions of their remaining pieces in the mature particle have been analysed only for β 7/Pre4 so far. The Pre4 propeptide including its eight-residue remnant piece that stays in the mature particle was found to be not required

for proteasome function (Jäger et al., 1999). In the work presented here the eight residue propeptide region of $\beta 3$ /Pup3 was similarly found to be dispensable for proteasome function, since its deletion did not affect cell growth. Hence, this prosequence does not contribute any substantial function to the proteasome. Surprisingly, introducing *pre7* mutant alleles expressing $\beta 6$ /Pre7 without the complete propeptide into yeast cells led to drastically reduced survival rate and an extreme growth defect of surviving clones (Fig 7C). Thus, this propeptide plays an essential role for yeast cell viability. However, partial deletion of the Pre7 propeptide revealed that the region cleaved off by the neighboring active β -type subunit $\beta 2$ /Pup1 is dispensable and that the remaining C-terminal nine prosequence residues staying in the mature particle are sufficient for normal cell growth. The minimal length still allowing survival was determined by further truncations of this residual propeptide region from the N-terminus: the six residues in the Pre7 propeptide (position -6 to -1) were found to be absolutely required for survival (Fig 8). Nevertheless, a proline at -6 position is dispensable for the propeptide remnant function. Remarkably, the growth phenotype of the viable mutants was strengthened gradually along with the propeptide remnant truncation (Fig 8B and 10A)

The requirement of prosequences for generation of the functional protein species is a widespread feature among proteases. They are synthesized as precursors bearing prosequences that are eventually removed generating the active form of the protein. Besides avoiding premature proteolytic activity these propeptides are often needed to mediate the folding of the mature moiety (Baker et al., 1993; Khan and James, 1998). The propeptides of proteasomal β -subunits could play similar roles in proteasome biogenesis (Arendt and Hochstrasser, 1999). Since Pre7 is an inactive subunit, the role of its propeptide might be restricted to correct folding of this subunit in order to allow incorporation into the 20S particle. Interestingly, the Pre2 propeptide, when provided *in trans*, can function in the assembly of active proteasomes as efficiently as in its covalently, precursor-bound form (Chen and Hochstrasser, 1996). Here, the propeptide was reported to serve a chaperone-like function in assisting the assembly and maturation process (Chen and Hochstrasser, 1996). However, expression of the HA epitope-tagged Pre7 propeptide as separate peptide did not rescue growth of cells harbouring the Pre7 subunit without covalently bound propeptide region. Hence, the function of this propep-

tide might be accomplishable only in its covalently bound state. However it cannot be excluded here that the short propeptide was degraded due to lack of any folding which might require covalent linkage to the Pre7 precursor subunit. As described in the beginning, the contribution of β -subunit propeptides to particle assembly is unequal, which is paralleled by a high degree of divergence among each other in primary structure and in length (Arendt and Hochstrasser, 1997; Jäger et al., 1999; Zühl et al., 1997a; Zwickl et al., 1994). By sequence replacement analysis, the function of the Pre7 propeptide remnant was found to specifically depend on its amino acid sequence because replacing this region by corresponding prosequence stretches of similar length from the active Pre3 or the inactive Pup3 subunit did not rescue the deletion phenotype. This is in line with the assumption that the propeptides play subunit specific roles to fold and incorporate the subunit into the nascent proteasome (Chen and Hochstrasser, 1996; Yang et al., 1995). However, the propeptides do not seem to be essential for positioning of β -subunits within the ring (Schmidt et al., 1999; Schmidtke et al., 1996). The Pre7 propeptide might be involved in folding of the Pre7 subunit and/or to mediate specific contacts with neighbouring subunits or other proteins aiding in the assembly pathway. It could also be required to transduce conformational changes during particle assembly to the Pre7 core moiety. Finally, a putative role of the Pre7 propeptide remnant in the mature 20S proteasome to prevent deleterious interactions between protein substrates and the inner surface of the active chamber could not be excluded in the beginning of this study. However, the ensuing biochemical analysis of Pre7 mutants and their genetic interplay with the proteasome assembly and maturation factor Ump1 lent the focus of the propeptide role towards particle biogenesis. Cells carrying Pre7 subunits with 7- or 6- residue propeptide remnant are impaired to form functional proteasomes (see below). Further shortening this propeptide remnant probably obstructs the proteasome assembly process due to formation of dead-end assembly products. Recently, such assembly products or half-proteasomes were shown to accumulate due to replacement of the β -subunit propeptide in the proteasome of the archaebacterium *A. fulgidus* by human $\beta 5$ propeptide sequences of different length (Mullapudi et al., 2004).

5.2 Additional requirements for proteasome assembly

In addition to β -subunit propeptides, assembly and maturation of the proteasome requires additional molecular chaperones (Schmidtke et al., 1997). In yeast, a short-lived chaperone named Ump1 was found that is required for correct assembly and proper maturation of the proteasome and, after completion of these steps, is degraded inside the activated proteasome (Ramos et al., 1998). Interestingly, the Pre2 propeptide that is essential for formation of functional proteasomes became dispensable in the absence of the Ump1 protein (Ramos et al., 1998). Surprisingly, also the nine residue propeptide remnant piece of Pre7 which stays in the mature the proteasome was no more required for assembly of functional proteasomes when the *UMP1* gene was deleted (Fig 10). The function of Ump1 was reported to enhance dimerization of two half-proteasomes and to trigger particle maturation (Ramos et al., 1998). During this processes, the propeptides seem to play a critical role. If the involvement of the Pre7 propeptide remnant is essential in these stages to guarantee the execution of Ump1's function, its deletion could become incompatible with formation of functional proteasomes in the presence of Ump1. Alternatively, retardation of proteasome assembly and maturation in the absence of the Ump1 protein (Ramos et al., 1998) could allow incorporation or correct folding of the truncated Pre7 subunit, which in the normally proceeding process might be inefficient. If this indirect effect were true, other mutations that affect the half-proteasome dimerization or maturation process could be compatible with the otherwise lethal Pre7 mutations. When combining the *pre7* mutations with the *pre1-1* mutation that was reported to affect particle maturation due to defective association between the β 4/Pre1 and the β 5/Pre2 subunits from opposed halves of the proteasome (Chen and Hochstrasser, 1996), no suppression of growth defects originating from Pre7 propeptide truncations was observed. Instead, the *pre1-1* mutation even enhanced these phenotypes (Fig 12B). Nevertheless, it cannot be excluded that other mutations that specifically affect the half-proteasome dimerization might suppress the phenotype caused by Pre7 truncations.

Since expression of Ump1 protein in Pre7 mutants caused severe defects, its function must somehow be coupled to the Pre7 propeptide remnant piece. An important question would be at which stage the Pre7 propeptide function is linked to that of Ump1. As proposed for the Pre2 propeptide (Ramos et al., 1998), the Pre7 propeptide might play

a role through a specific interaction with Ump1 to induce structural alteration or displacement of this factor to allow proceeding of the assembly process. Absence of either propeptide would leave Ump1 in a position that is incompatible with the formation of active proteasomes.

If the function of the Ump1 protein depends on the availability of propeptides, they must interact with each other at any stage of the assembly processes. Analysis of some of the late incorporating β -type subunits such as $\beta 5/\text{Pre}2$, $\beta 6/\text{Pre}7$ and $\beta 7/\text{Pre}4$ for their interaction with Ump1 *in vitro* revealed that these subunits are indeed capable to interact individually with the Ump1 protein (Fig 14C), although the necessity of their propeptides for this association has not been proven in this kind of experiment. Thus, the interaction of Ump1 with assembly intermediates obviously is mediated by multiple contacts to individual β -subunit precursors. Due to these multiple interactions, the Ump1 binding is coupled with the formation of half-proteasome precursors, because from *ump1 Δ* cell extracts an array of proteasomal subunits, presumably stemming from half-proteasomes or earlier assembly intermediates containing a subset of α - and β -subunits, was pulled down effectively using immobilized GST-Ump1. Whereas in cells containing endogenous Ump1, the protein seems to occupy its place in assembly intermediates such as the half-proteasome and therefore might compete for binding of the GST-bound Ump1 protein (Fig 14B). Remarkably, the amount of material binding to GST-Ump1 was not affected by truncations in the Pre7 propeptide. Hence, the residues -9 to -7 in the Pre7 propeptide remnant regions are not essential for a putative interaction with Ump1. Unfortunately, binding of Ump1 with assembly intermediates synthesized in strains carrying Pre7 propeptide remnants shorter than six residues was not analysed, which might have given clues to a different binding behaviour as encountered in a *UMPI* background, where this might be responsible for lethality. At this stage, it is clear that the formation of half-proteasome precursor complexes is coupled with incorporation of Ump1, for which the late incorporating subunits or their propeptides seem to play a crucial role. Studies on yeast Ump1 (Ramos et al., 1998) or its homologue hUmp1 in human cells (Burri et al., 2000) gave detailed insights into its functional domains required to interact with assembly intermediates. They propose that the C-terminal region of this protein is specifically required for interaction with assembly intermediates (Burri et al.,

2000; Ramos et al., 1998), but it is still not known whether these assembly complexes are complete half-proteasomes or earlier assembly intermediates. At present, propeptides are believed to interact with Ump1 during this process, although there is no published experimental evidence proving the interaction of Ump1 only with precursor subunits but not with their mature counterparts.

As discussed above, the Pre7 and Pre2 propeptides are absolutely required for the function of Ump1. The propeptides of other β -subunits (Pre3 and Pre4) were found to be dispensable for normal cell viability, excluding a major function in proteasome biogenesis, in contrast to the Pup1 propeptide, whose deletion impaired cell growth (Jäger et al., 1999). To investigate the unknown nature of the assembly promoting function of the Pup1 propeptide and to explore a putative involvement of the Pre3 and Pre4 propeptides in particle assembly, the requirement or dispensability of these propeptides in the absence of Ump1 was analysed as well. This genetic analysis elucidated that these propeptides operate in parallel with Ump1 during proteasome biogenesis. In all cases, synthetic growth defects were observed, when deletions of Ump1 and any of these propeptide were combined (Fig 13). Thus, the requirement for these propeptides in the absence of Ump1 appears to be much higher than in its presence. It is interesting to note that the combined deletion of the propeptides from both Pup1 and Pre3 subunits also caused a significantly stronger phenotype than that seen in either single mutant (Arendt and Hochstrasser, 1999; Jäger et al., 1999). Likewise, deletion of the Pre7 propeptide combined with deletion of the Pre2 or Pre4 propeptides strikingly caused lethality either in the presence or in the absence of Ump1 (not shown). Therefore, these propeptides are considered to function in a coordinative manner to assist proteasome assembly. Removing Ump1 together with any of these propeptides or deleting any of these propeptides in combination thus causes severe defects in the proteasome assembly process.

5.3 Defects in proteasome function up-regulate the precursor expression

The proteasome is essential for cell viability, and so any gross defects in its assembly would be lethal. Truncation of the Pre7 propeptide remnant region caused a severe growth phenotype due to perturbation in the proteasome assembly and/or maturation

process (see below). Such defects have already been reported for Pre2 and Pup1 propeptide deletion mutants (Chen and Hochstrasser, 1996; Jäger et al., 1999). These type of primary defects affecting the assembly or maturation of the proteasome can be compensated by increasing the amounts of proteasomal precursors in the cell (Chen and Hochstrasser, 1996; Ramos et al., 1998; Ramos et al., 2004). Apparently, also truncations in the Pre7 subunit lead to a dramatic up-regulation of proteasome subunit expression (see Fig 17). Analyzing the assembly products from Pre7 mutants by fractionation studies showed a high amount of precursors that are predominantly incorporated into proteasome assembly intermediates (Fig 18A). Recent studies have demonstrated, that up-regulation of the proteasomal gene expression upon impaired proteasome function is mediated by the transcription factor Rpn4 (Ju and Xie, 2004; Mannhaupt et al., 1999). The Rpn4 protein itself is a substrate of the 26S proteasome and thus its level depends on proteasomal activity, suggesting that it is a key component in a feedback regulation of the proteasome (London et al., 2004; Xie and Varshavsky, 2001). Evidently, in *ump1Δ* background the levels of proteasome precursors are similar for all Pre7 mutants. This means that the absence of Ump1 already causes maximal up-regulation of precursor expression even in cells carrying the wild-type Pre7 subunit, because proteasome assembly and maturation is substantially impaired in *ump1Δ* strains.

5.4 Complete maturation of 20S proteasomes requires the function of propeptides and accurate particle assembly

Autocatalytic processing of β -subunit precursors is a late event in proteasome assembly, since the 13-15S assembly intermediates are inactive, whereas the active 20S core particle contains only mature subunits (Frentzel et al., 1994; Schmidtke et al., 1996). By the fractionation studies carried out in this work, a minor defect in autocatalytic processing of precursors was even found in strains expressing the Pre7 subunit with those nine propeptide residues that are preserved in the mature particle. This result enlightens that the part of the Pre7 propeptide that is removed by processing *in trans* also contributes somewhat to proper proteasome maturation. Shortening the propeptide remnant region from -9 to -7 leads to accumulation of precursor subunits such as Pre2 in fractions that

contain 20S or 26S proteasomes (Fig 18). Accordingly, in these fractions the chymotrypsin-like activity was reduced along with stepwise truncations in the Pre7 propeptide remnant region. These defects are most pronounced in the MY-5 strain carrying Pre7 with a six residue propeptide remnant. Interestingly, only in case of the MY-5 strain traces of the intermediately processed Pre2 subunit were found in the 20S fractions. Since these Pre2 species are likely to be produced by Pre3 and/or Pup1 cleavage, the autocatalytic processing of these other β -type subunits seems to be affected by Pre7 truncations as well. Although the maturation of the Pre3 and Pup1 subunits was not analysed in this work, the dramatic decrease in PGPH activity in the Pre7 mutants supports general defects in particle maturation. As reported, active sites are only activated when the two half-proteasomes have been associated correctly and specific interactions between subunits were formed thereby (Chen and Hochstrasser, 1996). The Pre7 propeptide remnant must contribute a crucial role in this process entailing formation of functional proteasomes. The catalytic activity of the Pre2 subunit is known to be central for *in vivo* protein degradation and cell growth (Arendt and Hochstrasser, 1997; Chen and Hochstrasser, 1996; Jäger et al., 1999), since any defects in Pre2 activity substantially affect the cell growth. Thus, the reduced Pre2 precursor processing observed along with propeptide truncations of Pre7 might at least in part be responsible for the gradually increasing growth defect (Fig 8B). Remarkably, in *ump1 Δ* cells the 20S/26S fractions contained more material of processed and intermediately processed Pre2 than precursor form. Indeed, this pattern was not significantly changed by truncations in the Pre7 subunit. In the mutant expressing the Pre7 subunit with six residue propeptide remnant *inter* and *intra*-molecular processing even seems to occur significantly better in the absence of Ump1 than in its presence (Fig 18 and 19). These results show that the effect of Pre7 propeptide truncations on cell viability is coupled to the availability of Ump1 in the cell. Conformational changes in Ump1 or alterations in its position in the nascent or pre-holoproteasome seem to be crucial for generation of functional proteasomes and the contribution of the Pre7 propeptide in this process is indispensable (see below).

Defects in the maturation process converting precursors to mature subunits are compensated by an increased precursor synthesis, which finally increases the amount of

correctly matured proteasomes (Ramos et al., 1998; Ramos et al., 2004; Seemüller et al., 1996). According to pulse-chase experiments the formation of active proteasome from precursors in mammals ranges from few to several hours, depending on the cell type (Frentzel et al., 1994; Nandi et al., 1997; Yang et al., 1995). In yeast this process seems to be faster and requires only 30 to 40 minutes (Chen and Hochstrasser, 1996; Ramos et al., 1998). Analysis of *inter*-molecular processing of the Pre4 subunit in Pre7 mutants by pulse-chase experiments revealed that most of the precursors remain unprocessed even after a 120 min chase (see Fig 20). In this kind of experiment, it cannot be distinguished whether precursors have been incorporated into proteasome complexes or remained free in the cell. However, most of the precursors were detected in the fractions containing 13S, 20S and 26S complexes (Fig 18) showing that most of them have been incorporated into assembly intermediates. Thus, defects in proteasome maturation due to impaired autocatalytic processing seem to be mainly responsible for precursor accumulation, and not their inefficient incorporation. Interestingly, no intermediately processed form of Pre4 was detected in the pulse-chase analysis in any of the Pre7 mutants either in the presence or in the absence of Ump1. It is known that processing of the Pre4 propeptide depends on its nearest neighbor active subunit, Pup1. Only if Pup1 activity is missing intermediate processing is exerted by Pre3 or Pre2 (Heinemeyer et al., 1997). After a 120 min chase, the small amount of processed Pre4 detectable in all viable Pre7 mutants corresponds to the completely matured species, indicating that in the Pre7 truncation mutants gain of the PGPH and/or chymotrypsin-like activities of Pre3 and Pre2 is more affected when compared to the trypsin-like activity of Pup1.

All the results discussed above imply that in Pre7 mutants the assembly of the proteasome is retarded in presence of Ump1; in addition, the particle maturation is dramatically reduced in viable mutants, whereas these steps might be completely obstructed in non-viable mutants. However, in the absence of Ump1 such defects are identical in strains expressing either Pre7 mutants or wild-type Pre7. Interestingly, a putative assembly complex (Fig 21B; §) that migrates slower than the 20S complex was enriched over 20S particles in Pre7 mutants in *ump1Δ* background. These complexes are clearly distinguishable from 20S and 26S complexes in the native-gel system and thus might contain the 20S particle associated with some other proteins. These putative

assembly products show a migration behaviour comparable to that of core particles containing the Blm3 protein, as identified by using a similar gel-electrophoresis system (Fehlker et al., 2003). In contrast to PA200, a mammalian homologue of Blm3 that acts as an activator of the 20S proteasome, the yeast Blm3 was reported to function as a checkpoint protein by preventing premature activation of the nascent proteasome. In contrast to this, the putative complexes accumulating in Pre7 mutants show peptidase activity like 20S or 26S proteasomes, which disputes against the assumption that these complexes represent Blm3/20S core particle associations. If these were indeed proteasome/Blm3 complexes, it would not be clear at this stage whether Blm3 is required to prevent premature activation or whether it functions as regulator of the yeast 20S proteasome in a different way. However, it is intriguing to speculate that an impaired assembly or maturation process due to truncations in the Pre7 propeptide region or lack of Ump1 might be compensated by binding of a novel complex or Blm3 to the nascent proteasome.

5.5 Proteasome assembly occurs via half-proteasome

Under normal conditions, precursor complexes of proteasomes are less abundant than mature proteasomes due to the fact, that the half-lives of these precursors are shorter or inhomogeneous *in vivo* (Nandi et al., 1997; Rodriguez-Vilarino et al., 2000). Upon truncations in the Pre7 propeptide, such putative early intermediates accumulated in the cell (Fig 21A, H?). Indeed, these complexes are not active and migrate faster than the purified 20S proteasome. According to this behaviour, these complexes are considered as 13S-15S early assembly intermediates. Unfortunately, presence or absence of the Pre7 subunit in these complexes was not detectable in the native-gel system by the available antibody. Therefore, accumulation of such assembly products in the Pre7 mutants can be explained by two scenarios. First, the truncations in the Pre7 subunit might inhibit its incorporation into those assembly intermediates or, second, the presence of the mutant subunit in this complex is incompatible with proceeding of the assembly process. The requirement of the Pre7 propeptide for incorporation of the subunit into early assembly intermediates cannot be excluded. As discussed in the beginning, the propeptides are

known to play an essential role during this process, for instance Pre2 in yeast or its mammalian homologue Lmp7 cannot be incorporated into proteasomes *in vivo* without their propeptides (Cerundolo et al., 1995; Chen and Hochstrasser, 1996). In addition to this function, the interaction ability of Ump1 with early assembly products seems to be influenced by the propeptide region of Pre7 (see above). Such proteasome assembly intermediates or half-proteasomes with sedimentation constants of 13S or 15S have been described in mammalian cells (Yang et al., 1995), however, not all of the β -subunits were detected in the most abundant species of assembly intermediate (Nandi et al., 1997). In yeast, such early assembly intermediates have not been identified and analysed as yet, except for the complete half-proteasome complex containing the Ump1 protein (Ramos et al., 1998). It is possible that mutations in the Pre7 subunit result in structural perturbations that affect the proceeding of the assembly process and lead both to accumulation of the early assembly products and, at the late assembly stages, affect critical conformational changes in the pre-holoproteasomes or nascent proteasomes that are required for particle maturation.

5.6 Induction of Ump1 in Pre7 truncation mutants causes defects in the proteasome assembly process

The interaction of Ump1 with proteasome assembly intermediates containing the Pre7 subunit with propeptide remnant shorter than six residues might be a rate-limiting step in proteasome assembly. Whereas all Pre7 mutants grew homogeneously in the absence of Ump1, induction of Ump1 in these cells strikingly changed their growth behaviour (Fig 22 or 24A). Growth of the strain carrying wild-type Pre7 became better than that of strains expressing Pre7 with truncated propeptides with 9 to 6 residues and evidently, growth of the strain possessing the propeptide remnant shortened to 5 residues was obstructed after few division cycles (see Fig 22 or 24). Accordingly, the precursor maturation kinetics was strongly slowed down in strains carrying the Pre7 propeptide remnant with 7, 6 or 5 residues (Fig 22 and 24B) compared to strains with the wild-type Pre7 propeptide. Similarly, in *ump1Δ* cells the amounts of 20S and 26S proteasomes were equal in all Pre7 truncation mutants and not different to those found in a similar

strain carrying wild-type Pre7 (Fig 25A), but upon appearance of Ump1 the concentration of these complexes was somewhat reduced in strains expressing Pre7 with a propeptide remnant of 5 residues (Fig 25B). Whereas the expression of Ump1 in strains carrying wild-type Pre7 or Pre7 with 7 or 6 residue propeptide did not change the amount of 20S and 26S proteasome considerably (Fig 25B), the two latter mutant strains show a strong accumulation of proteasome assembly intermediates (§ and *), which is comparable with the strain expressing Pre7 with 5 residues propeptide remnant. Interestingly, detection of Ump1 in these assembly intermediates revealed that the binding of Ump1 to early assembly intermediates is completely obstructed in strains expressing Pre7 with a 5 residue propeptide remnant (Fig 25B, III), but the shorter truncations did not affect this association (lane 13 to 15). However, Ump1 is still able to incorporate into the slower migrating intermediate, probably the half-proteasome or 15S complex. Since binding of Ump1 to early assembly intermediates does not occur in strains expressing Pre7 with 5 residue propeptide remnant, the incorporation of Ump1 at this state might be a much more efficient way to let the assembly process proceed than incorporation at the stage of the half-proteasome. Alternatively, the assembly intermediates with Pre7 subunits containing propeptide remnants with nine to six residues are compatible with Ump1 binding and induction of critical conformational changes during the assembly process, whereas Pre7 versions with longer propeptide truncations might be inadequate in this process.

5.7 Genetic dissection of structural requirements in Pre7 for proper Ump1 function

Mutation analysis of the Pre7 subunit revealed that even minor modifications in its structure can cause malfunction of the subunit. At first addition of any kind of epitope tag at the C-terminus or into an internal loop region of Pre7 caused severe defects in its function. In addition, truncations or replacement of the Pre7 propeptide caused dead-end proteasome assembly products and so led to lethality. This suggests that incorporation of Pre7 into assembly intermediates or into half-proteasomes depends on a strict preservation of its tertiary structure, which might be required either to fit this subunit in a right

conformation and/or to induce structural alterations in order to promote further steps in particle biogenesis.

Strikingly, the structure of the Pre7 subunit that is compatible with normal proceeding of the assembly process depends on amino acid residues, which have been conserved among the orthologues subunits during proteasome evolution (see Fig 26). In the propeptide remnant region, a tyrosine at position -5 is necessary for its function because replacing it by alanine was lethal, whereas an exchange to phenylalanine was still functional. Thus, the aromatic side chain of tyrosine is essential whereas its hydroxyl group is dispensable. However, the mutation of Tyr-5 to alanine did not cause lethality in a *ump1Δ* background. Interestingly, the yeast 20S proteasome crystal structure reveals that the aromatic side chain of this tyrosine resides in a hydrophobic pocket, which is formed by a highly conserved stretch of hydrophobic amino acids from Pre7 itself (Fig 27). Two phenylalanines in the hydrophobic pocket are essential only when Ump1 is present in the cell, like the tyrosine from the propeptide region, indicating that these residues play a crucial role which is absolutely required for Ump1 function during the assembly or maturation process. This could be explained by the fact that the exposure of a hydrophobic site in the Pre7 surface, due to the absence of the propeptide or its inability to cover this region, might lead to unfavorable interactions of Ump1 or even other proteins or propeptides with this region. Besides that, the Pre7 propeptide might be needed to interact directly with Ump1, thereby inducing conformational changes in Ump1 during the assembly and maturation process, probably in cooperation with other propeptides.

If the accessibility of the hydrophobic pocket is incompatible with Ump1 function during particle assembly and maturation, destruction of this region by mutations could let the assembly process proceed. But unexpectedly, replacing the tyrosine in the propeptide region in combination with the exchange of any of the hydrophobic amino acids in the hydrophobic pocket to alanines caused a severe growth phenotype even in *ump1Δ* cells (see Fig 28). This unexpected result could be confirmed by exchanging all conserved hydrophobic residues, that form the hydrophobic pocket to alanines, which substantiated the conclusion that these preserved residues in the Pre7 subunit are foremost essential for its structural integrity.

In brief, the conserved hydrophobic amino acid cluster apparently is essential to allow folding of the Pre7 subunit into an incorporation-competent conformation. The appearance of the hydrophobic surface formed by the conserved hydrophobic residues is evidently incompatible with Ump1 function during particle assembly and maturation and the contacts between the hydrophobic pocket and the propeptide region are indispensable to avoid deleterious interactions with this region during particle biogenesis.

6 A model of the yeast 20S proteasome biogenesis

The assembly of functional yeast 20S proteasomes requires the coordinated association of 14 different subunits in a fixed order with the involvement of other factors (Groll et al., 1997; Heinemeyer et al., 2004). Such proteins contributing to the proteasome biogenesis have been described in recent years (Ramos et al., 1998). However, the early steps in the assembly process are not understood neither in yeast nor in mammalian cells (Gerards et al., 1998; Schmidtke et al., 1997). Obviously, more work is required, to clearly define the assembly pathway of the eukaryotic 20S proteasome and to specify the exact role of chaperones in this process. In consideration of the results presented in this work, the following model can be proposed for yeast 20S proteasome biogenesis (see Fig 29).

1. The earliest detectable assembly intermediate in mammalian cells was shown to contain a complete α -ring and a subset of β -subunits (Frentzel et al., 1994; Nandi et al., 1997; Yang et al., 1995). The yeast homologues of these early incorporating β -subunits are β 2/Pup1, β 3/Pup3 and β 4/Pre1. Under the presumption of a conserved assembly pathway in mammals and yeast, these subunits would associate with a complete α -ring yielding the first long-lived assembly intermediate in yeast cells (highlighted with dark background). It is still unclear whether this assembly process is initiated via rings of α -subunits that serve as a matrix for docking of the β -subunits (white arrows), as found for the *Thermoplasma* proteasome biogenesis (Zwickl et al., 1994) or whether the assembly is initiated by α/β heterodimer formation (blue arrows) as demonstrated for *Rhodococcus* (Zühl et al., 1997a).

2. Incorporation of the remaining β -subunits β 1/Pre3, β 5/Pre2, β 6/Pre7 and β 7/Pre4 into the early assembly intermediates obtained above leads to complete half-proteasomes (Nandi et al., 1997). These subunits might be incorporated either as a preassembled sub-complex (white arrows) or individually (blue arrows). In both pathways, binding of the Ump1 protein to half-proteasomes seems to be strongly influenced by these subunits and might mutually depend on their propeptides. Thus, the propeptides of β 5/Pre2 and β 6/Pre7 might be involved directly or indirectly in the association of Ump1 with the half-proteasome complex (A). Truncations or deletion of the β 6/Pre7 propeptide region might obstruct the assembly process because of two possible reasons (B). The first might be the inability of the mutant Pre7 to fold into a conformation that is

compatible with its incorporation into any of the assembly intermediates (highlighted with yellow circle). The second possibility would be that truncations or deletion of the propeptide region lead to exposure of the hydrophobic area on the surface of $\beta 6/\text{Pre}7$ (pointed by hand symbol), which leads to a wrong positioning of Ump1. The data obtained in this study clearly demonstrate that in the absence of Ump1 the mutant Pre7 protein is capable to incorporate effectively into assembly intermediates that allow the assembly process to proceed. This largely excludes the first possible reason, an effect on the folding and incorporation of Pre7 by deletion of its propeptide and favours the model that the appearance of the hydrophobic pocket causes improper binding of Ump1 to the β -sub-complexes and/or to half-proteasomes. Assembly of the putative sub-complex with mutant $\beta 6/\text{Pre}7$ in the presence of Ump1 might induce unfavorable conformational constraints in this complex, which is either incompatible with its incorporation or lead to incorporation in a unsuitable conformation (white arrows with question marks). Alternatively, if these subunits were incorporated individually (shown in blue arrows) into the nascent half-proteasomes, Ump1 would still be capable to associate because of its ability to interact with most of the late incorporating subunits. However, the presence of mutant Pre7 with exposed hydrophobic surface in half-proteasomes would lead to an unproductive interaction with Ump1, and thus interfere with or inhibit further steps.

3. The β -subunits in the half-proteasome seem to undergo conformational changes to induce dimerization (Mullapudi et al., 2004). In addition, structural alteration of Ump1 by the influence of propeptides in the half-proteasome could be crucial to enhance dimerization of two half-proteasomes into an instable intermediate or pre-holoproteasome (Ramos et al., 1998). The presence of truncated or mutated Pre7 in the half-proteasome together with Ump1 might obviate the conformational changes required to trigger the dimerization process. Alternatively, the absence of the Pre7 propeptide might cause Ump1 to fall in a wrong position inside the half-proteasomes. Thus, the appearance of the hydrophobic surface might interfere with the proper function of Ump1 in both scenarios. In all cases, the dimerization process is obstructed and so leads to accumulation of half-proteasome complexes with Ump1. In contrast to this, when the Ump1 protein is missing, the Pre7 propeptide is dispensable at least during the assembly process.

4. The conversion of active β -subunit precursors to the mature form by autocatalytic processing in the pre-holoproteasome is the final step to reach the mature 20S proteasome (Chen and Hochstrasser, 1996; Heinemeyer et al., 1997; Schmidt et al., 1997). In this step, Ump1 seems to play a crucial role in positioning the propeptides in a conformation that induces the maturation process (Ramos et al., 1998). This step was shown to be affected dramatically even in viable strains carrying Pre7 with a propeptide remnant of 7 to 6 residues. Obviously, this stage is not reached or absolutely blocked in Pre7 mutants carrying longer truncations in the propeptide region beyond position -6. If Ump1 is missing, all the β -subunit propeptides seem to function in a coordinative manner that guarantees normal proteasome maturation to an extent that is still sufficient for survival.

Fig 29
Models of 20S proteasome biogenesis

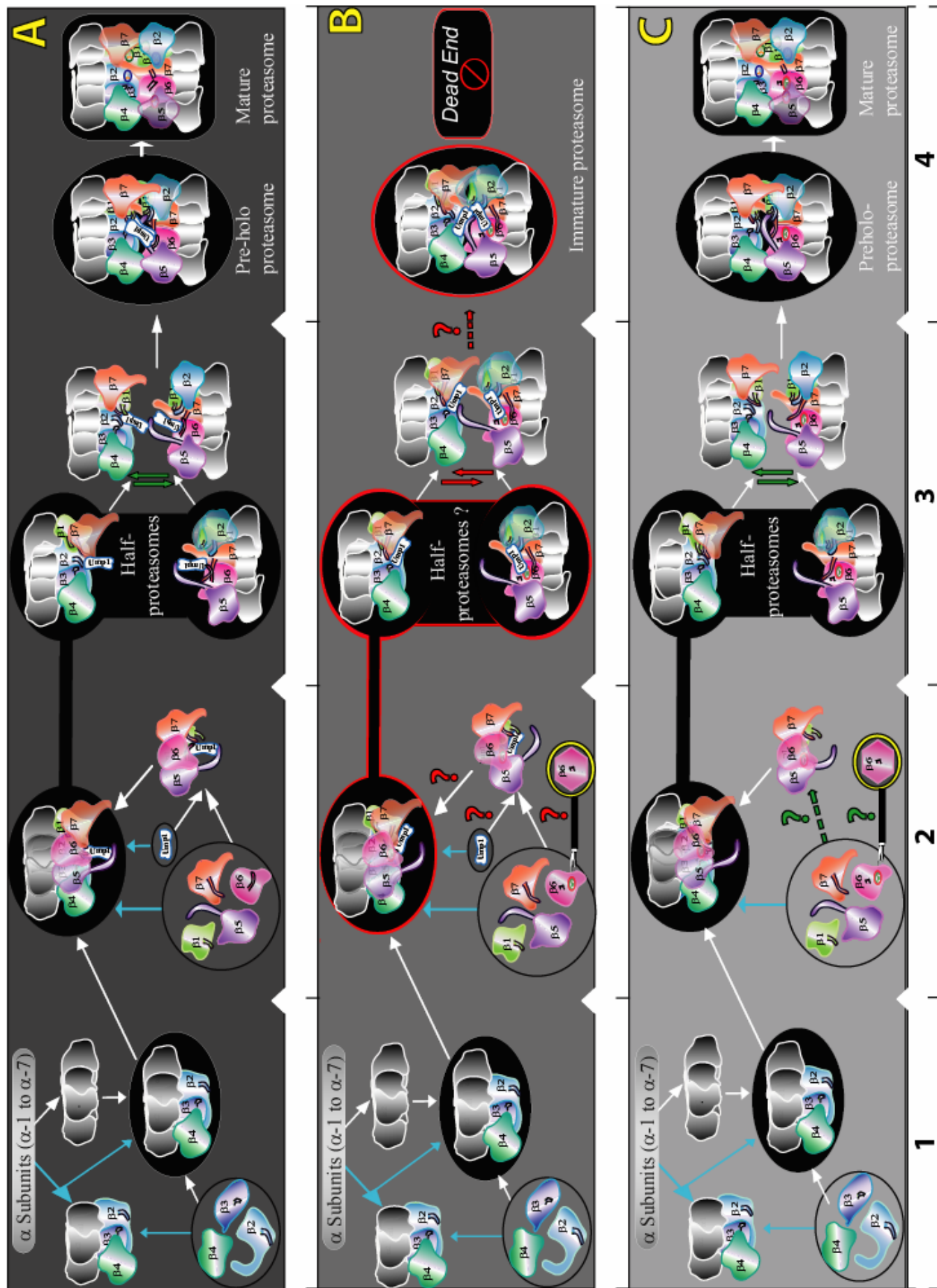
A. Assembly steps in proteasome biogenesis in wild-type cells. **B.** The assembly process in strains expressing mutant $\beta 6$ /Pre7 subunits with indication of possible obstruction stages. **C.** Proteasome assembly steps in the absence of the assembly and maturation factor Ump1 in $\beta 6$ /Pre7 mutants. The cartoons of the subunits represented here are based on their conformation in the crystal structure of the yeast 20S proteasome. For simplification, all α -subunits (α -1 to α -7) are shown in grey color, whereas β -subunits and their propeptides (tail-like extensions on the subunits) are shown in different colors ($\beta 1$: light green, $\beta 2$: light blue, $\beta 3$: dark blue, $\beta 4$: dark green, $\beta 5$: pink, $\beta 6$: purple and $\beta 7$: orange). Groups of free subunits are circled. Blue and white arrows in step 1 and 2 represent putative alternative routes in generation of a relatively long-lived early assembly intermediate and the half-proteasome (shown inside the dark circles), respectively. The small proteasome assembly and maturation factor Ump1 is shown in white color. The β -subunits in the front of the ring ($\beta 5$ and $\beta 6$) are drawn transparently in step 2, and these subunits are removed in step 3 and 4 in order to allow a view into the interior chamber of the proteasome. Similarly, subunits $\beta 3$ and $\beta 4$ are removed from the other half-proteasome in order to view the interior chamber containing the $\beta 5$ and $\beta 6$ subunits. In both cases, two adjacent α -subunits are removed as well for similar purpose. Mutations in the $\beta 6$ subunit might either affect its tertiary structure (highlighted with yellow circle) which could be incompatible with its incorporation at any stage of the assembly process or lead to exposure of a hydrophobic pocket on its surface (green dotted circle, indicated through hand symbol). The truncations or deletion of the $\beta 6$ propeptide could cause binding of Ump1 in a wrong conformation, as indicated in step 2. Processes proceeding efficiently (green arrows and question marks) and transformations that are possibly obstructed due to mutations in the $\beta 6$ subunit (red arrows and question marks) are indicated in step 2 and 3. Dead-end assembly products are highlighted with red circles. The models are represented in four stages: formation of early assembly intermediates (step 1), formation of complete half-proteasomes (step 2), conformational changes that are required to initiate dimerization of two half-proteasome complexes (step 3) and finally the conversion of the pre-holo-proteasome into mature 20S proteasome (step 4).

Step 1 represents the formation of a stable early assembly intermediate that contains a complete α -ring with a subset of β -subunits (highlighted by dark background). This complex is either assembled via the complete α -ring that served as a docking platform for the respective β -type subunits (white arrows) or assembly is initiated by α/β heterodimers as earliest oligomerisation products (blue arrows).

Step 2 indicates the incorporation of the four remaining β -subunits (circled) either individually (blue arrow) or as a pre-assembled sub-complex (white arrows) resulting in the half-proteasome. In both scenarios, their assembly is coupled with binding of the Ump1 protein into the complete half-proteasome (A). The exposure of a hydrophobic pocket (hinted by hand symbol) on the surface of the $\beta 6$ subunit due to truncations or deletion of $\beta 6$ propeptide is shown to affect binding of Ump1 in a right conformation either in the sub-complexes or in half-proteasomes (B). In addition, the yellow-circled hexagonal $\beta 6$ subunit indicates mutations that might generally affect the $\beta 6$ subunit tertiary structure thus avoiding its incorporation into any assembly intermediate in the presence of Ump1 (B and C).

Step 3 reflects the possible conformational changes in both of the half-proteasomes in order to initiate dimerization of the two halves of the proteasome precursor complexes. During this process, the propeptides are shown to be involved in structural alteration of β -subunits as well as in positioning of Ump1 (A), which is mutually distracted when these complexes bear mutant $\beta 6$ subunits (B).

Step 4 represents the maturation process, in which the final conformational changes of the subunits occur. In (A) the Ump1 protein and propeptides are shown to be fixed in a right position in order to initiate autocatalytic processing. In contrast, when mutant $\beta 6$ subunits are present in this complex the maturation event is obstructed in the presence of Ump1 (B) due its structural interference with the exposed hydrophobic surface, which is incompatible with initiation of particle maturation. However, in the absence of Ump1, the maturation process can proceed, at least partially, even in presence of truncated or mutated $\beta 6$ subunits (C).



7 References

- Arendt, C. S., and Hochstrasser, M. (1997). Identification of the yeast 20S proteasome catalytic centers and subunit interactions required for active-site formation. *Proc Natl Acad Sci U S A* *94*, 7156-7161.
- Arendt, C. S., and Hochstrasser, M. (1999). Eukaryotic 20S proteasome catalytic subunit propeptides prevent active site inactivation by N-terminal acetylation and promote particle assembly. *EMBO J* *18*, 3575-3585.
- Arrigo, A. P., Tanaka, K., Goldberg, A. L., and Welch, W. J. (1988). Identity of the 19S 'prosome' particle with the large multifunctional protease complex of mammalian cells (the proteasome). *Nature* *331*, 192-194.
- Ausubel, F., Brent, R., Kingston, R.E., Moore, D.D., Seidman, J.G., Smith, J.A., Struhl, K. (1995). *Current Protocols in Molecular Biology*. John Wiley & Sons, Inc.
- Ausubel, F., R, Brent, R. Kingston, D. Moore, J. Seidman and J.S., Smith (1991). *Current Protocol in Molecular Biology*. New York: John Wiley and Sons, Inc.
- Baker, D., Shiau, A. K., and Agard, D. A. (1993). The role of pro regions in protein folding. *Curr Opin Cell Biol* *5*, 966-970.
- Baker, D., Shiau, K., Goldberg, A.L., and Welch, W.J. (1988). The role of proregions in protein folding. *Curr Opin Cell Biol* *5*, 966-970.
- Bartel, B., Wunning, I., and Varshavsky, A. (1990). The recognition component of the N-end rule pathway. *EMBO J* *9*, 3179-3189.
- Baumeister, W., Dahlmann, B., Hegerl, R., Kopp, F., Kuehn, L., and Pfeifer, G. (1988). Electron microscopy and image analysis of the multicatalytic proteinase. *FEBS Lett* *241*, 239-245.
- Baumeister, W., Walz, J., Zühl, F., and Seemüller, E. (1998). The proteasome: paradigm of a self-compartmentalizing protease. *Cell* *92*, 367-380.
- Bochtler, M., Ditzel, L., Groll, M., and Huber, R. (1997). Crystal structure of heat shock locus V (HslV) from *Escherichia coli*. *Proc Natl Acad Sci U S A* *94*, 6070-6074.
- Bohley, P., and Seglen, P. O. (1992). Proteases and proteolysis in the lysosome. *Experientia* *48*, 151-157.

- Bradford (1976). A rapid and sensitive method for the quantitation of microgram quantities of protein utilizing the principle of protein-dye binding. *Anal Biochem* 7, 248-254.
- Brannigan, J. A., Dodson, G., Duggleby, H. J., Moody, P. C., Smith, J. L., Tomchick, D. R., and Murzin, A. G. (1995). A protein catalytic framework with an N-terminal nucleophile is capable of self-activation. *Nature* 378, 416-419.
- Burri, L., Hockendorff, J., Boehm, U., Klamp, T., Dohmen, R. J., and Levy, F. (2000). Identification and characterization of a mammalian protein interacting with 20S proteasome precursors. *Proc Natl Acad Sci U S A* 97, 10348-10353.
- Cerundolo, V., Kelly, A., Elliott, T., Trowsdale, J., and Townsend, A. (1995). Genes encoded in the major histocompatibility complex affecting the generation of peptides for TAP transport. *Eur J Immunol* 25, 554-562.
- Chen, P., and Hochstrasser, M. (1996). Autocatalytic subunit processing couples active site formation in the 20S proteasome to completion of assembly. *Cell* 86, 961-972.
- Ciechanover, A. (1998a). The ubiquitin-proteasome pathway: on protein death and cell life. *EMBO J* 17, 7151-7160.
- Ciechanover, A. And Schwartz, A. (1998b). The ubiquitin-proteasome pathway: the complexity and myriad functions of proteins death. *Proc Natl Acad Sci U S A* 95, 2727-2730.
- Ciechanover, A., Orian, A., and Schwartz, A. L. (2000). Ubiquitin-mediated proteolysis: biological regulation via destruction. *Bioessays* 22, 442-451.
- Cioffi, C. L., Liu, X. Q., Kosinski, P. A., Garay, M., and Bowen, B. R. (2003). Differential regulation of HIF-1 alpha prolyl-4-hydroxylase genes by hypoxia in human cardiovascular cells. *Biochem Biophys Res Commun* 103 (3), 947-53
- Ciechanover, A. (2003). The ubiquitin proteolytic system and pathogenesis of human diseases: a novel platform for mechanism-based drug targeting. *Biochem Soc Trans* 31, 474-481.
- Coligan J.E, Dunn B.M, Speicher D.W and Wingfield P.D (2001). *Current Protocols in Protein Science*.
- Dahlmann, B., Kopp, F., Kuehn, L., Niedel, B., Pfeifer, G., Hegerl, R., and Baumeister, W. (1989). The multicatalytic proteinase (prosome) is ubiquitous from eukaryotes to archaeobacteria. *FEBS Lett* 251, 125-131.

- Ditzel, L., Huber, R., Mann, K., Heinemeyer, W., Wolf, D. H., and Groll, M. (1998a). Conformational constraints for protein self-cleavage in the proteasome. *J Mol Biol* 279, 1187-1191.
- Ditzel, L., Huber, R., Mann, K., Heinemeyer, W., Wolf, D. H., and Groll, M. (1998b). Conformational constraints for protein self-cleavage in the proteasome. *J Mol Biol* 279, 1187-1191.
- Driscoll, J., and Goldberg, A. L. (1990). The proteasome (multicatalytic protease) is a component of the 1500-kDa proteolytic complex which degrades ubiquitin-conjugated proteins. *J Biol Chem* 265, 4789-4792.
- Egner, R., Thumm, M., Straub, M., Simeon, A., Schuller, H. J., and Wolf, D. H. (1993). Tracing intracellular proteolytic pathways. Proteolysis of fatty acid synthase and other cytoplasmic proteins in the yeast *Saccharomyces cerevisiae*. *J Biol Chem* 268, 27269-27276.
- Emori, Y., Tsukahara, T., Kawasaki, H., Ishiura, S., Sugita, H., and Suzuki, K. (1991). Molecular cloning and functional analysis of three subunits of yeast proteasome. *Mol Cell Biol* 11, 344-353.
- Enenkel, C., Lehmann, H., Kipper, J., Guckel, R., Hilt, W., and Wolf, D. H. (1994). PRE3, highly homologous to the human major histocompatibility complex-linked LMP2 (RING12) gene, codes for a yeast proteasome subunit necessary for the peptidylglutamyl-peptide hydrolyzing activity. *FEBS Lett* 341, 193-196.
- Etlinger, J. D., Li, S. X., Guo, G. G., and Li, N (1977). A soluble ATP-dependent protolytic system responsible for the degradation of abnormal proteins in reticulocytes. *Proc Natl Acad Sci U S A* 74, 54 - 48.
- Eytan, E., Ganoth, D., Armon, T., and Hershko, A. (1989). ATP-dependent incorporation of 20S protease into the 26S complex that degrades proteins conjugated to ubiquitin. *Proc Natl Acad Sci U S A* 86, 7751-7755.
- Fehlker, M., Wendler, P., Lehmann, A., and Enenkel, C. (2003). Blm3 is part of nascent proteasomes and is involved in a late stage of nuclear proteasome assembly. *EMBO Rep* 4, 959-963.
- Frentzel, S., Pesold-Hurt, B., Seelig, A., and Kloetzel, P. M. (1994). 20 S proteasomes are assembled via distinct precursor complexes. Processing of LMP2 and LMP7 proproteins takes place in 13-16 S preproteasome complexes. *J Mol Biol* 236, 975-981.
- Fu, H., Doelling, J. H., Arendt, C. S., Hochstrasser, M., and Vierstra, R. D. (1998). Molecular organization of the 20S proteasome gene family from *Arabidopsis thaliana*. *Genetics* 149, 677-692.

- Gerards, W. L., de Jong, W. W., Boelens, W., and Bloemendal, H. (1998). Structure and assembly of the 20S proteasome. *Cell Mol Life Sci* 54, 253-262.
- Gerards, W. L., Enzlin, J., Haner, M., Hendriks, I. L., Aebi, U., Bloemendal, H., and Boelens, W. (1997). The human alpha-type proteasomal subunit HsC8 forms a double ringlike structure, but does not assemble into proteasome-like particles with the beta-type subunits HsDelta or HsBPROS26. *J Biol Chem* 272, 10080-10086.
- Glickman, M. H., Rubin, D. M., Coux, O., Wefes, I., Pfeifer, G., Cjeka, Z., Baumeister, W., Fried, V. A., and Finley, D. (1998a). A subcomplex of the proteasome regulatory particle required for ubiquitin-conjugate degradation and related to the COP9-signalosome and eIF3. *Cell* 94, 615-623.
- Glickman, M. H., Rubin, D. M., Fried, V. A., and Finley, D. (1998b). The regulatory particle of the *Saccharomyces cerevisiae* proteasome. *Mol Cell Biol* 18, 3149-3162.
- Glickman, M. H., and Ciechanover, A. (2002). The ubiquitin-proteasome proteolytic pathway: destruction for the sake of construction. *Physiol Rev* 82, 373-428.
- Glickman, M. H. Adir N., (2004). The Proteasome and the Delicate Balance between Destruction and Rescue. *PLoS Biol* 2, E13.
- Griffin, T. A., Slack, J. P., McCluskey, T. S., Monaco, J. J., and Colbert, R. A. (2000). Identification of proteasemblin, a mammalian homologue of the yeast protein, Ump1p, that is required for normal proteasome assembly. *Mol Cell Biol Res Commun* 3, 212-217.
- Groettrup, M., Standera, S., Stohwasser, R., and Kloetzel, P. M. (1997). The subunits MECL-1 and LMP2 are mutually required for incorporation into the 20S proteasome. *Proc Natl Acad Sci U S A* 94, 8970-8975.
- Groll, M., Bajorek, M., Kohler, A., Moroder, L., Rubin, D. M., Huber, R., Glickman, M. H., and Finley, D. (2000). A gated channel into the proteasome core particle. *Nat Struct Biol* 7, 1062-1067.
- Groll, M., Ditzel, L., Lowe, J., Stock, D., Bochtler, M., Bartunik, H. D., and Huber, R. (1997). Structure of 20S proteasome from yeast at 2.4 Å resolution. *Nature* 386, 463-471.
- Grziwa, A., Baumeister, W., Dahlmann, B., and Kopp, F. (1991). Localization of subunits in proteasomes from *Thermoplasma acidophilum* by immunoelectron microscopy. *FEBS Lett* 290, 186-190.

- Grziwa, A., Maack, S., Puhler, G., Wiegand, G., Baumeister, W., and Jaenicke, R. (1994). Dissociation and reconstitution of the *Thermoplasma* proteasome. *Eur J Biochem* *223*, 1061-1067.
- Guthrie, C., and Fink, G. R. (1991). *Guide to Yeast Genetics and Molecular Cloning*. 194.
- Harris, J. R. (1968). Release of a macromolecular protein component from human erythrocyte ghosts. *Biochim Biophys Acta* *150*, 534-537.
- Harris, J. R. (1988). Erythrocyte cylindrin: Possible identity with the ubiquitous 20S high molecular weight protease complex and the prosome partical,. *Indian j Biochem Biophys* *25*.
- Hase, J., Kobashi, K., Nakai, N., Mitsui, K., Iwata, K., and Takadera, T. (1980). The quaternary structure of carp muscle alkaline protease. *Biochim Biophys Acta* *611*, 205-213.
- Hegerl, R., Pfeifer, G., Puhler, G., Dahlmann, B., and Baumeister, W. (1991). The three-dimensional structure of proteasomes from *Thermoplasma acidophilum* as determined by electron microscopy using random conical tilting. *FEBS Lett* *283*, 117-121.
- Heinemeyer, W., Fischer, M., Krimmer, T., Stachon, U., and Wolf, D. H. (1997). The active sites of the eukaryotic 20 S proteasome and their involvement in subunit precursor processing. *J Biol Chem* *272*, 25200-25209.
- Heinemeyer, W., Gruhler, A., Mohrle, V., Mahe, Y., and Wolf, D. H. (1993). PRE2, highly homologous to the human major histocompatibility complex-linked RING10 gene, codes for a yeast proteasome subunit necessary for chrymotryptic activity and degradation of ubiquitinated proteins. *J Biol Chem* *268*, 5115-5120.
- Heinemeyer, W., Kleinschmidt, J. A., Saidowsky, J., Escher, C., and Wolf, D. H. (1991). Proteinase yscE, the yeast proteasome/multicatalytic-multifunctional proteinase: mutants unravel its function in stress induced proteolysis and uncover its necessity for cell survival. *EMBO J* *10*, 555-562.
- Heinemeyer, W., Ramos, P. C., and Dohmen, R. J. (2004). The ultimate nanoscale mincer: assembly, structure and active sites of the 20S proteasome core. *Cell Mol Life Sci* *61*, 1562-1578.
- Heinemeyer, W., Trondle, N., Albrecht, G., and Wolf, D. H. (1994). PRE5 and PRE6, the last missing genes encoding 20S proteasome subunits from yeast? Indication for a set of 14 different subunits in the eukaryotic proteasome core. *Biochemistry* *33*, 12229-12237.

- Hershko, A., and Ciechanover, A. (1998). The ubiquitin system. *Annu Rev Biochem* 67, 425-479.
- Hideshima, T., Chauhan, D., Hayashi, T., Podar, K., Akiyama, M., Mitsiades, C., M. Itsiades N, Gong, B., Bonham, L., de Vries, P., Munshi, N., Richardson, P. G., Singer, J. W., and Anderson, K. C. (2003). Antitumor activity of lysophosphatidic acid acyltransferase-beta inhibitors, a novel class of agents, in multiple myeloma. *Cancer Res* 63, 8428-8436.
- Hilt, W., and Wolf, D. H. (2004). The ubiquitin-proteasome system: past, present and future. *Cell Mol Life Sci* 61, 1545.
- Hough, R., Pratt, G., and Rechsteiner, M. (1987). Purification of two high molecular weight proteases from rabbit reticulocyte lysate. *J Biol Chem* 262, 8303-8313.
- Ishiura, S., and Sugita, H. (1986). Ingensin, a high-molecular-mass alkaline protease from rabbit reticulocyte. *J Biochem (Tokyo)* 100, 753-763.
- Jäger, S., Strayle, J., Heinemeyer, W., and Wolf, D. H. (2001). Cic1, an adaptor protein specifically linking the 26S proteasome to its substrate, the SCF component Cdc4. *EMBO J* 20, 4423-4431.
- Jäger, S., Groll, M., Huber, R., Wolf, D. H., and Heinemeyer, W. (1999). Proteasome beta-type subunits: unequal roles of propeptides in core particle maturation and a hierarchy of active site function. *J Mol Biol* 291, 997-1013.
- Jentsch, S., and Schlenker, S. (1995). Selective protein degradation: a journey's end within the proteasome. *Cell* 82, 881-884.
- Ju, D., and Xie, Y. (2004). Proteasomal Degradation of RPN4 via Two Distinct Mechanisms, Ubiquitin-dependent and -independent. *J Biol Chem* 279, 23851-23854.
- Khan, A. R., and James, M. N. (1998). Molecular mechanisms for the conversion of zymogens to active proteolytic enzymes. *Protein Sci* 7, 815-836.
- Kleinschmidt, J. A., Hugle, B., Grund, C., and Franke, W. W. (1983). The 22 S cylinder particles of *Xenopus laevis*. I. Biochemical and electron microscopic characterization. *Eur J Cell Biol* 32, 143-156.
- Knop, M., Schiffer, H. H., Rupp, S., and Wolf, D. H. (1993). Vacuolar/lysosomal proteolysis: proteases, substrates, mechanisms. *Curr Opin Cell Biol* 5, 990-996.

- Kohler, A., Cascio, P., Leggett, D. S., Woo, K. M., Goldberg, A. L., and Finley, D. (2001). The axial channel of the proteasome core particle is gated by the Rpt2 ATPase and controls both substrate entry and product release. *Mol Cell* 7, 1143-1152.
- Kopp, F., Kristensen, P., Hendil, K. B., Johnsen, A., Sobek, A., and Dahlmann, B. (1995). The human proteasome subunit HsN3 is located in the inner rings of the complex dimer. *J Mol Biol* 248, 264-272.
- Laemmli, U. K. (1970). Cleavage of Structural proteins during the assembly of the head of bacteriophage T4. *Nature* 227, 737-740.
- Larsen, C. N., and Finley, D. (1997). Protein translocation channels in the proteasome and other proteases. *Cell* 91, 431-434.
- Larsen, K. E., and Sulzer, D. (2002). Autophagy in neurons: a review. *Histol Histopathol* 17, 897-908.
- London, M. K., Keck, B. I., Ramos, P. C., and Jurgen Dohmen, R. (2004). Regulatory mechanisms controlling biogenesis of ubiquitin and the proteasome. *FEBS Lett* 567, 259-264.
- Löwe, J., Stock, D., Jap, B., Zwickl, P., Baumeister, W., and Huber, R. (1995). Crystal structure of the 20S proteasome from the archaeon *T. acidophilum* at 3.4 Å resolution. *Science* 268, 533-539.
- Ma, J., Katz, E., and Belote, J. M. (2002). Expression of proteasome subunit isoforms during spermatogenesis in *Drosophila melanogaster*. *Insect Mol Biol* 11, 627-639.
- Mannhaupt, G., Schnall, R., Karpov, V., Vetter, I., and Feldmann, H. (1999). Rpn4p acts as a transcription factor by binding to PACE, a nonamer box found upstream of 26S proteasomal and other genes in yeast. *FEBS Lett* 450, 27-34.
- McGuire, M. J., and DeMartino, G.N (1986). Purification and characterization of a high molecular weight proteinase (macropain) from human erythrocytes. *Biochim Biophys Acta* 873.
- Missiakas, D., Schwager, F., Betton, J. M., Georgopoulos, C., and Raina, S. (1996). Identification and characterization of HsIV HsIU (ClpQ ClpY) proteins involved in overall proteolysis of misfolded proteins in *Escherichia coli*. *EMBO J* 15, 6899-6909.
- Monaco, J.J., and McDevitt, H.O. (1984). H-2-Linked low-molecular weight polypeptide antigens assemble into an unusual macromolecular complex. *Nature* 309, 797-799.

- Mullapudi, S., Pullan, L., Khalil, H., Stoops, J. K., Tastan-Bishop, A. O., Beckmann, R., Kloetzel, P. M., Krueger, E., and Penczek, P. A. (2004). Rearrangement of the 16S precursor subunits is essential for the formation of the active 20S proteasome. *Biophys J*. (published online)
- Mumberg D, Muller R, Funk M. (1994). Regulatable promoters of *Saccharomyces cerevisiae*: comparison of transcriptional activity and their use for heterologous expression. *Nucleic Acids Res* 22, 5767-5768.
- Mumberg D, Muller R, and Funk M. (1995). Yeast vectors for the controlled expression of heterologous proteins in different genetic backgrounds. *Gene* 156, 119-122.
- Nandi, D., Woodward, E., Ginsburg, D. B., and Monaco, J. J. (1997). Intermediates in the formation of mouse 20S proteasomes: implications for the assembly of precursor beta subunits. *EMBO J* 16, 5363-5375.
- Narayan, K. S., and Rounds, D. E. (1973). Minute ring-shaped particles in cultured cells of malignant origin. *Nat New Biol* 243, 146-150.
- Norbury, C. C., Basta, S., Donohue, K. B., Tschärke, D. C., Princiotta, M. F., Berglund, P., Gibbs, J., Bennink, J. R., and Yewdell, J. W. (2004). CD8+ T cell cross-priming via transfer of proteasome substrates. *Science* 304, 1318-1321.
- Orlowski, M., and Wilk, W., (1988). Multicatalytic proteinase complex or multicatalytic proteinase: A high Mr endopeptidase. *Biochem J* 255, 751.
- Papandreou, C. N., Daliani, D. D., Nix, D., Yang, H., Madden, T., Wang, X., Pien, C. S., Millikan, R. E., Tu, S. M., Pagliaro, L., *et al.* (2004). Phase I trial of the proteasome inhibitor bortezomib in patients with advanced solid tumors with observations in androgen-independent prostate cancer. *J Clin Oncol* 22, 2108-2121.
- Peekhaus, N. T., Chang, T., Hayes, E. C., Wilkinson, H. A., Mitra, S. W., Schaeffer, J. M., and Rohrer, S. P. (2004). Distinct effects of the antiestrogen Faslodex on the stability of estrogen receptors- α and - β in the breast cancer cell line MCF-7. *J Mol Endocrinol* 32, 987-995.
- Peters, J. M., Cejka, Z., Harris, J. R., Kleinschmidt, J. A., and Baumeister, W. (1993). Structural features of the 26 S proteasome complex. *J Mol Biol* 234, 932-937.
- Pühler, G., Weinkauff, S., Bachmann, L., Müller, S., Engel, A., Hegerl, R., and Baumeister, W. (1992). Subunit stoichiometry and three-dimensional arrangement in proteasomes from *Thermoplasma acidophilum*. *EMBO J* 11, 1607-1616.

- Ramos, P. C., Hockendorff, J., Johnson, E. S., Varshavsky, A., and Dohmen, R. J. (1998). Ump1p is required for proper maturation of the 20S proteasome and becomes its substrate upon completion of the assembly. *Cell* 92, 489-499.
- Ramos, P. C., Marques, A. J., London, M. K., and Dohmen, R. J. (2004). Role of C-terminal extensions of subunits beta2 and beta7 in assembly and activity of eukaryotic proteasomes. *J Biol Chem* 279, 14323-14330.
- Rock, K. L., Gramm, C., Rothstein, L., Clark, K., Stein, R., Dick, L., Hwang, D., and Goldberg, A. L. (1994). Inhibitors of the proteasome block the degradation of most cell proteins and the generation of peptides presented on MHC class I molecules. *Cell* 78, 761-771.
- Rodriguez-Vilarino, S., Arribas, J., Arizti, P., and Castano, J. G. (2000). Proteolytic processing and assembly of the C5 subunit into the proteasome complex. *J Biol Chem* 275, 6592-6599.
- Rohrwild, M., Coux, O., Huang, H. C., Moerschell, R. P., Yoo, S. J., Seol, J. H., Chung, C. H., and Goldberg, A. L. (1996). HslV-HslU: A novel ATP-dependent protease complex in *Escherichia coli* related to the eukaryotic proteasome. *Proc Natl Acad Sci U S A* 93, 5808-5813.
- Rose, M. D., Winston, F., Hieter, P. (1990). *Methods in Yeast Genetics; A Laboratory Course Manual*. Cold Spring Harbor Laboratory Press, Cold Spring Harbor, NY.
- Sambrook, J., Fritsch, E.F., Maniatis, T. (1989). *Molecular Cloning, A Laboratory Manual*. Cold Spring Harbor Laboratory Press, Cold Spring Harbor, NY.
- Schauer, T. M., Nesper, M., Kehl, M., Lottspeich, F., Muller-Taubenberger, A., Gerisch, G., and Baumeister, W. (1993). Proteasomes from *Dictyostelium discoideum*: characterization of structure and function. *J Struct Biol* 111, 135-147.
- Schmidt, M., and Kloetzel, P. M. (1997). Biogenesis of eukaryotic 20S proteasomes: the complex maturation pathway of a complex enzyme. *Faseb J* 11, 1235-1243.
- Schmidt, M., Schmidtke, G., and Kloetzel, P. M. (1997). Structure and structure formation of the 20S proteasome. *Mol Biol Rep* 24, 103-112.
- Schmidt, M., Zantopf, D., Kraft, R., Kostka, S., Preissner, R., and Kloetzel, P. M. (1999). Sequence information within proteasomal prosequences mediates efficient integration of beta-subunits into the 20 S proteasome complex. *J Mol Biol* 288, 117-128.
- Schmidtke, G., Kraft, R., Kostka, S., Henklein, P., Frommel, C., Lowe, J., Huber, R., Kloetzel, P. M., and Schmidt, M. (1996). Analysis of mammalian 20S proteasome

- biogenesis: the maturation of beta-subunits is an ordered two-step mechanism involving autocatalysis. *EMBO J* 15, 6887-6898.
- Schmidtke, G., Schmidt, M., and Kloetzel, P. M. (1997). Maturation of mammalian 20 S proteasome: purification and characterization of 13 S and 16 S proteasome precursor complexes. *J Mol Biol* 268, 95-106.
- Seemüller, E., Lupas, A., and Baumeister, W. (1996). Autocatalytic processing of the 20S proteasome. *Nature* 382, 468-471.
- Seemüller, E., Lupas, A., Stock, D., Lowe, J., Huber, R., and Baumeister, W. (1995a). Proteasome from *Thermoplasma acidophilum*: a threonine protease. *Science* 268, 579-582.
- Seemüller, E., Lupas, A., Zuhl, F., Zwickl, P., and Baumeister, W. (1995b). The proteasome from *Thermoplasma acidophilum* is neither a cysteine nor a serine protease. *FEBS Lett* 359, 173-178.
- Shelton, E., Kuff, E. L., Maxwell, E. S., and Harrington, J. T. (1970). Cytoplasmic particles and aminoacyl transferase I activity. *J Cell Biol* 45, 1-8.
- Sikorski RS, and P., H. (1989). A system of shuttle vectors and yeast host strains designed for efficient manipulation of DNA in *Saccharomyces cerevisiae*. *Genetics* 122, 19-27.
- Smulson, M. (1974). Subribosomal particles of Hela cells. *Exp Cell Res* 87, 253-258.
- Tamura, T., Nagy, I., Lupas, A., Lottspeich, F., Cejka, Z., Schoofs, G., Tanaka, K., De Mot, R., and Baumeister, W. (1995). The first characterization of a eubacterial proteasome: the 20S complex of *Rhodococcus*. *Curr Biol* 5, 766-774.
- Tanaka, K. (2004). [Ubiquitin and proteasome]. *Tanpakushitsu Kakusan Koso* 49, 1033-1039.
- Towbin, H., T. Staehelin and J. Gordon (1979). Electrophoretic transfer of proteins from polyacrylamide gels to nitrocellulose sheets: procedure and some applications. *Proc Natl Acad Sci, USA* 76, 4350-4354.
- Unno, M., Mizushima, T., Morimoto, Y., Tomisugi, Y., Tanaka, K., Yasuoka, N., and Tsukihara, T. (2002a). Structure determination of the constitutive 20S proteasome from bovine liver at 2.75 Å resolution. *J Biochem (Tokyo)* 131, 171-173.
- Unno, M., Mizushima, T., Morimoto, Y., Tomisugi, Y., Tanaka, K., Yasuoka, N., and Tsukihara, T. (2002b). The structure of the mammalian 20S proteasome at 2.75 Å resolution. *Structure (Camb)* 10, 609-618.

- Ustrell, V., Hoffman, L., Pratt, G., and Rechsteiner, M. (2002). PA200, a nuclear proteasome activator involved in DNA repair. *EMBO J* 21, 3516-3525.
- Varshavsky, A. (1995). The N-end rule. *Cold Spring Harb Symp Quant Biol* 60, 461-478.
- Velichutina, I., Connerly, P. L., Arendt, C. S., Li, X., and Hochstrasser, M. (2004). Plasticity in eucaryotic 20S proteasome ring assembly revealed by a subunit deletion in yeast. *EMBO J* 23, 500-510.
- Vigouroux, S., Furukawa, Y., Farout, L., S, J. K., Briand, M., and Briand, Y. (2003). Peptidase activities of the 20/26S proteasome and a novel protease in human brain. *J Neurochem* 84, 392-396.
- Voges, D., Zwickl, P., and Baumeister, W. (1999). The 26S proteasome: a molecular machine designed for controlled proteolysis. *Annu Rev Biochem* 68, 1015-1068.
- Wang, J. H., J. A. and Flanagan, J. M. (1997). The Structure of ClpP at 2.3 Å resolution suggests a model for ATP-dependent proteolysis. *Cell* 91, 447-456.
- White, B. A. (1993). Current Methods and Applications. *Methods in molecular biology* 15.
- Witt, E., Zantopf, D., Schmidt, M., Kraft, R., Kloetzel, P. M., and Kruger, E. (2000). Characterisation of the newly identified human Ump1 homologue POMP and analysis of LMP7(beta 5i) incorporation into 20 S proteasomes. *J Mol Biol* 301, 1-9.
- Wu, Q., Lin, X. F., Ye, X. F., Zhang, B., Xie, Z., and Su, W. J. (2004). Ubiquitinated or sumoylated retinoic acid receptor alpha determines its characteristic and interacting model with retinoid X receptor alpha in gastric and breast cancer cells. *J Mol Endocrinol* 32, 595-613.
- Xie, Y., and Varshavsky, A. (2001). RPN4 is a ligand, substrate, and transcriptional regulator of the 26S proteasome: a negative feedback circuit. *Proc Natl Acad Sci U S A* 98, 3056-3061.
- Yang, Y., Fruh, K., Ahn, K., and Peterson, P. A. (1995). In vivo assembly of the proteasomal complexes, implications for antigen processing. *J Biol Chem* 270, 27687-27694.
- Yoshimura, T., Kameyama, K., Takagi, T., Ikai, A., Tokunaga, F., Koide, T., Tanahashi, N., Tamura, T., Cejka, Z., Baumeister, W., and et al. (1993). Molecular characterization of the "26S" proteasome complex from rat liver. *J Struct Biol* 111, 200-211.

- Zühl, F., Seemüller, E., Golbik, R., and Baumeister, W. (1997a). Dissecting the assembly pathway of the 20S proteasome. *FEBS Lett* *418*, 189-194.
- Zühl, F., Tamura, T., Dolenc, I., Cejka, Z., Nagy, I., De Mot, R., and Baumeister, W. (1997b). Subunit topology of the *Rhodococcus* proteasome. *FEBS Lett* *400*, 83-90.
- Zwickl, P., Grziwa, A., Puhler, G., Dahlmann, B., Lottspeich, F., and Baumeister, W. (1992). Primary structure of the *Thermoplasma* proteasome and its implications for the structure, function, and evolution of the multicatalytic proteinase. *Biochemistry* *31*, 964-972.
- Zwickl, P., Kleinz, J., and Baumeister, W. (1994). Critical elements in proteasome assembly. *Nat Struct Biol* *1*, 765-770.

8 Acknowledgments

I would like to thank Prof. Dr. Dieter H. Wolf who provided this great opportunity to perform my Ph.D. thesis work in his laboratory and for his encouragements throughout this scientific cruise. I am indeed very thankful for his valuable criticisms.

I really stuck when I search for words to evince my thanks to Dr. Wolfgang Heinemeyer for his grateful helps and his tremendous supports during this scientific ordeal. Without him, this adventure would have been implausible for me. I express my deep heart full thanks to him.

I am indebted Dr. W. Hilt, Dr. B. Singer-krüger and Dr. H. Rudolph for their valuable support and advice during this period. I thank to Elisabeth and Helga for their friendly assistance. Thanks to Jojo, Tom, Park, Harish and RuiE who gave convivial and colorful life in lab. I feel heartily and deeply grateful for my special friend Julia for her lively support that ameliorated me.

Again, my special thanks are flying to my friends: appukootan Sharath, Ponni and Subee, as well to VGV, Kusmith, Geetha and others for their marvelous support during my studies. I am indebted to Dr. Yi-ling-lin, Dr. E.long-lin , Dr. Chihmao-su and Dr. Krishnan who initiated my scientific life.

My special incredible thanks to chappathi Ajoy, who is there to help me always. As well, I would like to acknowledge my special thanks to karamban Veera who fetched me to abroad, which tuned my scientific life. A big hugging thanks to Sara, Sha and SPs for their valuable company.

It is impossible to express how blessed I was to be a son for my parents and to get greatest family members on earth. Their patience and buoyancy made and will make me to cheer up my life.

Good luck

Curriculum Vitae

Personal information

Name : Saravanakumar Iyappan
Date of birth : 10.06.1976
Sex : Male
Nationality : Indian

Educational/Research qualifications

- 1994-1997** : **Bachelor of Science in Zoology**,
University of Madras, Chennai, India.
- 1997-1999** : **Master of Science in Biotechnology**,
Bharathidasan University, Tiruchirappalli, India.
- [05th -17th Jan-1998] : Research training program on vaccine production against
“Diphtheria toxin (DPT) and Rabbis virus”,
Pasteur Institute of India, Coonnor, India.
- [02nd -06th Mar-1998] : Research training program on “Fundamentals engineering on
Engineering fundamentals in fermentation technology”,
Central Food Technological Research Institute, Mysore, India.
- [25th May-25th June, 1998] : Student summer training program
National Institute of Virology, Pune, India.
Topic: “Purification of virus (*Dengue*, *Japanese encephalitis* and
West Nile) specific monoclonal antibody IgG and its application in
diagnosis”
- [Dec1998-May1999] : Diploma thesis
Bharathidasan University, Tiruchirappalli, India.
Topic:
**Impact of kinetin on the major haemolymph protein
(MHP) during the development of silk worm *Bombyx mori* L**
“Funded by Tamilnadu State Council for Science & Technology
(TNSCST)”, Government of India.
- Oct 1999-Dec 2000** : Research assistant,
Institute of Biomedical Sciences, Academia Sinica, Taipei, Taiwan.
Topic: The *Japanese Encephalitis* viral proteins and their
involvement in inhibition of the antiviral protein kinase PKR.
- Dec 2000-Dec 2004** : Doctorate student,
Institute of Biochemistry,
Universität Stuttgart,
Stuttgart, Germany.
Topic:
**The function of the β 6/Pre7 propeptide for 20S proteasome
biogenesis in baker’s yeast**
“Funded by Deutsche Forschungsgemeinschaft (DFG)”, Germany

9 Declaration

Hiermit versichere ich, dass ich die vorgelegte Arbeit selbstständig angefertigt und keine anderen als die angegebenen Quellen and Hilfsmittel verwendet wurden.

Stuttgart, den
November 2004

Iyappan Saravanakumar